OPTIMIZATION OF POLYELECTROLYTE COMPLEX PRODUCTION: IMPLICATIONS OF MOLECULAR CHARACTERISTICS ON PHYSICOCHEMICAL AND BIOLOGICAL PROPERTIES

By

Sean Michael Hartig

Dissertation

Submitted to the Faculty of the

Graduate School of Vanderbilt University

in partial fulfillment of the requirements

for the degree of

DOCTOR OF PHILOSOPHY

in

Chemical Engineering

December, 2006

Nashville, Tennessee

Approved:

Professor G. Kane Jennings

Professor Bridget Rogers

Professor Ken Debelak

Professor Scott Guelcher

Professor Jeffrey Davidson

Professor Ales Prokop

‘so it always is: when you escape to the desert, the silence shouts in your ear’

To my parents, June and Charles Hartig, but especially Mom who has carried me here and will continue to be the light that guides me.

ACKNOWLEDGMENTS

There are many people who deserve thanks for helping me succeed at Vanderbilt. I would like to thank my advisors, Drs. Davidson and Prokop, for their helpful guidance and support throughout my graduate work. I am appreciative of everything they have done for me, particularly for overseeing my professional development as a researcher, and am grateful for the three years I was able to work under their supervision. My accomplishments are directly related to their patience, uncanny ability to cultivate my ideas, and advice when I needed it the most. They gave me a wonderful opportunity, when the prospects of a Ph.D. looked pretty bleak. They have my utmost respect and admiration. I hope that I can make them proud. I will particularly miss the meetings Dr. Prokop and I had almost daily where he constantly challenged me in ways I never thought possible and, more importantly, became my friend; I will not forget his contributions to my success and well-being. Hopefully, our meetings will continue, although they will not be as often. I am also appreciative to the faculty members that served on my Ph.D. committee: even though the project and some of the circumstances were atypical: Dr. Bridget Rogers, Dr. Ken Debelak, Dr. Kane Jennings, and Dr. Scott Guelcher. I thank each of them for their time.

For the many people I have met and worked with during my time at Vanderbilt and who made life during these past 5+ years better, I am deeply grateful. Since I have been here for a good bit, I have gotten to know the faculty and staff of the chemical engineering department very well. I thank the staff of chemical engineering for putting up with me all these years and aiding me numerous times in various ways, and for always

being supportive of my efforts. Fellow graduate students, past and present, and especially fellow members of my research group have always been willing to help me in whatever way possible, have been a joy to work with, and made direct contributions to my success: Rachel Greene, Jin-Hua Liu, Jayasri DasGupta. Two people that I am particularly thankful to are Gianluca Carlesso and Evgeni Kozlov. They were people that I initially only associated with work, but became close friends, confidants, and friendships I will maintain even after I leave Vanderbilt. Jim Higginbotham played a huge part towards the end of the project providing me free access to expensive machinery and helping me hammer out ideas and experiments. Along with the people I worked with, I am grateful to Eric Brantley and Tiffany Rau for making my time in graduate school at Vanderbilt a little bit more bearable. They listened to my complaining and were supportive of me even when I knew they were sick of hearing the constant whining. Also, my life-long friends, Manoj Viswanathan and Spooner Ward deserve shout-outs.

Finally, and most importantly, I am grateful for the undying support of my family and love you all: Kate, Pat, Leslie, Mom, and Dad. Their infinite love never relented while I was miles away struggling and trying to figure out what I wanted to do with my life. There really aren't any words to describe the thanks they deserve for standing next to me when I wanted to pack up and quit. This was the most difficult, both emotionally and mentally, experience of my life and they knew something that I didn't: the sun does come up eventually, even after the darkest and longest nights.

TABLE OF CONTENTS

LIST OF TABLES

LIST OF FIGURES

SYMBOLS AND ACRONYMS

Acronym/Symbol	Definition
2-DOG	2-deoxyglucose
%CUM	Cumulative Protein Released
%EE	Entrapment Efficiency
%R	%protein retained after 7d
%REL	%protein release at time, t
a	Path Length
A_{353}	Absorbnace at 353 nm
α-xyl, a-xyl	4-nitrophenyl-α-D-xylopyranoside
ACA	Alkylcyanoacrylate
AF750	AlexaFluor750
APC	Allophycocyanin
ANOVA	Analysis of Variance
ATP	Adenosine triphosphosphate
β-xyl, b-xyl	4-nitrophenyl-β-D-xylopyranoside
BLG	β-lactoglobulin
C14	Carbon-14
CHO	Chinese Hamster Ovary
CLSM	Confocal Laser Scanning Microscopy
CPM	Counts Per Minute
Cyt C	Cytochrome C

ρ	Density
d_H	Hydrodynamic Diameter
D(equation 2-1)	Diffusion Constant
D(equation 2-13)	Pipe Diameter
DMEM	Dulbecco's Minimum Essential Medium
DMSO	Dimethyl Sulfoxide
ε	Extinction Cofficient
EC(s)	Endothelial Cell(s)
EDAC	1-ethyl-(3-dimethyl-aminopropyl) carbodiimide
EDTA	Ethylenediaminetetraacetic Acid
Epox	Epoxomicin
EPR	Enhanced Permeability and Retention Effect
FACS	Fluorescence Activated Cell Sorting, Flow Cytometry
FCS	Fetal Calf Serum
FFR	Fast Field Reversing
FGF	Fibroblast Growth Factor
FITC	Fluorescein Isothiocyanate
FSC	Forward Scattered Light
HBSS	Hank's Balanced Salt Solution
HEPES	4-(2-hydroxymethyl)-1-piperazineethansulfonic acid
HMVEC(s)	Human Microvascular Endothelial Cell(s)
HMW	High Molecular Weight
HSD	Honestly Significant Difference

HSPG(s)	Heparan Sulfate Proteoglycan(s)
hTNF	Human Tumor Necrosis Factor Alpha
ICG	Iodocyanine Green
k(equation 2-1)	Boltzmann's Constant
k(equation 4-2)	Correlation Constant
K_d	Equilibrium Dissociation Constant, Binding Constant
$[L_{Free}]$	Free Ligand Concentration
LDV	Laser Doppler Velocimetry
LMW	Low Molecular Weight
M_{inf}	Total Mass Incorporated, Maximum Possible Release
M_t	Mass Released at time, t
MES	2-(N-morpholino)-ethane sulfonic acid
MF(I)	Median Fluorescence (Index)
MRI	Magnetic Resonance Imaging
MTT	3-(4,5-dimethylthiazol 2-yl)-2,5-diphenyl tetrazolium bromide
μ	viscosity
μ_{AF750}	Mean AlexaFluor 750 Fluorescence with ICG Filter
μ_{PBS}	Mean PBS Fluoresnce with ICG Filter
n	Diffusional Constant for Fickian/Non-Fickian Transport
NHS	N-hydroxysuccinimide
NIBS	Non-Invasive Back Scattering
NIR(F)	Near-Infrared (Fluorescence)
NP(s)	Nanoparticle(s)

N Re, Re	Reynolds Number
PBS	Phosphate Buffered Saline
PCS	Photon Correlation Spectroscopy
PDI	Polydispersity Index
PDTC	Pyrrolidine Dithiocarbamate
PEC(s)	Polyelectrolyte Complex Dispersion(s)
PEG	Polyethylene Glycol
PEO	Polyethylene Oxide
PET	Positron Emission Tomography
pI	Isoelectric Point
PI	Propidium Iodide
PLGA	Poly(lactic-co-glycolic) Acid
PMCG	Poly(methylene-co-guanidide)
PMT	Photomultiplier Tube
PPO	Polypropylene Oxide
PS	Phosphatidylserine
RES	Reticuloendothelial System
$[R_{Free}]$	Free Receptor Concentraiton
[R:L]	Receptor-Ligand Complex, [Bound]
ROI	Region of Interest
$[R_{total}]$	Maximum Number of Receptors
Rxn	Reaction Mixture
SOP	Standard Operating Procedure

SSC	Side Scattered Light
STI	Soybean Trypsin Inhibitor
t	Time
T	Temperature
TB	Trypan Blue
TCEP	Tris(2-carboxyethyl)-phosphine
TEM	Transmission Electron Microscopy
TMRA	Tetramethylrhodamine
TSP	Thrombospondin
U/ml	Units/ml
v	Velocity
VEGF	Vascular Endothelial Growth Factor
ZP	Zeta Potential

CHAPTER I

INTRODUCTION

Nanotechnology and Medicine

Nanotechnology is an area of science devoted to the manipulation of atoms and molecules leading to the assembly of structures in the nanometer (1 to 1000 nm) scale size range. Research in the "nanorealm" began in physics and chemistry in the early 1970's but soon spread into medicine and biology. Specifically, a wide array of nanotechnologies is beginning to change the foundations of disease diagnosis, treatment, and prevention. These advanced innovations, referred to as nanomedicine by the National Institutes of Health[1], have the potential for widespread patient benefits. Because molecules and structures inside cells operate at the nano- and micro-scale, the evolution of nanomedicine as an offshoot of nanotechnology has become a key component for the future of research in medical intervention. A few of the current nanomedical approaches include carbon nanotubes that act as biological mimetics[2], polymeric nanoconstructs for tissue engineering[3,4], and nanoscale microfabrication-based devices[5]. Furthermore, the use of nanoparticulate technologies as targeted forms of diagnostics, drug, and gene delivery is at the forefront of nanomedicine, and it has led to collaborative efforts between disciplines that were typically segregated: engineering and molecular biology, chemistry and virology, physics and surgery.

Drug Development and Limitations in Protein and Peptide Trafficking

In recent years, biotechnology derived drugs including peptides, proteins, and monoclonal antibodies/fragments have become a central focus of pharmaceutical research and developmental efforts[6]. The fate of these drugs after administration in vivo are determined by a combination of several processes: distribution, metabolism, and elimination when given intravenously (systemically) while an local (topical), extravascular dose, is controlled by absorption, distribution, metabolism, and elimination[7].

Bioavailability, the ratio of drug accumulation at its site of action to the amount delivered to the body, is a significant limitation in the use of protein or peptide biologics. Typically, these molecules have a short half-life in blood plasma or other biological fluids, 1.5 min to 150 min for some peptides. Drug distribution among various tissues is equally important. Thus, the use of naked proteins/peptides in vivo has limited utility, necessitating advanced delivery systems which can act locally. The carrier platform should be non-toxic, compatible with the drug applied, preserve its activity, and deliver the payload with reproducible pharmacodynamics. This criteria is especially critical for substances that are labile and sensitive to components in biological fluids[8]. Drug incorporation into delivery systems offers many advantages, particularly the enhancement of the therapeutic potential of many drugs, alteration of pharmacokinetics and biodistribution, and sustained release reservoirs.

Other benefits include:

- in vivo predictability of release rate for optimization of plasma levels and reduction of adverse reactions
- decreased dosing frequency and improved patient compliance
- reduction of systemic drug toxicity[9]
- drug stabilization[10]
- effective accumulation in a target tissue[11]

The development of formulations that can combine these benefits with a low cost, simple design is critical for highly efficient delivery systems.

Nanoplatforms for Targeted Drug Delivery

Nanoparticles (NPs), first observed around 1970, are defined as solid colloidal particles less than 1 μm in size consisting of macromolecular compounds. They were initially devised as carriers for vaccines and anticancer drugs. NPs can be fabricated from a multitude of materials, including synthetic polymers and biopolymers (proteins and polysaccharides). Drug integration of peptide segments, proteins, and/or small molecules with both targeting and therapeutic abilities into delivery systems in the form of nanoparticulate polymer matrices offers many benefits. These benefits include controlled drug release and protection, prolonged blood circulation times, and countless other adjustable characteristics[12,13].

There are numerous engineered constructs, assemblies, architectures, and particulate systems being studied as drug delivery platforms. These include polymeric micelles, dendrimers, virus-derived capsid nanoparticles, polyplexes, and liposomes[14-18].

Incorporation of therapeutic and diagnostic agents can be achieved by encapsulation, covalent attachment, or surface adsorption. Many carriers can be engineered for activation by pH, chemical stimuli, radiation, magnetic fields, or heat. Many systems are being designed for multifuctionality that combine targeted tissue delivery, organelle trafficking, and imaging[19,20]. These nanovehicles do not behave similarly; their behavior within the biological microenvironment, stability, extracellular and cellular distribution varies with their chemical makeup, morphology and size.

The advantages of using nanoparticles for drug delivery result from their two basic properties. First, NPs, due to their small size, penetrate within even small capillaries and are taken up within cells, which allows for efficient drug accumulation at the target sites in the body[21,22]. Second, the use of biodegradable materials for NP preparation allow for the sustained drug release within the target site over a period of days or even weeks after injection[23], establishing many of the concepts described above. Table 1-1 introduces some nanovehicular drug delivery approaches.

Table 1-1. Current drug delivery platforms

NP Platform	Size(nm)	Therapeutic Application
Polymeric	10-1000	Brain tumors[24-26], bone healing[27], vaccine adjuvant[28], restenosis[29, 30], diabetes[31]
Ceramic	<100	Photodynamic[32], insulin delivery[33]
Metallic	<50	Cancer[34, 35], imaging[36]
Polymer Micelle	<100	Solid tumors[37-39], anti-fungal[40]
Liposome	50-100	HIV[41], tumors[42, 43], vaccine delivery[44]
Dendrimer	<10	Bacterial infections[45], cancer[46, 47], HIV treatment[48]

Polymer-based Nanoparticles and Polyelectrolyte Complex Dispersions

Most NP systems, particularly polymer-based, can be formed from a variety of preparation techniques, many of which are derived from potentially toxic components and harmful solvents. The most common methods involve polymerization reactions, such as emulsion, dispersion, and inverse microemulsion polymerization using both biodegradable and non-biodegradable polymers[49]. Some of these polymerization techniques use mineral oils and strong organic solvents, which may remain in the formulation along with other unreacted monomers, initiators, and surfactants, and these present safety issues in the final product. In particular, a widely used polymer for NP systems, polylactide-glycolide co-polymer (PLGA), uses a toxic organic solvent (methylene chloride), which adds regulatory approval problems. Alkylcyanoacrylate (ACA) nanotechnology suffers from toxic breakdown products[50].

One strategy to circumvent these processing limitations has involved the use of water-soluble, biodegradable, polymeric, polyelectrolyte NPs. This technology is a type of NP that has evolved because of the limitations of the currently available systems. Biodegradable polymeric polyelectrolytes degrade at a very slow rate and do not alter normal cell function[51,52]. The polyelectrolytes permit the environmentally attractive use of water as a solvent, a major advantage for products that may be used as drug delivery systems in humans. These nanoparticulate architectures, termed polyelectrolyte complex dispersions (PECs), result from strong electrostatic interactions between charged microdomains of at least two oppositely charged polyelectrolytes[53]. The mixing of solutions of polyanions and polycations leads to the spontaneous formation of insoluble PECs under certain conditions. The formation of PECs are governed by the strength and

location of ionic sites, polymer chain rigidity, precursor chemistries, pH, temperature, ionic strength, mixing intensity, and other controllable factors which will affect the PEC product. Classically, PECs have been applied in gene delivery[54-56] and microencapuslation of various cell and tissue types[57,58].

The most predominant molecular forces for PEC assembly are the strong electrostatic interactions. However, hydrogen bonding, hydrophobic interactions and van der Waals forces complement PEC formation, and they are related to the physical characteristics listed previously[59]. Two major steps dictate PEC complexation: (1) the kinetic diffusion process of mutual entanglement between polymers, occurring at relatively short times, depending on molar size differences, and (2) thermodynamic rearrangement of the already formed simplex aggregate due to conformational changes and disentanglement. The latter process occurs at rather long times leading to a source of instability in the PEC, and it is a consequence of phase separation in aqueous medium. Stop flow measurements showed that the PEC formation takes place in less than 5 ms, nearly corresponding to the diffusion-controlled collision of polyion coils[60].

Three different types of PECs have been prepared in water[61]:

- soluble PEC, i.e. macroscopically homogeneous systems containing small PEC aggregates
- turbid colloidal, PEC systems in the transition range to phase separation exhibiting an observable light scattering or Tyndall effect
- two-phase systems of supernatant liquid and precipitated PEC, which are readily separated as a solid after washing and drying (not desirable).

As borderline cases for the resulting structures of PECs, two models are discussed in literature, dictated by the characteristics of the polyion groups, stoichiometry, and molecular weights: (1) the ladder-like structure, where complex formation takes place on a molecular level via conformational adaptation, and (2) the scrambled-egg model, where a high number of chains are incorporated into particle architecture[60]. The ladder-like structure consists of hydrophilic single-stranded and hydrophobic double-stranded segments. These phenomena result from the mixing of polyelectrolytes having weak ionic groups and large differences in molecular dimensions and can lead to populations of water-soluble and insoluble PECs, an unwanted consequence. The oppositely charged ions complex according to a "zip" mechanism where there is often insufficient ion pairing. In some cases, a high molecular weight polyion with a weak charge density is titrated into a shorter, smaller molecular weight counterion (oligomer) nonstoichiometrically to form initially soluble PECs. Through continued addition of the high molecular weight polyion, insoluble PECs can form[62]. The scrambled-egg model refers to complexes that are the product of the combination of polyions with strong ionic groups and comparable molar masses yielding insoluble and highly aggregated complexes under a strict 1:1 stoichiometry. Figure 1-1 shows, schematically, these representations.

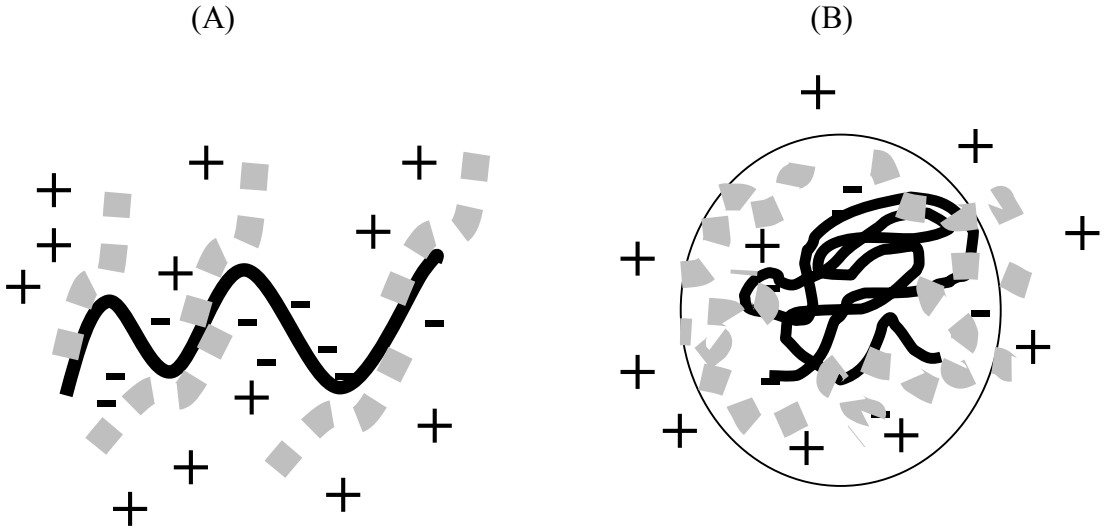

Figure 1-1. Schematic representation of ladder and scrambled egg structures**.** Black represents the large polyion (negative) while gray represents a polyion of opposite charge (positive). (A) shows the ladder representation where insufficient ion pairing occurs under certain stoichiometric conditions leading to macromolecular aggregates, insoluble, and soluble PECs. (B) shows the scrambled egg model where polymers of comparable size complex yielding insoluble PECs under certain conditions.

As the stoichiometry is adjusted under dilute conditions (10^{-4} g/ml), colloidal, Tyndall effect PECs consisting of a neutral and stoichiometric core surrounded by excess binding polyelectrolytes are stabilized against aggregation, and they provide a practical nano-and micro-scale product[53]. The excess polyelectrolyte provides stability in different medium conditions[63], i.e. surplus cation bound to a neutralized anionic core leads to stability at low pH. Both the routes ladder and scrambled egg assemblies share the same steps of polyelectrolyte interaction, but they only result in the desired structures (insoluble stoichiometric complexes) under certain conditions. An important stride

towards functional and practical use of PEC complexes for drug delivery would be assemblies that form under easily understood and controllable conditions such as simple stream mixing in a continuous or batch design.

Nanoparticle/PEC Size and Zeta Potential Drive Cellular Interactions

The size of nanoparticulate or PEC species is critical for cell binding and internalization[64-66]. Due to their sub-cellular and sub-micron size, NPs introduced intravascularly can penetrate deep into tissues through fine capillaries. They are generally taken up by cells and have a higher intracellular uptake compared to microparticles[30]. For example, 100 nm size NPs showed 2.5 fold greater uptake compared to 1 μm particles and they had 6 fold higher uptake compared to 10 μm particles in Caco-2 (human colon) cells[67]. This type of behavior, increased intracellular uptake, has been observed not only in Hepa 1-6, Hep G2, and KLN 205 cell lines, but also in perfused rat tissues[68].

Intracellular uptake studies have mostly focused on liposome[69-71] and polymer delivery systems[27,72,73], process that are driven by endocytosis: a means of cellular ingestion by which the plasma membrane folds inward to bring substances inside cells. The process of endocytosis begins with diffusion of particles to the cell surface and binding either to receptors or via electrostatic interactions between the anionic cell surface and cationic charge domains. Subsequent to the binding, NPs can remain bound to the surface, dissociate, or accumulate in coated or non-coated invaginations. Following this size-dependent event, NPs may be delivered to lysosomes where their contents may be degraded by lysosomal peptidases and hydrolases. Another possible fate

may be nanovehicle fusion with the endosomal membrane and pH-dependent release/degradation of the NP[30,74]. Endocytosis has been shown to be concentration, energy, time, and size dependent, but saturable. Specific mechanisms may include phagocytosis, fluid phase pinocytosis, or receptor-mediated uptake[74] and may be probed by applying various inhibitor strategies[75]. Figure 1-2 schematizes the NP internalization process.

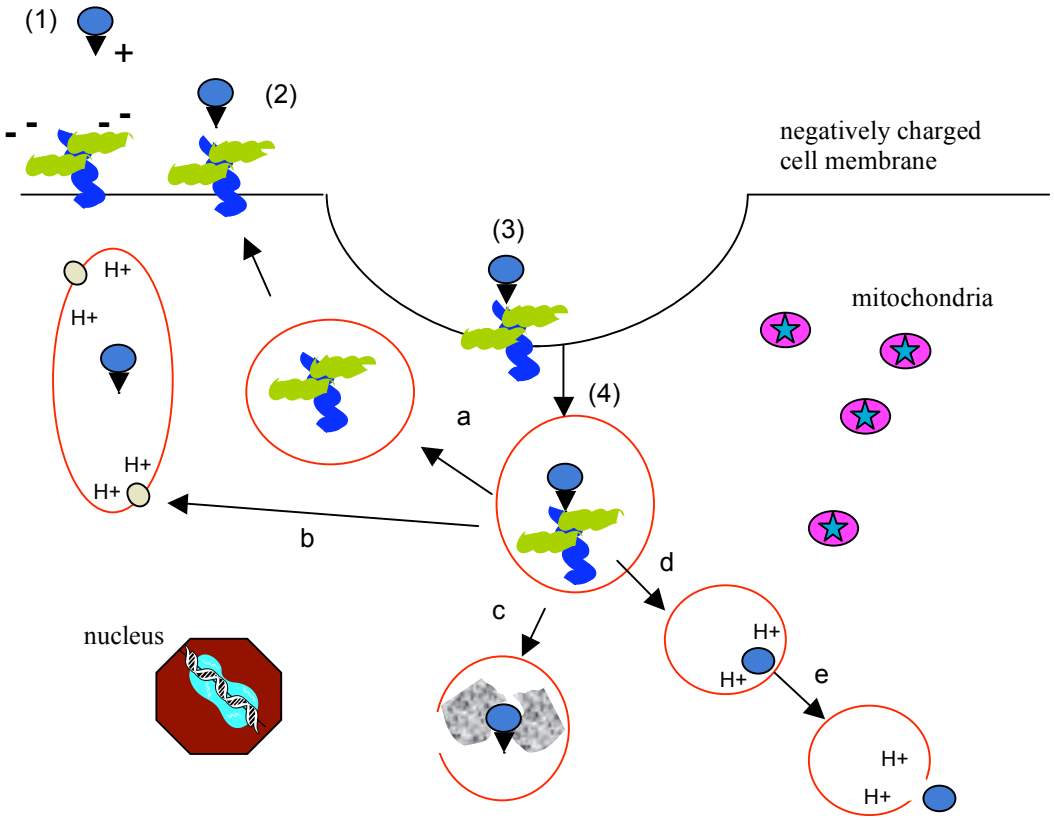

Figure 1-2. Potential fates of PECs. (1) PECs diffuse and (2) attach to the cell surface via receptors or ionic interactions . Upon binding to the membrane, PECs can remain bound at the cell surface, dissociate, or (3) accumulate in coated or non-coated invaginations. Following (4) size-dependent endocytosis, PECs can be delivered to (b) lysosomes, after endosomal acidification, where their contents may be degraded by lysosomal peptidases and hydrolases. Another possibility, following acidification of the endosomal lumen, PECs are designed to either (d) fuse with the endosomal membrane, (e) releasing their contents or escaping directly into the cytoplasm, or become destabilized and subsequently destabilize the endosomal membrane (c) resulting in leakage of the endosomal contents into the cytosol. Receptors may be recycled back to the cell surface (a) or targeted for degradation in the lysosome (b).

Zeta potential, or mean surface charge, is a surrogate marker for the colloidal stability of PECs/NPs[76,77]. The charge develops as a function of the excess polymer and is controlled by an ordered PEC assembly process. Zeta potential is rarely addressed mechanistically in the literature, since it is easily altered by modification of environmental conditions, but it has important connotations for surface modification, size retention/aggregation, and targeting. The classical colloidal theory has long held that one of the major interactive forces that controls particle stability in aqueous liquid suspension is electrostatic forces at the particle surface represented by zeta potential[76-78]. Simply put, the presence of significantly positive or negative surface charge causes charge repulsion and prevents further aggregation by virtue of fewer collisions and ionic attraction. This range of stable zeta potential in aqueous suspension has been empirically defined as greater than $|\pm 30|$ mV[78]. Therefore, it is of great interest for biological systems to have a sufficient zeta potential for preservation of colloidal stability and nano-scale size for drug delivery.

Variation of the surface charge could potentially control binding and direct NPs to cellular compartments both in vivo and in vitro. Cellular surfaces are dominated by negatively charged sulfated proteoglycans, molecules that play pivotal roles in cellular proliferation, migration, and motility[79]. Proteoglycans consist of a core protein anchored to the membrane and linked to one or more glycosaminoglycans side chains (heparan, dermatan, and chondroitin sulfates) to produce a structure that extends away from the cell surface. Glycosaminoglycans are highly anionic, and the interactions between proteoglycans and NP shells, if positively charged, tend to be largely ionic[80]. Once inside

the cell, degradation of polymers may occur, but targeting specific intracellular organelles is possible depending on the surface charge and attached ligands[30].

Specific Modes of Endocytosis

Small molecules, such as amino acids, sugars, and ions, can traverse the plasma membrane through the action of membrane protein pumps or channels. Larger macromolecular species must be carried into the cell in membrane-bound vesicles derived by the invagination and pinching-off of pieces of the plasma membrane. Virtually all cells use endocytosis to take up nutrients from the external environment and modulate the expression of cell surface molecules. Endocytosis occurs through two broad mechanisms which are delineated by the size of the payload: phagocytosis (cell eating) for large particles and pinocytosis (cell drinking) for uptake of fluid and solutes. The specific endocytic modes are phagocytosis, macropinocytosis, clathrin-mediated, caveolin-mediated, and clathrin/caveolin-independent endocytosis[81].

Phagocytosis is conducted primarily by specialized cells, including macrophages, monocytes, and neutrophils, which function to clear pathogens such as bacteria, yeast and large debris usually larger than 1 μm. It is an active and highly regulated process that involves cell-surface receptors and intracellular signaling cascades, followed by actin-controlled engulfment of the particle to be internalized[82]. There are multiple modes of phagocytosis that are determined by the particle to be ingested and the receptor recognition mechanism.

Similar to phagocytosis, macropinocytosis is an actin-driven process that accompanies growth factor and signaling cascades. Membrane protrusions and ruffling result in the formation of macropinosomes. Macropinosomes (~250 nm in diameter) form at the site of ruffling and fuse with the plasma membrane resulting in non-selective endocytosis of solute macromolecules[83].

Caveolae, ~70 nm in diameter, are flask-shaped invaginations of the plasma membrane and are theorized to mediate the transcellular shuttling of serum proteins from or extracellular environment. They are dynamic elements, largely postulated to be regulated by the molecule dynamin, and will fuse with macromolecules after initial binding resulting in a vesicular structure[84]. The size and shape of caveolae are determined by caveolin, a dimeric protein that binds cholesterol, and self-associates to form a striated caveolin coat on the surface of membrane invaginations[81]. Caveolae are activated by tyrosine phosphorylation and slowly internalized.

Clathrin-mediated endocytosis, also dynamin-directed, occurs constitutively in all mammalian cells and carries out the continuous uptake of essential nutrients, such as low density lipoprotein and transferrin; its size limit has been observed to be as high as 120 nm. The process is controlled by high affinity transmembrane receptors and their bound ligands into 'coated pits' on the plasma membrane that are formed by the accumulation of cytosolic coat proteins, the main unit being clathrin. Clathrin monomers assemble into a lattice structure which helps to deform the plasma membrane into a coated pit. The extracellular cargo fuses with the coated pit, an invagination, followed a 'pinching off' of the endocytic vesicle. The process and its components can be recycled by an uncoating reaction after internalization of the payload[85].

The mechanisms that govern caveolae- and clathrin-independent endocytosis remain poorly understood. It is likely that these pathways fulfill unique functions in the cell and varies mechanistically not only in how the vesicles are formed, but in terms of which cargo molecules they transport, to what intracellular destination their cargo is delivered, and how their entry is regulated. These processes are possibly controlled by the formation of lipid rafts, 40-50 nm in diameter, that diffuse freely on the cell surface and can be presumably captured by, and internalized within any endocytic vesicle[86].

Current Polymeric Targeting Strategies and Approach For PECs

Great progress has been made in targeted drug delivery. It is now possible to deliver agents (peptides, nucleotides, hydrophobic drugs) to selected extracellular and intracellular targets[87]. The blood circulatory system is the container and distributor of oxygen and nutrients throughout the body, and thus the normal function of each cell vitally depends on the mechanisms that operate at the level of blood vessels. All blood vessels are lined with endothelial cells, making them accessible to circulatory macromolecules[88]. Strategies have included coupling of surface ligands to liposomal systems[43,89,90] (active targeting) and the enhanced permeability and retention effect (EPR)[91,92] (passive targeting), a unique pathophysiology of the tumor vasculature. Some example systems include dendrimer[47,93], polymeric[94,95], and liposomal[90] nanoparticles conjugated with folate for specificity to cancer cells that overexpress its receptor. Other polymeric nanostructures[96,97], PECs[98], and liposomes[43] target cellular adhesion molecules, integrins, expressed on vascular endothelial cells in solid tumors.

Liposomes[22], PECs[55], and polymer conjugates[97] have utilized vascular endothelial growth factor (VEGF) for targeting the VEGF receptor on the vasculature.

The process of new and remodeled blood vessels, defined as angiogenesis, is a promising targeting strategy due the presence of unique, tissue-specific markers accessible to circulation. These vascular networks are lined with endothelial cells (ECs), critical players in a number of pathological processes: cancer (dysregulated angiogenesis), wound healing, inflammation, oxidative stress, and thrombosis[43,99]. For instance, angiogenesis is critical for tumor metastasis (cancer) to distant tissues and for expansion of small clusters of malignant cells into a clinically relevant tumor. Cancer cells can co-opt host vessels and sprout new vessels from existing ones and recruit EC from bone marrow (vasculogenesis). The resultant vasculature is structurally and functionally abnormal and the endothelial lining has an aberrant morphology. Structural irregularities contribute to temporal and spatial heterogeneity in tumor blood flow. The result is an abnormal tumor microenvironment with endothelial cells unique to the disease state[100]. During angiogenesis, endothelial cells show increased expression of cell surface molecules that potentiate cell invasion and proliferation that can be used as targets for soluble and particulate ligands[101]. Furthermore, the accessibility of these endothelial cells from the blood stream is an important advantage over other target candidates such as tumor cells.

Several extracellular molecules have moieties that interact with the vascular endothelium and have been exploited as an anti-angiogenic strategy. One of these molecules, thrombospondin-1 (TSP-1), is a large, multimeric molecule that associates with cells and the extracellular matrix through multiple interactions that are revealed in

specific domains of the macromolecule[102,103]. Intact TSP-1 suppresses angiogenesis by interaction with the CD36 receptor, leading to apoptosis of endothelial cells, and the collapse of the tumor vasculature[104]. Although, the 450 kDa TSP-1 macromolecule can diminish tumor growth by affecting the vasculature, its use clinical use is limited due to its size, complications in large-scale preparations, and concerns about side effects. Small, TSP-1 derived peptide mimetics that can be targeted to a specific receptor offer an attractive alternative. TSP521, a peptide derived from the type 1 repeat of TSP-1, binds cell surface heparan sulfate proteoglycans (HSPG), which are overexpressed on tumor endothelial cells[105,106]. In addition to HSPG affinity, TSP521 can act as an angiostatic agent by interfering with growth factor binding, translocation and, therefore, cell proliferation. Additionally, TSP521 has shown selective accumulation in the vasculature in experimental brain tumor models[107], leading to its application as a ligand for a PEC targeting strategy. The incorporation of TSP521 into NPs/PECs can be performed by two methods:

- passive entrapment after addition of polyethylene glycol (PEG) to achieve both a geometric and flexible presentation[87], decreased susceptibility to circulatory proteolytic enzymes, improved phamacokinetic properties[108]
- direct coupling by 1-ethyl-3-(3-dimethyl-aminopropyl) carbodiimide (EDAC)/N-hydroxysuccinimide (NHS) two-step, zero-length cross-linking[109] of the aspartic acid carboxylic acid to surface PEC amines.

Both approaches may allow for heparin binding site of TSP521 to interact efficiently with ubiquitous HSPGs present in vascular endothelial models. Figure 1-3 is a representation of the strategy.

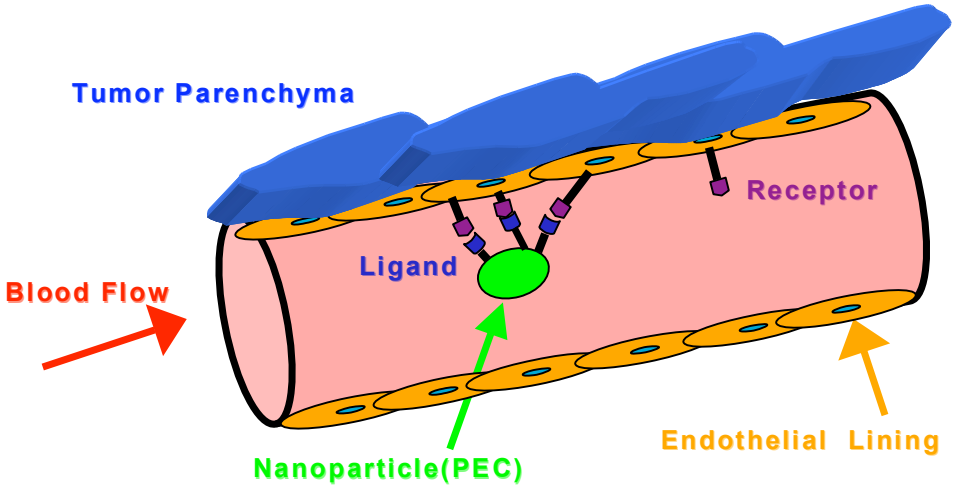

Figure 1-3. Targeted PEC conceptualization**.** PECs can be directed to overexpressed HSPG groups omnipresent on the tumor endothelium by functionalization of the complex with TSP521. Ideally, targeted PECs are administered intravenously and home to the tumor vasculature. PECs, due to their nanoscale architecture, are internalized and the payload (DNA, drug, peptide, protein) delivered.

Binding Theory

The interactions of biological macromolecules, in terms of ligands with cell surface receptors, can often be described by a model of reversible binding and characterized by an equilibrium constant. At equilibrium, the chemical reaction between free receptor (equation 1-1), where $[R_{free}]$, $[L_{free}]$ are the free receptor and ligand, respectively, and [R:L] is the bound, [Bound], receptor:ligand complex:

$$[R_{Free}] + [L_{Free}] \underset{k_{-1}}{\overset{k_1}{\leftrightarrows}} [R:L] \qquad (1\text{-}1)$$

At equilibrium, the mass action expression becomes equation 1-2, where K_d is the equilibrium dissociation constant (binding constant):

$$\frac{[R_{Free}][L_{Free}]}{[Bound]} = \frac{k_{-1}}{k_1} = K_d \tag{1-2}$$

Equation 1-2 can be rewritten, after substitution of $[R_{Free}]$, as equation 1-3, where R_{total} represents the sum of $[R_{Free}]$ and [Bound]:

$$\frac{[R_{Total} - Bound][L_{Free}]}{[Bound]} = \frac{k_{-1}}{k_1} = K_d \tag{1-3}$$

Rearrangement yields a Michaelian expression as shown in equation 1-4, where the brackets are dropped only for convenience:

$$Bound = \frac{R_{total}L_{Free}}{K_d + L_{Free}} \tag{1-4}$$

Equation 1-4 is the equation for a rectangular hyperbola with a horizontal asymptote corresponding to 100% saturation of R_{total}, such that [Bound]=$[R_{total}]$. Experimentally, the relevant parameters are collected with concentration-dependent, saturation binding experiments. The quantitation of physical constants defining classical ligand-receptor interactions must follow assumptions from the law of mass action (Clark's Theory)[110]: (1) the interaction of ligand and receptor is reversible, association is bimolecular while the dissociation is unimolecular; (2) all receptor molecules homogeneous and independent; (3) the biological response is proportional to the number of occupied receptor sites; (4) interaction and response are measured after the reaction has reached equilibrium; and (5) the ligand only exists as free, unbound, or attached to the receptor and it does not undergo degradation or participate in other reactions.

Saturation data that follow these assumptions and equation 1-4 is classically linearized by Scatchard's plots[111]. Scatchard representations plot the ratio bound to free ligand on x-axis versus bound ligand on the abscissa. Linearity of this transformation yields a slope of $-1/K_d$ and y-intercept of R_{total}/K_d. This allows graphical assessment of the parameters in equation 1-4 and relative ligand affinities. Countless studies have applied this analysis for summarizing receptor-ligand interactions, the prominent work being for epidermal growth factor[112,113]. Currently, there are no Scatchard analyses of nanoparticulate drug delivery vehicles, with or without active targeting moieties.

Overview of Dissertation

The work contained herein is focused on the development of nanoparticulate polyelectrolyte complex formulations for targeted delivery to endothelial cells. Recent research to avoid use of harmful materials has involved application of water-soluble, biodegradable, polymeric, polyelectrolyte nanoparticles and the results appear to be promising due to the biocompatibility and complete degradability of polymers[114,115]. Rationalizing the assembly mechanisms and tailoring the size, charge, and loading capability to desirable levels are essential to advance biodegradable, polymeric, polyelectrolyte nanoparticles as efficient drug delivery vehicles. The current technology applied in this study has utilized a water-based approach for producing the PECs under the prevailing assembly and complexation theory. Typically, one interacting pair of oppositely charged polymers does not result in a thermodynamically stable system. Therefore, the PECs are produced using a multipolymeric mixture with a minimum of two pairs. This inherently increases the number of possible reacting pairs. The

electrostatic interaction of the polymer pairs also allows controlled incorporation of molecules such as proteins or targeting peptides. Also, the multipolymeric nature allows more rational selection of polymers to meet specific criteria essential for creating a uniform process for preparing biodegradable, water-based PECs for targeted delivery.

According to the literature, there are several PEC characteristics favorable for cellular uptake and colloidal stability, including hydrodynamic diameter less than or equal to 200 nm[30,54], surface charge of greater than 30 mV or less than –30 mV, spherical morphology, and a low polydispersity index indicative of a homogeneous size distribution[76,78,116]. The PEC properties of size, charge, polydispersity index (PDI), and morphology, are highly dependent on environmental complexation properties and molecular parameters of the polyions used. In particular, the complexation process between polyelectrolytes having significantly different molecular weights leads to the formation of water-insoluble aggregates[117-119]. This effect is undesirable because structures with diameter greater than 1000 nm can cause blockage of blood capillaries and inflammatory tissue responses[30,120,121].

Based on these considerations, the following foci have been investigated and will be addressed in subsequent chapters:

1. Determine the PEC system (similar or dissimilar molecular weights) that will provide the most suitable and controllable product for further in vitro testing. Systems will be examined based on the following qualifications: spherical morphology via TEM, decreased hydrodynamic radius with a goal of 200 nm (good for cellular uptake), low PDI of approximately 0.200, and zeta potential greater than +30 mV or less than -30 mV, the benchmark for colloidal stability.
2. Establish PEC stability as a function of pH for dissimilar and similar molecular weight chemistry by measuring the size and zeta potential during and after processing/centrifugation steps. Systems must be stable at physiological pH (pH=7.4).
3. Evaluate PEC binding and uptake mechanisms for naked and targeted particles using fluorescent labeling in vitro, human microvascular endothelial cells (HMVEC-1) while separately measuring protein release from the polyelectrolyte complex. Compare two methods of TSP521 incorporation: (1) passive PEG-conjugated TSP521 and (2) direct conjugation of TSP521 by EDAC/NHS isopeptide linkage to coronal PEC amines. Demonstrate protein loading and measure release kinetics for proteins carrying acidic and basic isoelectric points. Investigate the biocompatibility in vitro and in vivo. Systems must meet the engineering criteria defined in aim 1 and be stable at biological pH.

4. Assess the scale up ability by applying Kenics static mixer technology under simple two-stream mixing at laminar flow conditions.

References

1. Moghimi, S. M.; Hunter, A. C.; Murray, J. C. "Nanomedicine: current status and future prospects" *Faseb Journal* **2005,** 19, 311-330.

2. Bianco, A.; Kostarelos, K.; Prato, M. "Applications of carbon nanotubes in drug delivery" *Current Opinion In Chemical Biology* **2005,** 9, 674-679.

3. Khademhosseini, A.; Langer, R.; Borenstein, J.; Vacanti, J. P. "Microscale technologies for tissue engineering and biology" *Proceedings Of The National Academy Of Sciences Of The United States Of America* **2006,** 103, 2480-2487.

4. Lavik, E.; Langer, R. "Tissue engineering: current state and perspectives" *Applied Microbiology And Biotechnology* **2004,** 65, 1-8.

5. Catimel, B.; Domagala, T.; Nerrie, M.; Weinstock, J.; White, S.; Abud, H.; Heath, J.; Nice, E. "Recent applications of instrumental biosensors for protein and peptide structure-function studies" *Protein And Peptide Letters* **1999,** 6, 319-340.

6. Tang, L.; Persky, A. M.; Hochhaus, G.; Meibohm, B. "Pharmacokinetic aspects of biotechnology products" *Journal Of Pharmaceutical Sciences* **2004,** 93, 2184-2204.

7. Barratt, G. "Colloidal drug carriers: achievements and perspectives" *Cellular and Molecular Life Sciences* **2003,** 60, 21-37.

8. Baldwin, S. P.; Saltzman, W. M. "Materials for protein delivery in tissue engineering" *Advanced Drug Delivery Reviews* **1998,** 33, 71-86.

9. Herman, E. H.; Zhang, J.; Hasinoff, B. B.; Chadwick, D. P.; Clark, J. R.; Ferrans, V. J. "Comparison of the protective effects against chronic doxorubicin cardiotoxicity and the rates of iron (III) displacement reactions of ICRF-187 and other bisdiketopiperazines" *Cancer Chemotherapy And Pharmacology* **1997,** 40, 400-408.

10. Yokoyama, M.; Fukushima, S.; Uehara, R.; Okamoto, K.; Kataoka, K.; Sakurai, Y.; Okano, T. "Characterization of physical entrapment and chemical conjugation of adriamycin in polymeric micelles and their design for in vivo delivery to a solid tumor" *Journal Of Controlled Release* **1998,** 50, 79-92.

11. Cleland, J. L.; Daugherty, A.; Mrsny, R. "Emerging protein delivery methods" *Current Opinion In Biotechnology* **2001,** 12, 212-219.

12. Taylor, S.; Qu, L. W.; Kitaygorodskiy, A.; Teske, J.; Latour, R. A.; Sun, Y. P. "Synthesis and characterization of peptide-functionalized polymeric nanoparticles" *Biomacromolecules* **2004,** 5, 245-248.

13. Vinogradov, S. V.; Bronich, T. K.; Kabanov, A. V. "Nanosized cationic hydrogels for drug delivery: preparation, properties and interactions with cells" *Advanced Drug Delivery Reviews* **2002,** 54, 135-147.

14. Kramer, M.; Stumbe, J. F.; Grimm, G.; Kaufmann, B.; Kruger, U.; Weber, M.; Haag, R. "Dendritic polyamines: simple access to new materials with defined treelike structures for application in nonviral gene delivery" *Chembiochem* **2004,** 5, 1081-1087.

15. Allen, T. M.; Cullis, P. R. "Drug delivery systems: entering the mainstream" *Science* **2004,** 303, 1818-1822.

16. Haag, R.; Vogtle, F. "Highly branched macromolecules at the interface of chemistry, biology, physics, and medicine" *Angewandte Chemie-International Edition* **2004,** 43, 272-273.

17. Moghimi, S. M.; Hunter, A. C.; Murray, J. C. "Long-circulating and target-specific nanoparticles: Theory to practice" *Pharmacological Reviews* **2001,** 53, 283-318.

18. Verderone, G.; van Craynest, N.; Boussif, O.; Santaella, C.; Bischoff, R.; Kolbe, H. V. J.; Vierling, P. "Lipopolycationic telomers for gene transfer: synthesis and evaluation of their in vitro transfection efficiency" *Journal Of Medicinal Chemistry* **2000,** 43, 1367-1379.

19. Panyam, J.; Zhou, W. Z.; Prabha, S.; Sahoo, S. K.; Labhasetwar, V. "Rapid endo-lysosomal escape of poly(DL-lactide-co-glycolide) nanoparticles: implications for drug and gene delivery" *Faseb Journal* **2002,** 16.

20. Drummond, D. C.; Zignani, M.; Leroux, J. C. "Current status of pH-sensitive liposomes in drug delivery" *Progress In Lipid Research* **2000,** 39, 409-460.

21. Winet, H.; Hollinger, J. O.; Stevanovic, M. "Incorporation of polylactide-polyglycolide in a cortical defect - neoangiogenesis and blood-supply in a bone chamber" *Journal of Orthopaedic Research* **1995,** 13, 679-689.

22. Monsky, W. L.; Fukumura, D.; Gohongi, T.; Ancukiewcz, M.; Weich, H. A.; Torchilin, V. P.; Yuan, F.; Jain, R. K. "Augmentation of transvascular transport of macromolecules and nanoparticles in tumors using vascular endothelial growth factor" *Cancer Research* **1999,** 59, 4129-4135.

23. Guzman, M.; Molpeceres, J.; Garcia, F.; Aberturas, M. R. "Preparation, characterization and in vitro drug release of poly-epsilon-caprolactone and hydroxypropyl methylcellulose phthalate ketoprofen loaded microspheres" *Journal of Microencapsulation* **1996,** 13, 25-39.

24. Kreuter, J.; Ramge, P.; Petrov, V.; Hamm, S.; Gelperina, S. E.; Engelhardt, B.; Alyautdin, R.; von Briesen, H.; Begley, D. J. "Direct evidence that polysorbate-80-coated poly(butylcyanoacrylate) nanoparticles deliver drugs to the CNS via specific mechanisms requiring prior binding of drug to the nanoparticles" *Pharmaceutical Research* **2003,** 20, 409-416.

25. Olivier, J. C.; Fenart, L.; Chauvet, R.; Pariat, C.; Cecchelli, R.; Couet, W. "Indirect evidence that drug brain targeting using polysorbate 80-coated polybutylcyanoacrylate nanoparticles is related to toxicity" *Pharmaceutical Research* **1999,** 16, 1836-1842.

26. Vinogradov, S. V.; Batrakova, E. V.; Kabanov, A. V. "Nanogels for oligonucleotide delivery to the brain" *Bioconjugate Chemistry* **2004,** 15, 50-60.

27. Labhasetwar, V.; Bonadio, J.; Goldstein, S. A.; Levy, J. R. "Gene transfection using biodegradable nanospheres: results in tissue culture and a rat osteotomy model" *Colloids and Surfaces B-Biointerfaces* **1999,** 16, 281-290.

28. Coester, C.; Nayyar, P.; Samuel, J. "In vitro uptake of gelatin nanoparticles by murine dendritic cells and their intracellular localisation" *European Journal Of Pharmaceutics And Biopharmaceutics* **2006,** 62, 306-314.

29. Guzman, L. A.; Labhasetwar, V.; Song, C. X.; Jang, Y. S.; Lincoff, A. M.; Levy, R.; Topol, E. J. "Local intraluminal infusion of biodegradable polymeric nanoparticles - a novel approach for prolonged drug delivery after balloon angioplasty" *Circulation* **1996,** 94, 1441-1448.

30. Panyam, P.; Labhasetwar, V. "Biodegradable nanoparticles for drug and gene delivery to cells and tissue" *Advanced Drug Delivery Reviews* **2003,** 55, 329-347.

31. Watnasirichaikul, S.; Davies, N. M.; Rades, T.; Tucker, I. G. "Preparation of biodegradable insulin nanocapsules from biocompatible microemulsions" *Pharmaceutical Research* **2000,** 17, 684-689.

32. Roy, I.; Ohulchanskyy, T. Y.; Pudavar, H. E.; Bergey, E. J.; Oseroff, A. R.; Morgan, J.; Dougherty, T. J.; Prasad, P. N. "Ceramic-based nanoparticles entrapping water-insoluble photosensitizing anticancer drugs: A novel drug-carrier system for photodynamic therapy" *Journal Of The American Chemical Society* **2003,** 125, 7860-7865.

33. Cherian, A. K.; Rana, A. C.; Jain, S. K. "Self-assembled carbohydrate-stabilized ceramic nanoparticles for the parenteral delivery of insulin" *Drug Development And Industrial Pharmacy* **2000,** 26, 459-463.

34. Bergen, J. M.; Von Recum, H. A.; Goodman, T. T.; Massey, A. P.; Pun, S. H. "Gold nanoparticles as a versatile platform for optimizing physicochemical parameters for targeted drug delivery" *Macromolecular Bioscience* **2006,** 6, 506-516.

35. Wang, S. Z.; Gao, R. M.; Zhou, F. M.; Selke, M. "Nanomaterials and singlet oxygen photosensitizers: potential applications in photodynamic therapy" *Journal Of Materials Chemistry* **2004,** 14, 487-493.

36. Gao, X. H.; Cui, Y. Y.; Levenson, R. M.; Chung, L. W. K.; Nie, S. M. "In vivo cancer targeting and imaging with semiconductor quantum dots" *Nature Biotechnology* **2004,** 22, 969-976.

37. Kataoka, K.; Harada, A.; Nagasaki, Y. "Block copolymer micelles for drug delivery: design, characterization and biological significance" *Advanced Drug Delivery Reviews* **2001,** 47, 113-131.

38. Yamamoto, Y.; Nagasaki, Y.; Kato, Y.; Sugiyama, Y.; Kataoka, K. "Long-circulating poly(ethylene glycol)-poly(D,L-lactide) block copolymer micelles with modulated surface charge" *Journal Of Controlled Release* **2001,** 77, 27-38.

39. Yokoyama, M.; Miyauchi, M.; Yamada, N.; Okano, T.; Sakurai, Y.; Kataoka, K.; Inoue, S. "Characterization and anticancer activity of the micelle-forming polymeric anticancer drug adriamycin-conjugated poly(ethylene glycol)-poly(aspartic acid) block copolymer" *Cancer Research* **1990,** 50, 1693-1700.

40. Yu, F. Q.; Liu, Y. P.; Zhu, R. X. "A novel method for the preparation of core-shell nanoparticles and hollow polymer nanospheres" *Journal of Applied Polymer Science* **2004,** 91, 2594-2600.

41. Kamps, J.; Swart, P. J.; Morselt, H. W. M.; Pauwels, R.; DeBethune, M. P.; DeClercq, E.; Meijer, D. K. F.; Scherphof, G. L. "Preparation and characterization of conjugates of (modified) human serum albumin and liposomes: drug carriers with an intrinsic anti-HIV activity" *Biochimica Et Biophysica Acta-Biomembranes* **1996,** 1278, 183-190.

42. Deverdiere, A. C.; Dubernet, C.; Nemati, F.; Poupon, M. F.; Puisieux, F.; Couvreur, P. "Uptake of doxorubicin from loaded nanoparticles in multidrug-resistant leukemic murine cells" *Cancer Chemotherapy And Pharmacology* **1994,** 33, 504-508.

43. Hallahan, D.; Geng, L.; Qu, S. M.; Scarfone, C.; Giorgio, T.; Donnelly, E.; Gao, X.; Clanton, J. "Integrin-mediated targeting of drug delivery to irradiated tumor blood vessels" *Cancer Cell* **2003,** 3, 63-74.

44. Talsma, S. S.; Babensee, J. E.; Murthy, N.; Williams, I. R. "Development and in vitro validation of a targeted delivery vehicle for DNA vaccines" *Journal Of Controlled Release* **2006,** 112, 271-279.

45. Chen, C. Z. S.; Cooper, S. L. "Interactions between dendrimer biocides and bacterial membranes" *Biomaterials* **2002,** 23, 3359-3368.

46. Kukowska-Latallo, J. F.; Candido, K. A.; Cao, Z. Y.; Nigavekar, S. S.; Majoros, I. J.; Thomas, T. P.; Balogh, L. P.; Khan, M. K.; Baker, J. R. "Nanoparticle targeting of anticancer drug improves therapeutic response in animal model of human epithelial cancer" *Cancer Research* **2005,** 65, 5317-5324.

47. Thomas, T. P.; Majoros, I. J.; Kotlyar, A.; Kukowska-Latallo, J. F.; Bielinska, A.; Myc, A.; Baker, J. R. "Targeting and inhibition of cell growth by an engineered dendritic nanodevice" *Journal Of Medicinal Chemistry* **2005,** 48, 3729-3735.

48. Witvrouw, M.; Fikkert, V.; Pluymers, W.; Matthews, B.; Mardel, K.; Schols, D.; Raff, J.; Debyser, Z.; De Clercq, E.; Holan, G.; Pannecouque, C. "Polyanionic (i.e., polysulfonate) dendrimers can inhibit the replication of human immunodeficiency virus by interfering with both virus adsorption and later steps (reverse transcriptase/integrase) in the virus replicative cycle" *Molecular Pharmacology* **2000,** 58, 1100-1108.

49. Vauthier-Holtzscherer, C.; Benabbou, S.; Spenlehauer, G.; Veillard, M.; Couvreur, P. "Methodology for the preparation of of ultra-dispersed polymer systems" **1991,** 2, 109-116.

50. Cruz, T.; Gaspar, R.; Donato, A.; Lopes, C. "Interaction between polyalkylcyanoacrylate nanoparticles and peritoneal macrophages: MTT metabolism, NBT reduction, and NO production" *Pharmaceutical Research* **1997,** 14, 73-79.

51. Hanafusa, S.; Matsusue, Y.; Yasunaga, T.; Yamamuro, T.; Oka, M.; Shikinami, Y.; Ikada, Y. "Biodegradable plate fixation of rabbit femoral-shaft osteotomies - a comparative-study" *Clinical Orthopaedics and Related Research* **1995,** 315, 262-271.

52. Matsusue, Y.; Hanafusa, S.; Yamamuro, T.; Shikinami, Y.; Ikada, Y. "Tissue reaction of bioabsorbable ultra-high strength poly(L-lactide) rod - a long-term study in rabbits" *Clinical Orthopaedics and Related Research* **1995,** 317, 246-253.

53. Schatz, C.; Lucas, J. M.; Viton, C.; Domard, A.; Pichot, C.; Delair, T. "Formation and properties of positively charged colloids based on polyelectrolyte complexes of biopolymers" *Langmuir* **2004,** 20, 7766-7778.

54. Carlesso, G.; Kozlov, E.; Prokop, A.; Unutmaz, D.; Davidson, J. M. "Nanoparticulate system for efficient gene transfer into refractory cell targets" *Biomacromolecules* **2005,** 6, 1185-1192.

55. Fisher, K. D.; Ulbrich, K.; Subr, V.; Ward, C. M.; Mautner, V.; Blakey, D.; Seymour, L. W. "A versatile system for receptor-mediated gene delivery permits increased entry of DNA into target cells, enhanced delivery to the nucleus and elevated rates of transgene expression" *Gene Therapy* **2000,** 7, 1337-1343.

56. Wolfert, M. A.; Dash, P. R.; Nazarova, O.; Oupicky, D.; Seymour, L. W.; Smart, S.; Strohalm, J.; Ulbrich, K. "Polyelectrolyte vectors for gene delivery: Influence of cationic polymer on biophysical properties of complexes formed with DNA" *Bioconjugate Chemistry* **1999,** 10, 993-1004.

57. Thu, B.; Bruheim, P.; Espevik, T.; Smidsrod, O.; SoonShiong, P.; SkjakBraek, G. "Alginate polycation microcapsules.1. Interaction between alginate and polycation" *Biomaterials* **1996,** 17, 1031-1040.

58. Wang, T.; Lacik, I.; Brissova, M.; Anilkumar, A. V.; Prokop, A.; Hunkeler, D.; Green, R.; Shahrokhi, K.; Powers, A. C. "An encapsulation system for the immunoisolation of pancreatic islets" *Nature Biotechnology* **1997,** 15, 358-362.

59. Dragan, S.; Cristea, M.; Luca, C.; Simionescu, B. C. "Polyelectrolyte complexes.1. synthesis and characterization of some insoluble polyanion-polycation complexes" *Journal of Polymer Science Part a-Polymer Chemistry* **1996,** 34, 3485-3494.

60. Dautzenberg, H. "Light scattering studies on polyelectrolyte complexes" *Macromolecular Symposia* **2000,** 162, 1-21.

61. Webster, L.; Huglin, M. B.; Robb, I. D. "Complex formation between polyelectrolytes in dilute aqueous solution" *Polymer* **1997,** 38, 1373-1380.

62. Kabanov, A. V.; Kabanov, V. A. "DNA complexes with polycations for the delivery of genetic material into cells" *Bioconjugate Chemistry* **1995,** 6, 7-20.

63. Dautzenberg, H.; Kriz, J. "Response of polyelectrolyte complexes to subsequent addition of salts with different cations" *Langmuir* **2003,** 19, 5204-5211.

64. Foged, C.; Brodin, B.; Frokjaer, S.; Sundblad, A. "Particle size and surface charge affect particle uptake by human dendritic cells in an in vitro model" *International Journal Of Pharmaceutics* **2005,** 298, 315-322.

65. Rejman, J.; Oberle, V.; Zuhorn, I. S.; Hoekstra, D. "Size-dependent internalization of particles via the pathways of clathrin-and caveolae-mediated endocytosis" *Biochemical Journal* **2004,** 377, 159-169.

66. Wood, K. C.; Little, S. R.; Langer, R.; Hammond, P. T. "A family of hierarchically self-assembling linear-dendritic hybrid polymers for highly efficient targeted gene delivery" *Angewandte Chemie-International Edition* **2005,** 44, 6704-6708.

67. Desai, M. P.; Labhasetwar, V.; Walter, E.; Levy, R. J.; Amidon, G. L. "The mechanism of uptake of biodegradable microparticles in Caco-2 cells is size dependent" *Pharmaceutical Research* **1997,** 14, 1568-1573.

68. Sahoo, S. K.; Panyam, J.; Prabha, S.; Labhasetwar, V. "Residual polyvinyl alcohol associated with poly (D,L-lactide-co-glycolide) nanoparticles affects their physical properties and cellular uptake" *Journal of Controlled Release* **2002,** 82, 105-114.

69. Salvage, J. P.; Rose, S. F.; Phillips, G. J.; Hanlon, G. W.; Lloyd, A. W.; Ma, I. Y.; Armes, S. P.; Billingham, N. C.; Lewis, A. L. "Novel biocompatible phosphorylcholine-based self-assembled nanoparticles for drug delivery" *Journal Of Controlled Release* **2005,** 104, 259-270.

70. Wang, J. C.; Goh, B. C.; Lu, W. L.; Zhang, Q.; Chang, A.; Liu, X. Y.; Tan, T. M. C.; Lee, H. S. "In vitro cytotoxicity of Stealth liposomes co-encapsulating doxorubicin and verapamil on doxorubicin-resistant tumor cells" *Biological & Pharmaceutical Bulletin* **2005,** 28, 822-828.

71. Gref, R.; Minamitake, Y.; Peracchia, M. T.; Trubetskoy, V.; Torchilin, V.; Langer, R. "Biodegradable long-circulating polymeric nanospheres" *Science* **1994,** 263, 1600-1603.

72. Bulmus, V.; Woodward, M.; Lin, L.; Murthy, N.; Stayton, P.; Hoffman, A. "A new pH-responsive and glutathione-reactive, endosomal membrane-disruptive polymeric carrier for intracellular delivery of biomolecular drugs" *Journal Of Controlled Release* **2003,** 93, 105-120.

73. Davda, J.; Labhasetwar, V. "Characterization of nanoparticle uptake by endothelial cells" *International Journal Of Pharmaceutics* **2002,** 233, 51-59.

74. Panyam, J.; Labhasetwar, V. "Dynamics of endocytosis and exocytosis of poly(D,L-lactide-co-glycolide) nanoparticles in vascular smooth muscle cells" *Pharmaceutical Research* **2003,** 20, 212-220.

75. Huth, U. S.; Schubert, R.; Peschka-Suss, R. "Investigating the uptake and intracellular fate of pH-sensitive liposomes by flow cytometry and spectral bio-imaging" *Journal Of Controlled Release* **2006,** 110, 490-504.

76. Chern, C. S.; Lee, C. K.; Chang, C. J. "Electrostatic interactions between amphoteric latex particles and proteins" *Colloid and Polymer Science* **2004,** 283, 257-264.

77. Trimaille, T.; Pichot, C.; Elaissari, A.; Fessi, H.; Briancon, S.; Delair, T. "Poly(D,L-lactic acid) nanoparticle preparation and colloidal characterization" *Colloid and Polymer Science* **2003,** 281, 1184-1190.

78. Sugrue, S. "Predicting and controlling colloid suspension stability using electrophoretic mobility and particle size measurements" *American Laboratory* **1992,** 24, 64-71.

79. Bernfield, M.; Gotte, M.; Park, P. W.; Reizes, O.; Fitzgerald, M. L.; Lincecum, J.; Zako, M. "Functions of cell surface heparan sulfate proteoglycans" *Annual Review Of Biochemistry* **1999,** 68, 729-777.

80. Mislick, K. A.; Baldeschwieler, J. D. "Evidence for the role of proteoglycans in cation-mediated gene transfer" *Proceedings Of The National Academy Of Sciences Of The United States Of America* **1996,** 93, 12349-12354.

81. Conner, S. D.; Schmid, S. L. "Regulated portals of entry into the cell" *Nature* **2003,** 422, 37-44.

82. Aderem, A.; Underhill, D. M. "Mechanisms of phagocytosis in macrophages" *Annual Review Of Immunology* **1999,** 17, 593-623.

83. Swanson, J. A.; Watts, C. "Macropinocytosis" *Trends In Cell Biology* **1995,** 5, 424-428.

84. Schnitzer, J. E. "Caveolae: from basic trafficking mechanisms to targeting transcytosis for tissue-specific drug and gene delivery in vivo" *Advanced Drug Delivery Reviews* **2001,** 49, 265-280.

85. Mukherjee, S.; Ghosh, R. N.; Maxfield, F. R. "Endocytosis" *Physiological Reviews* **1997,** 77, 759-803.

86. Edidin, M. "Shrinking patches and slippery rafts: scales of domains in the plasma membrane" *Trends In Cell Biology* **2001,** 11, 492-496.

87. Lu, J.; Jeon, E.; Lee, B. S.; Onyuksel, H.; Wang, Z. J. J. "Targeted drug delivery crossing cytoplasmic membranes of intended cells via ligand-grafted sterically stabilized liposomes" *Journal Of Controlled Release* **2006,** 110, 505-513.

88. Simionescu, M.; Gafencu, A.; Antohe, F. "Transcytosis of plasma macromolecules in endothelial cells: a cell biological survey" *Microscopy Research And Technique* **2002,** 57, 269-288.

89. Farokhzad, O. C.; Jon, S. Y.; Khadelmhosseini, A.; Tran, T. N. T.; LaVan, D. A.; Langer, R. "Nanopartide-aptamer bioconjugates: a new approach for targeting prostate cancer cells" *Cancer Research* **2004,** 64, 7668-7672.

90. Gabizon, A.; Horowitz, A. T.; Goren, D.; Tzemach, D.; Mandelbaum-Shavit, F.; Qazen, M. M.; Zalipsky, S. "Targeting folate receptor with folate linked to extremities of poly(ethylene glycol)-grafted liposomes: in vitro studies" *Bioconjugate Chemistry* **1999,** 10, 289-298.

91. Schraa, A. J.; Kok, R. J.; Moorlag, H. E.; Bos, E. J.; Proost, J. H.; Meijer, D. K. F.; de Leu, L.; Molema, G. "Targeting of RGD-modified proteins to tumor vasculature: a pharmacokinetic and cellular distribution study" *International Journal Of Cancer* **2002,** 102, 469-475.

92. Verbaan, F. J.; Oussoren, C.; Snel, C. J.; Crommelin, D. J. A.; Hennink, W. E.; Storm, G. "Steric stabilization of poly(2-(dimethylamino)ethyt methacrytate)-based polyplexes mediates prolonged circulation and tumor targeting in mice" *Journal Of Gene Medicine* **2004,** 6, 64-75.

93. Quintana, A.; Raczka, E.; Piehler, L.; Lee, I.; Myc, A.; Majoros, I.; Patri, A. K.; Thomas, T.; Mule, J.; Baker, J. R. "Design and function of a dendrimer-based therapeutic nanodevice targeted to tumor cells through the folate receptor" *Pharmaceutical Research* **2002,** 19, 1310-1316.

94. Kim, S. H.; Jeong, J. H.; Chun, K. W.; Park, T. G. "Target-specific cellular uptake of PLGA nanoparticles coated with poly(L-lysine)-poly(ethylene glycol)-folate conjugate" *Langmuir* **2005,** 21, 8852-8857.

95. Kim, S. H.; Jeong, J. H.; Joe, C. O.; Park, T. G. "Folate receptor mediated intracellular protein delivery using PLL-PEG-FOL conjugate" *Journal Of Controlled Release* **2005,** 103, 625-634.

96. Suh, W.; Han, S. O.; Yu, L.; Kim, S. W. "An angiogenic, endothelial-cell-targeted polymeric gene carrier" *Molecular Therapy* **2002,** 6, 664-672.

97. Kim, W. J.; Yockman, J. W.; Lee, M.; Jeong, J. H.; Kim, Y. H.; Kim, S. W. "Soluble Flt-1 gene delivery using PEI-g-PEG-RGD conjugate for anti-angiogenesis" *Journal Of Controlled Release* **2005,** 106, 224-234.

98. Park, J. H.; Kwon, S. G.; Nam, J. O.; Park, R. W.; Chung, H.; Seo, S. B.; Kim, I. S.; Kwon, I. C.; Jeong, S. Y. "Self-assembled nanoparticles based on glycol chitosan bearing 5 beta-cholanic acid for RGD peptide delivery" *Journal of Controlled Release* **2004,** 95, 579-588.

99. Hood, J. D.; Bednarski, M.; Frausto, R.; Guccione, S.; Reisfeld, R. A.; Xiang, R.; Cheresh, D. A. "Tumor regression by targeted gene delivery to the neovasculature" *Science* **2002,** 296, 2404-2407.

100. Jain, R. K. "Normalization of tumor vasculature: an emerging concept in antiangiogenic therapy" *Science* **2005,** 307, 58-62.

101. Schiffelers, R. M.; Mixson, A. J.; Ansari, A. M.; Fens, M.; Tang, Q. Q.; Zhou, Q.; Xu, J.; Molema, G.; Lu, P. Y.; Scaria, P. V.; Storm, G.; Woodle, M. C. "Transporting silence: design of carriers for siRNA to angiogenic endothelium" *Journal Of Controlled Release* **2005,** 109, 5-14.

102. Shafiee, A.; Penn, J. S.; Krutzsch, H. C.; Inman, J. K.; Roberts, D. D.; Blake, D. A. "Inhibition of retinal angiogenesis by peptides derived from thrombospondin-1" *Investigative Ophthalmology & Visual Science* **2000,** 41, 2378-2388.

103. Tolsma, S. S.; Volpert, O. V.; Good, D. J.; Frazier, W. A.; Polverini, P. J.; Bouck, N. "Peptides derived from two separate domains of the matrix protein thrombospondin-1 have anti-angiogenic activity" *Journal of Cell Biology* **1993,** 122, 497-511.

104. Reiher, F. K.; Volpert, O. V.; Jimenez, B.; Crawford, S. E.; Dinney, C. P.; Henkin, J.; Haviv, F.; Bouck, N. P.; Campbell, S. C. "Inhibition of tumor growth by systemic treatment with thrombospondin-1 peptide mimetics" *International Journal Of Cancer* **2002,** 98, 682-689.

105. Engelberg, H. "Actions of heparin that may affect the malignant process" *Cancer* **1999,** 85, 257-272.

106. Yu, H. N.; Tyrrell, D.; Cashel, J.; Guo, N. H.; Vogel, T.; Sipes, J. M.; Lam, L.; Fillit, H. M.; Hartman, J.; Mendelovitz, S.; Panel, A.; Roberts, D. D. "Specificities of heparin-binding sites from the amino-terminus and type 1 repeats of thrombospondin-1" *Archives Of Biochemistry And Biophysics* **2000,** 374, 13-23.

107. Bogdanov, A. A.; Marecos, E.; Cheng, H. C.; Chandrasekaran, L.; Krutzsch, H. C.; Roberts, D. D.; Weissleder, R. "Treatment of experimental brain tumors with trombospondin-1 derived peptides: an in vivo imaging study" *Neoplasia* **1999,** 1, 438-445.

108. Harris, J. M.; Chess, R. B. "Effect of pegylation on pharmaceuticals" *Nature Reviews Drug Discovery* **2003,** 2, 214-221.

109. Grabarek, Z.; Gergely, J. "Zero-length crosslinking procedure with the use of active esters" *Analytical Biochemistry* **1990,** 185, 131-135.

110. McLean, F. C. "Applicaiton of the law of chemical equilibrium (law of mass action) to biological problems" *Physiological Reviews* **1938,** 18, 495-523.

111. Scatchard, G. "The attractions of proteins for small molecules and ions" *Annals of the New York Academy of Sciences* **1949,** 51, 660-672.

112. Carpenter, G.; Lembach, K. J.; Morrison, M. M.; Cohen, S. "Characterization of binding of I-125-labeled epidermal growth-factor to human fibroblasts" *Journal Of Biological Chemistry* **1975,** 250, 4297-4304.

113. Wiley, H. S.; Cunningham, D. D. "A steady-state model For analyzing the cellular-binding, internalization and degradation of polypeptide ligands" *Cell* **1981,** 25, 433-440.

114. Alonso, M. J., Nanoparticulate drug carrier technology. In *Microparticulate systems for the delivery of proteins and vaccines*, Cohen, S.; Bernstein, H., Eds. Marcel Dekker: New York, 1998; pp 203-242.

115. Prokop, A.; Kozlov, E.; Carlesso, G.; Davidson, J. M. "Hydrogel-based colloidal polymeric system for protein and drug delivery: physical and chemical characterization, permeability control and applications" *Advances in Polymer Science* **2002,** 160, 119-173.

116. Fatouros, D. G.; Piperoudi, S.; Gortzi, O.; Ioannou, P. V.; Frederik, P.; Antimisiaris, S. G. "Physical stability of sonicated arsonoliposomes: Effect of calcium ions" *Journal of Pharmaceutical Sciences* **2005,** 94, 46-55.

117. Schatz, C.; Domard, A.; Viton, C.; Pichot, C.; Delair, T. "Versatile and efficient formation of colloids of biopolymer-based polyelectrolyte complexes" *Biomacromolecules* **2004,** 5, 1882-1892.

118. Reihs, T.; Muller, M.; Lunkwitz, K. "Preparation and adsorption of refined polyelectrolyte complex nanoparticles" *Journal of Colloid and Interface Science* **2004,** 271, 69-79.

119. Dautzenberg, H. "Polyelectrolyte complex formation in highly aggregating systems. 1. effect of salt: Polyelectrolyte complex formation in the presence of NaCl" *Macromolecules* **1997,** 30, 7810-7815.

120. Debuigne, F.; Cuisenaire, J.; Jeunieau, L.; Masereel, B.; Nagy, J. B. "Synthesis of nimesulide nanoparticles in the microemulsion epikuron/isopropyl myristate/water/n-butanol (or isopropanol)" *Journal of Colloid and Interface Science* **2001,** 243, 90-101.

121. Dev, V.; Eigler, N.; Fishbein, M. C.; Tian, Y. Q.; Hickey, A.; Rechavia, E.; Forrester, J. S.; Litvack, F. "Sustained local drug delivery to the arterial wall via biodegradable microspheres" *Catheterization and Cardiovascular Diagnosis* **1997,** 41, 324-332.

CHAPTER II

EXPERIMENTAL PROCEDURES AND CHARACTERIZATION METHODS

PEC Chemistries

Anionic solutions contain 0.5 mg/ml low molecular weight (LMW) or high molecular weight (HMW) polyions that were dissolved in type I distilled water. The components and their respective molecular weights are listed in Table 2-1. The HMW anionic solution contained HMW sodium alginate, M_r=540 kDa, (Kelco, San Diego, CA) and cellulose sulfate, M_r=1200 kDa, (Janssen Chimica, Geel, Belgium). For LMW formulations, LMW alginate, M_r=12 kDa (FMC Biopolymer, Drammen, Norway) and chondroitin sulfate, M_r=15 kDa, (Sigma Chemical Co., St. Louis, MO) were applied. The cationic solution contained 0.5 mg/ml spermine tetrahydrochloride, M_r=0.348 kDa, (Sigma Chemical Co., St. Louis, MO), poly (methylene-co-guanidine) hydrochloride (PMCG), M_r=5 kDa (Scientific Polymer Producs, Ontario, NY), calcium chloride (Sigma Chemical Co., St. Louis, MO), and 1% m/v Pluronic F-68 (Sigma Chemical Co., St. Louis, MO). All solutions were filtered through 0.22 μm nylon filters (Nalgene, Rochester, NY). With the exception of PMCG and Pluronic F-68, components all were derived from biological systems. PMCG is a synthetic oligomer composed of arginine side chains (guanidinium moieties). Table 2-2 describes the polymeric sources and current applications.

Table 2-1. Components of similar (LMW) and dissimilar (HMW) molecular weight PEC chemistries. PECs are prepared with and without the use of frequency dispergation to determine the effect of polyion molecular weight on efficiency of complexation determined by physicochemical observations. The cationic baths for both LMW and HMW PEC formulations contained 1% m/v Pluronic F-68.

Precursor		Component	MW (Da)
Anion	LMW	LMW Sodium Alginate	12000
		Chondroitin Sulfate	15000
	HMW	HMW, HV Sodium Alginate	540000
		Cellulose Sulfate	1200000
Cation		Spermine Tetrahydrochloride	348
		Poly-[Methylene co-Guanidine] (PMCG)	5000
		Calcium Chloride	111
		Pluronic F-68	8400

Table 2-2. Polyion sources and common uses.

Polymer	Source	Current Application
Sodium Alginate	Algal cell walls	Controlled release and bioadhesive systems[1]
Cellulose Sulfate	Plant-derived	anti-HIV clinical trials[2]
Chondroitin Sulfate	Animal cartilage, ligaments, tendons	Osteoarthritis management[3]
Spermine Tetrahydrochloride	Mammalian sperm	Cancer diagnosis and treatment[4]
Calcium Chloride	Ubiquitous salt in all organisms	Cell and tissue polyelectrolyte maintenance[5]
PMCG	Synthetic	Microencapsulation[6-8]

PEC Fabrication

A batchwise, nonstoichiometric process was used to create the PECs. The solution of two anionic polyions (2 ml) was titrated into a cationic bath (20 ml), containing Pluronic F-68, with or without 20 kHz (maximum) frequency dispergation under conditions of mild mechanical stirring, as described in Figure 2-1, defined as "one batch". The system consisted of a needle (#26 gauge) connected to a 5 ml syringe, which was inserted into an ultrasonic, hollow, titanium probe with a 1.85 mm ID conical tip. The probe was connected to a transducer and power generator (Misonix, Farmingdale, NY). Anionic solution was slowly extruded via controlled air pressure (3 psig) at 1 ml/min. The complexes formed instantaneously[9-11].

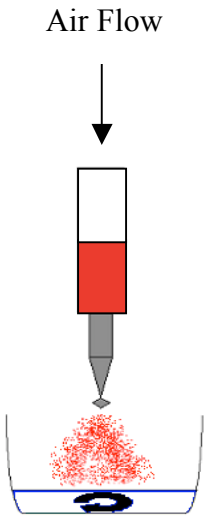

Figure 2-1. PEC fabrication. PECs can be formed instantaneously by extruding 2 ml anionic solution into the 20 ml cationic bath under mild stirring, defined as one batch. An ultrasonic dispergator converts anionic droplets into a fine mist via frequency input (0-20 kHz) where 0 kHz describes a dropwise titration under mechanical stirring.

Colloidal Stability

In preparation for biological study, stability of PEC systems was evaluated by suspending centrifuged preparations into various pH media and measuring their physicochemical response. After preparation of LMW and HMW PECs with and without frequency dispergation, the 22 ml reaction suspension was transferred to 50 ml polypropylene ultracentrifuge tubes (Nalgene, Rochester, NY), the pH was measured (Fisher Accumet, Fairlawn, NJ), and the colloidal suspension was pelleted 3 times at 35000x*g* at 4°C for 10 min (Beckman, Model L5-50, Rotor Type 60 Ti). Subsequent to the first two centrifugations, the pellet was resuspended in 1 mM sodium acetate buffer, pH 4.2. The final centrifugation was followed by dispersion in 10 ml of 1 mM buffer: pH 4.2 and 5.2 (sodium acetate/acetic acid), pH 6.2 (sodium citrate/citric acid), pH 7.2 and 8.2 (Trizma/HCl), or pH 9.2 (carbonate-bicarbonate). Each buffer was prepared in type I distilled water and filtered with a nylon 0.22 μm filter. Subsequent to washings and final preparations, PECs were sonicated using a 1.045 liters (L) water bath in a sonication cylinder (Laboratory Supplies, Model #G1128P1G, Hicksville, NY) for 30 s in 10 s intervals.

Transmission Electron Microscopy (TEM)

Reaction mixture preparations were analyzed for morphology and ZetaSizer validation by pipetting a 20 μl sample volume onto a dry, Formvar coated, 400 mesh copper grid (Electron Microscopy Sciences, Hatfield, PA). The volume was allowed to adsorb onto the grid surface for 30 s, after which the excess liquid was blotted carefully with filter paper. The specimen was then viewed with a Philips CM-12, 120 keV electron

microscope equipped with a CCD camera. PEC diameter was evaluated by using point-to-point pixel based measurements for a minimum of 280 individual observations using software complementary to the TEM CCD camera (Advanced Microscopy Techniques, Danver, MA).

PEC Size and Zeta Potential

Following colloidal preparations, washing and dispersion at varying pH, a 1 ml sample was removed for size and zeta potential measurement with the Malvern ZetaSizer Nano ZS (Malvern Instruments, Worcestershire, UK). Each measurement was performed in triplicate within 24 h of preparation. A 750 μl aliquot was added by micropipettor to a Malvern disposable polystyrene cell (Malvern Instruments, DTS0012, Worcestershire, UK). The cell is inserted into the Malvern ZetaSizer Nano ZS located in the Vanderbilt Institute for Nanoscale Science and Engineering (VINSE). A standard operating procedure (SOP) was set up on the instrument to measure size and charge consecutively in triplicate after a one-minute temperature equilibration time.

The particle-sizing device uses non-invasive back scattering (NIBS) with photon correlation spectroscopy (PCS), which has a particle sensitivity in the range of 0.6 nm to 10 μm. The instrument applies the concept of Brownian motion, the random movement of particles due to the bombardment of surrounding solvent molecules. The Brownian motion of particles inside the measurement cell, based on its size, is directly related to the intensity of light scattered in the area in which the NIBS is applied. The intensity of light, measured by a digital auto correlator, is reflected back and fluctuates over time based on the size of particles. Large particles will have a smaller change in intensity,

while small structures will induce large oscillations. The changes in these oscillations are related to the diameter by a correlation function and the Stokes-Einstein equation (2-1) where k is Boltzmann's constant, D is the diffusion coefficient, T temperature, μ viscosity, and d_H the hydrodynamic radius of the particle.

$$d_H = \frac{kT}{6\pi\mu D} \tag{2-1}$$

Size-related measurements are reported as z-average mean, hydrodynamic diameter, and polydispersity index (PDI). The z-average mean is classically the parameter most comparable to diameters measured by transmission electron microscopy[12]. PDI is a dimensionless number that describes the heterogeneity of the sample, and it is scaled such that values less than 0.05 are rarely seen. The maximum value is 1.000. Values greater than 0.700 indicate a very broad size distribution and a lack of sample homogeneity.

Zeta potential measurements involve laser doppler velocimetry (LDV) and fast field reversing (FFR) to reverse the electrical field, which induces an effective particle electroosmotic flow inside the cell. Eventually the particle will migrate back to its original position and the effective mobility between these two locations is used to calculate the electrophoretic mobility. The electrophoretic mobility is then used to directly calculate the zeta potential of the particles by a proprietary means.

Protein Iodination

Drug loading and release was simulated by radioactively labeling 'dummy' proteins of different charges, adding them to the anionic stream for passive incorporation, and monitoring the release of the protein in biological media. The prototype proteins used

were β-lactoglobulin (BLG), soybean trypsin inhibitor (STI), and cytochrome c (Cyt C). BLG, (Sigma Chemical Co. St. Louis, MO) are proteins with well-established primary, tertiary, and quaternary structures with no biological activity[13-16]. Table 2-3 displays the proteins and their respective molecular weights and isoeletric points. All protocols involving radioactive materials were carried out in Medical Center North (MCN).

Table 2-3. Properties of prototype proteins used for entrapment and release studies.

Protein	Molecular Weight (Da)	Isoelectric Point (pI)
β-lactoglobulin	18362	5.35
soybean trypsin inhibitor	12000	10.8
cytochrome c	21345	4.50

Proteins were labeled with I-125 through the use of IODO-BEADS® iodination reagent/kit (Pierce Biotechnology, Rockford. IL) and gel permeation chromatography. The IODO-BEADS® are N-chloro-benzenesulfonamide (sodium salt) immobilized on nonporous, polystyrene beads. Two beads were washed twice with 100 mM phosphate buffered saline (Invitrogen/Gibco, Carlsbad, CA), pH=7.2 twice. The beads were then transferred to a 1.5 ml microcentrifuge tube (Fisher, Fairlawn, NJ) and 150 µl fresh phosphate buffered saline (PBS) added. To the 10 µl carrier-free isotope solution (1 mCi, Amersham Biosciences, Pittsburgh, PA), 150 µl of PBS was added and the 160 µl pipetted to the separate IODO-BEADS/PBS mixture. The solution, IODO-BEADS and I-125, was incubated 5 min at room temperature. 500 µg of protein was subsequently

mixed and the reaction was allowed to proceed for 15 min. The reaction was stopped by removal of the solution from the microcentrifuge tube. The resultant volume was then eluted with distilled water through a Sephadex G-50 GPC column over 18-20 0.500 ml fractions (Millipore, 2.6 cm ID x 40 cm, Billerica, MA). After the column chromatography, the radioactivity each fraction (2 µl aliquot) was measured using a multi-purpose scintillation/gamma counter (Beckman Coulter LS 6500, Beckman Coulter). Fractions with protein, labeled and unlabeled, appeared after the void volume followed by a peak corresponding to unreacted I-125 (Figure 2-2). The peak containing protein was pooled and assayed for total protein content by the Micro BCA protein assay kit (Pierce Chemical Co., Rockford, IL)**.**

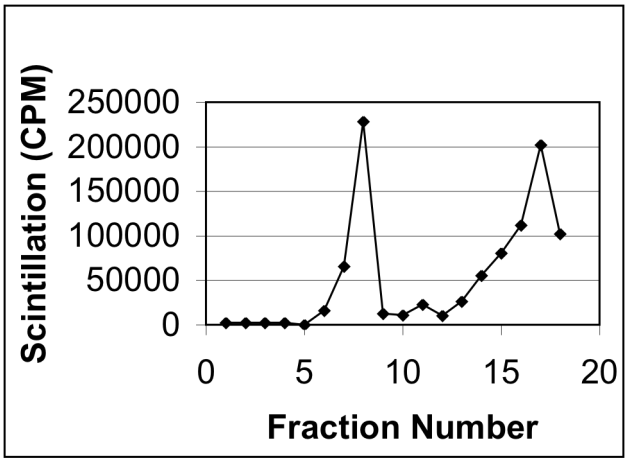

Figure 2-2. Chromatogram for the preparation of iodinated cytochrome c. Ordinate axis represents the radioactivity in terms of counts per minute (CPM).

PEC Protein Loading and Release Monitoring

Protein release and entrapment was monitored by incorporating radioactive, iodinated STI, BLG, or Cyt C into PECs. The PEC system was defined by initial physicochemistry and response to pH. Therefore, the complexes used for these experiments were only formulation(s) that fit specific engineering criteria.

PECs are prepared as described above in *PEC Fabrication* with 15 µg I-125 protein mixed into the standard anionic solution. The radioactivity of each sample accumulated during the course of an experiment was measured by multi-purpose scintillation/gamma counter with an output in terms of counts per minute (CPM). The PECs were isolated by centrifugation three times as outlined in *Colloidal Stability*. Subsequent to each centrifugation, 1 ml of the supernatant was sampled. Following the final centrifugation, supernatant decantment and sampling, the pellet is suspended in 1 ml of 100% fetal calf serum (Invitrogen/Gibco, Carlsbad, CA) to simulate mammalian blood plasma. The suspension was removed, transferred to sterile 1.5 ml microcentrifuge tubes (Fisher, Fairlawn, NJ), added to a rotisserie spinner (Labquake Rotisserie Shaker, Dubuque, IA) and incubated at 37°C, 5% CO_2, and 95% relative humidity**.** Prior to incubation, a 10 µl volume was removed to calculate the protein incorporation efficiency. The entrapment efficiency (%EE) was calculated by equation 2-2. PEC size of this volume was also measured as outlined in *PEC Size and Zeta Potential* after dilution with 750 µl fetal calf serum (FCS).

$$\%EE = \frac{\left(\frac{CPM_{10\mu l} - CPM_{bkg}}{0.010\,ml} \bullet 1ml\right)}{CPM_{15\mu g,initial}} \bullet 100 \qquad (2\text{-}2)$$

Release was assessed every 24 h for seven days by centrifugation at 15000x*g*, 4°C under vacuum and supernatant sampling (1 ml). The PEC pellet is then resuspended in 1 ml fresh fetal calf serum and re-incubated until experiment termination. At the outset of the experiment, 1 ml of FCS was added to the final pellet and the percent retained (%R) was analyzed by equation 2-3.

$$\%R = \frac{CPM_{pellet,t=168h} - CPM_{bkg}}{\left(\frac{CPM_{10\mu l,t=0h} - CPM_{bkg}}{0.010\,ml} \bullet 1ml\right)} \bullet 100 \tag{2-3}$$

The supernatants collected over the seven days can be used to calculate the percent released daily (%REL).

$$\%REL_{t=n} = \frac{CPM_{super,t=n} - CPM_{bkg}}{\left(\frac{CPM_{10\mu l,t=0h} - CPM_{bkg}}{0.010\,ml} \bullet 1ml\right)} \bullet 100 \tag{2-4}$$

The cumulative protein released (%CUM) was represented by equation 2-5.

$$\%CUM = \sum_{n=1}^{7} \%REL_{super} \tag{2-5}$$

Additionally, the radioactivity was proportionally converted to represent protein by mass with equation (2-6). Therefore, the quantities described by equations 2-2, 2-3, 2-4, and 2-5 were plotted against mass vertical axes.

$$\frac{Mass_{sample}}{CPM_{sample}} = \frac{15\mu g_{initial}}{CPM_{15\mu g_{initial}}} \tag{2-6}$$

Polymer Labeling

Two different fluorescent molecules, conjugated to the terminal amine of PMCG, were applied for tracking PEC behavior in vitro and in vivo. Fluorescent conjugates allowed the creation of colored particles and rapid, simple way to quantify cell-associated nanoparticles[17]. Fluorescein isothiocyanate (FITC, Sigma Chemical Co., St. Lous, MO) while AlexaFluor 750 (AF750, Molecular Probes/Invitrogen, Eugene, OR) was utilized for longitudinal, *in vivo* imaging. In both cases, fluorescent fractions were pooled for preparation of fluorescent PECs.

First, the amount of PMCG, adjusted to pH=9.0 with 100 mM NaOH, for a 15:1 FITC/polymer molar ratio was dissolved in the reaction buffer, 10 mM carbonate-bicarbonate, pH=9.0. The FITC powder was then added to a foil-wrapped beaker and allowed to react under stirring for 2 h. After 30 min of mixing, the solution was centrifuged at 15000*x*g for 30 min. The supernatant was removed and separated from unreacted FITC in a Sephadex G-50 GPC column (Millipore, 2.6 cm ID x 40 cm, Billerica, MA) using distilled water as elution solvent. Eighty 0.450 ml fractions are collected in 12x25 borosilicate glass tubes (VWR, Westchester, PA). The FITC labeled polymer is evaluated by measuring the fluorescence intensity of the fractions in a 96-well plate (Nunc, Rochester, NY) at λ_{ex} 485 nm, λ_{em} 530 nm (FL600 Bio-Tek Instruments, Winooski, VT). Again, the first peak that emerged after the void volume corresponded to the fractions of labeled constituent (Figure 2-3).

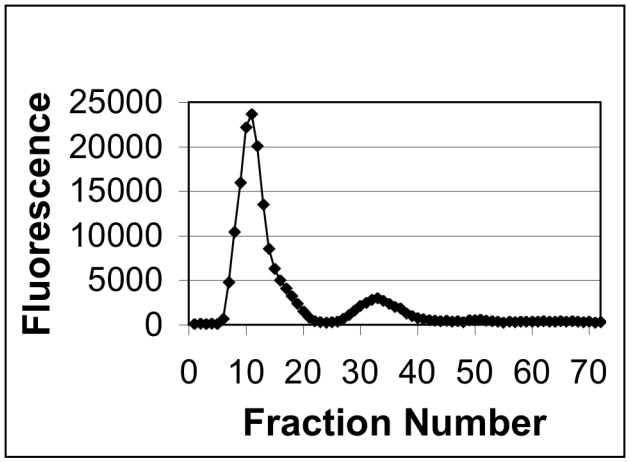

Figure 2-3. Separation of FITC-PMCG from unreacted FITC.

AF750 was conjugated to PMCG in 10 mM carbonate-bicarbonate buffer, pH=9. AF750 was suspended, first, in 100 µl 99% dimethyl sulfoxide (DMSO, Sigma Chemical Co., St. Louis, MO), then added to PMCG in a 200:1 PMCG/AF750 mass ratio with carbonate-bicarbonate buffer in a foil-wrapped beaker, total volume 2 ml. The reaction proceeded, under stirring, for 24 h at room temperature. The mixture is then spun down at 15000*x*g, 30 min. The supernatant was removed and separated from unreacted AF750 in a Sephadex G-50 GPC column (Millipore, 2.6 cm ID x 40 cm, Billerica, MA) using distilled water as elution solvent. Eighty 0.450 ml fractions are collected in 12x25 borosilicate glass tubes (VWR, Westchester, PA). Conjugated and free AF750 peaks were visualized by pipetting a small volume of each fraction to a 96-well plate. The fluorescence was measured with the iodocyanine green (ICG) filter (λ_{ex} 710-760 nm, λ_{em} 810-875 nm) on the Xenogen IVIS 200 Imaging System.

Fluorescent PEC Preparation

Fluorescent PECs were prepared by first adding 250 µl of pooled FITC or AF750 PMCG to the standard cationic solution, outlined in *PEC Chemistries*, under stirring for 30 min, followed by filtration through a nylon 0.22 µm filter. PECs are created as described by *PEC Fabrication*. The complexes were isolated by centrifugation three times as outlined in *Colloidal Stability*. After the final centrifugation and supernatant removal, the pellet was suspended in varied solutions depending on the application. The stability and effect of exchange reactions was evaluated by suspension of fluorescent PECs in physiological solutions (cell growth media and 10 mM HEPES buffer, pH=7.4) and tracking the release in a similar experimental and analytical manner described in *PEC Protein Release Monitoring*. The release of FITC in each buffer was less than 10% over 24 h.

Incorporation of TSP521: Direct Surface Coupling and Passive Entrapment

PEG-conjugated TSP521 (MW~20000 Da), was supplied by the Davidson Lab (VUMC Department of Pathology). TSP521 (Bio-Synthesis, Inc, Lewisville, TX) was synthetically prepared with one terminal cysteine. Upon PEGylation as described by Carlesso[18], TSP521 was dissolved in distilled water and treated with a fresh water solution of 50 mM Tris(2-carboxyethyl)-Phosphine HCl (TCEP, Sigma Chemical Co., St. Louis, MO) for 30 minutes at room temperature, in order to convert the peptide disulfide dimer to reactive monomer. After 30 min, the pH was adjusted to 6.5 and freshly water dissolved PEG-maleimide (provided by Dr. Yasuhiko Iwasaki of the Tokyo Medical & Dental University, Japan) was added in an equimolar ratio. The reaction was allowed to

proceed for 4 h at room temperature. The resulting PEGylated peptides were dialyzed using a Slidealizer Cassette (Pierce Chemical Co., Rockford, IL) with 5 kDa cutoff against four changes of 10 mM Tris-HCl, pH 7.3 at 4°C to remove free peptide. PEGylated TSP521 was incorporated into the PEC by addition of 0.750 mg PEGylated TSP521 to the anionic solution. PECs, fluorescent or standard, were prepared as described in *PEC Fabrication.* The complexes were isolated by centrifugation three times as outlined in *Colloidal Stability*. After the final centrifugation and supernatant removal, the pellet was suspended in varied solutions depending on the application. Additionally the incorporation of PEGylated TSP521 was evaluated by using FITC-labeled TSP521 (Bio-Synthesis, Inc, Lewisville, TX) followed by PEG conjugation. The incorporation efficiency of conjugate was calculated by equation 2-7, where $F_{0,TSP521}$ is the fluorescence of the anionic or cationic stock and $F_{final,TSP521}$ is the fluorescence of the final suspension. The fluorescence intensity of the preparation was measured in a 96-well plate (Nunc, Rochester, NY) at λ_{ex} 485 nm, λ_{em} 530 nm (FL600 Bio-Tek Instruments, Winooski, VT).

$$EE_{TSP\,521}\% = \frac{F_{0,TSP\,521} - F_{final,TSP\,521}}{F_{0,TSP\,521}} \bullet 100 \qquad (2\text{-}7)$$

TSP521 was coupled directly to the PEC surface using 1-ethyl-3-(3-dimethyl-aminopropyl) carbodiimide (EDAC)/N-hydroxysuccinimide (NHS) two-step, zero-length cross-linking. TSP521 only contains one amino acid with a reactive carboxylic acid, aspartate, which allowed for its direct conjugation. One PEC batch, fluorescent or standard, was coupled to 0.100 mg TSP521 by a procedure described by Grabarek and Gergely[19]. The third centrifugation was followed by PEC suspension in 500 µl 100 mM

2-[N-morpholino]-ethane sulfonic acid (MES, Sigma Chemical Co. St. Louis, MO), pH 6.0.

Separately, 100 µg 1 mg/ml TSP521 (Biosynthesis Inc., Lewisville, TX), 100 µl 4 mg/ml 1-ethyl-3-[3-dimethylaminopropyl] carbodiimide hydrochloride (EDAC, Sigma Chemical Co., St. Louis, MO), and 60 µl 4 mg/ml N-hydroxysuccinimide (NHS, Sigma Chemical Co., St. Louis, MO were mixed in a total volume of 500 µl MES buffer, pH=6.0. This step, activation of TSP521, was allowed to react for 30 min at room temperature on a rotisserie spinner (Labquake Rotisserie Shaker, Dubuque, IA). The reaction was terminated by addition of 3 µl 99% β-mercaptoethanol. TSP521/EDAC/NHS was then added to the 500 µl PEC suspension, followed by incubation at room temperature for 2 h. The 1 ml suspension was transferred to 50 ml polypropylene ultracentrifuge tubes (Nalgene, Rochester, NY) and centrifuged once at 35000x*g* at 4°C for 10 min. The supernatant was discarded and pellet suspended in various buffers or biological media. Analogous to the determination of incorporation efficiency of PEGylated TSP521, the effectiveness of direct conjugation was calculated by an identical expression.

Cell Line and Maintenance

The cell line used for these studies is a human microvascular endothelial cell line (HMVEC-1) generously provided by R. Swerlick of Emory University. The cells are maintained in MCDB 131 medium supplemented with 5% FCS (Invitrogen/Gibco, Carlsbad, CA), 20 mM L-Glutamine, 100 U/ml penicillin, 100 µg/ml streptomycin, 500 µg/ml hydrocortisone, 0.001 µg/ml epidermal growth factor (maintenance medium).

During maintenance, the cells are cultured in T-flasks (Corning, Corning, NY) at 33°C, 5% CO_2, and 95% relative humidity. After 3-4 days, cells are detached using 0.25% trypsin/0.1% EDTA, counted by hemacytometer, and resuspended in fresh growth medium.

Confocal Microscopy

FITC-labeled PECs were prepared as described in *Fluorescent PECs*. The PECs were suspended in 20 ml MCDB 131 complete media in preparation for microscopic studies. One day prior to PEC fabrication, confluent cells at approximately day 4 of culture, viability of 90% or greater by trypan blue exclusion, are detached from one T-75 cm^2 parent flask, diluted, and seeded to 8-well microscope slides (Lab-Tek™ II Chamber Slide System, Electron Microscopy Sciences, Hatfield, PA) at 5000 cell/well. Cells are allowed to attach overnight at 37°C, 5% CO_2, and 95% relative humidity in regular maintenance medium. After the 24 h incubation, FITC-PMCG complexes (400 µl/chamber) were added. Cells were allowed to interact with PECs for up to 24 h, followed by aspiration and three washing steps with 4°C PBS. The cultures were then fixed with cold methanol (200 µl) at -20°C for 30 min. The nuclei were stained with TOPRO-3 (Molecular Probes/Invitrogen, Eugene, OR), 150 µl 200 ng/ml, for 10 min. The stain was then removed along with the chambers and mounted with a glass coverslip. Images were then visualized and collected with a 3-track confocal microscope (Zeiss LSM-510, Thornwood, NY) using the appropriate fluorescence filters: λ_{em}=488 nm (FITC), λ_{em}=543 nm (Rhodamine), λ_{em}=633 nm (AlexaFluor 647, Cy-5). A technique called z-sectioning, was applied to determine if PECs localized in the same optical plane

as cells. By varying the distance between the objective pinhole and the specimen over fixed increments, a 'z-series' was generated that dissects and collects images through the specimen.

Flow Cytometric (FACS) Detection of PEC/Cell Interactions

Flow cytometry measures and then analyzes multiple physical characteristics of single particles, usually cells, as they flow in a fluid stream through a beam of light. The properties measured include a particle's relative size, relative granularity or internal complexity, and relative fluorescence intensity. These characteristics are determined using an optical-to-electronic coupling system that records how the cell or particle scatters incident laser light and emits fluorescence.

A typical flow cytometer is made up of 3 systems: fluidics, optics, and electronics. In a flow cytometer, particles or cells are carried to the laser intercept in a fluid stream. Any suspended material from ~0.200 μm to 150 μm in size is suitable for analysis. When particles pass through the laser intercept, they scatter laser light. Any fluorescent molecules present on the particle fluoresce. The scattered and fluorescent light is collected by appropriately positioned lenses. A combination of beam splitters and filters steers the scattered and fluorescent light to the appropriate detectors. The detectors produce electronic signals proportional to the optical signals striking them. Two types of scattered light, in addition to the fluorescence, are analyzed and displayed in Figure 2-4:

- Forward-scattered light (FSC): proportional to cell surface area or size
- Side-scattered light (SSC): proportional to cell granularity or internal complexity.

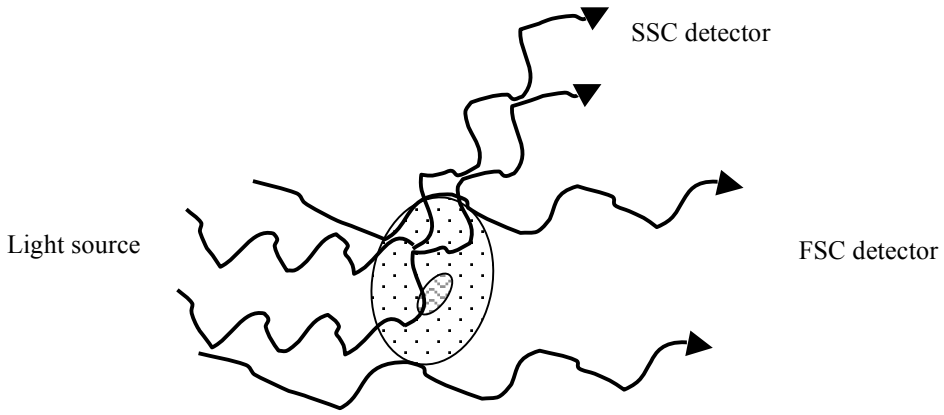

Figure 2-4. Light-scattering properties of a cell. Correlated measurements of FSC and SSC can allow for differentiation of different cell types.

Flow cytometric evalution of cellular interactions with PECs were performed by first, seeding cells to 48-well plates (Nunc, Rochester, NY) 24 h previous to the experiment. Confluent cells at approximately day 4 of culture are detached and counted by hemacytometer from 2 T-75 cm^2 parent flasks. The volumes were combined and volumes equivalent to 50000 cell/well are added to each well. HMVECs were permitted to attach overnight at 37°C, 5% CO_2, and 95% relative humidity in complete MCDB131. Following the ~24 h incubation, experiments were performed by exposing HMVECs to PECs under various concentration and inhibitor schemes (detailed later). At the outset of an experiment, the test media containing PECs was removed and the cultures washed thrice with 4°C PBS. Cells are then detached with 200 µl 0.25% trypsin/0.1% EDTA (2 min) or 5 min exposure to 5 mM EDTA in 4-(2-hydroxyethyl)-1-piperazineethanesulfonic acid (HEPES, Sigma Chemical Co., St. Louis MO), depending on the experiment. The majority of experiments were detached with EDTA as discussed in later chapters. Detachment was terminated by the addition of FACS buffer (3% FCS

in PBS). The detachment was followed by cell suspension transfer to 4 ml FACS tubes (BD Falcon, San Jose, CA) and centrifugation at 200*x*g for 10 min. The supernatant was removed and cells suspended in 200 μl FACS buffer. The tubes were kept on ice until arrival at the FACS instrumentation. Excitation of samples was performed with a 15 mW 488 nm (λ_{ex} 485 nm) argon ion laser and detected with either λ_{em} =515-545 nm (FITC) or λ_{em} =564-606 nm filters.

A standard experiment included acquisition of HMVECs in the absence of PECs to establish a background. The samples exposed to PECs were then acquired. SSC, FSC, and FITC outputs were collected in list mode form and analyzed with FloJo (Treestar, Inc., Ashland, OR). The first round of acquisition yielded the total amount of cell-associated fluorescence (MF_{total}), due to FITC PECs. MF also represents the median fluorescent index (MFI). The internalized fluorescence was determined by adding 120 μl 0.4 mg/ml trypan blue (TB, Mediatech, Herndon, VA) and re-acquiring the sample to give MF_{inside}. TB quenches extracellular FITC[20-22], giving the opportunity to evaluate the cellular compartmentalization of PECs (equation 2-8):

$$MF_{total} = MF_{surface} + MF_{inside} \tag{2-8}$$

Saturation PEC-Cell Association Kinetics

Fluorescent PECs were prepared as described above and suspended in 20 ml complete MCDB 131. Cell exposure, in 48-well plates, to 400 μl PECs was monitored for t=0, 5, 10, 15, 20, 30, 60, and 120 min. The 2 h incubation was followed by aspiration, washing, detachment, centrifugation, and addition of FACS buffer. Flow

cytometric measurements, minimally 10000 events, with and without TB were performed within 30 minutes using a 4-color FACSCalibur (BD Biosciences, Mountain View, CA)

PEC Acute Toxicity by Propidium Iodide (PI)

Acute toxicity of fluorescent PECs was detected by propidium iodide (PI, Molecular Probes/Invitrogen, Eugene, OR) as described by Rasola, and Geuna[23]. Cells were exposed to PECs as described in *Saturation PEC Cell Association Kinetics*, detached after 2 h PEC exposure using 0.25% trypsin/0.1% EDTA, centrifuged and resuspended in 200 μl FACS buffer. PI, 40 μl 0.01 mg/ml, was added to each sample 1 min prior to FACS acquisition. The cytometer applied was the 4-color FACSCalibur (BD Biosciences, Mountain View, CA) cytometer. For each sample, 10000 events were collected. The PI fluorescence was collected through a λ_{em} =564-606 nm filter after excitation of the fluorochrome at 488 nm (λ_{em}). The toxicity was represented as percent control, control being cultures without PECs.

Treatment of Cells with Various Inhibitors

HMVEC-1 cells were prepared as described above. At the end of the exposure, cells were washed, detached and analyzed by flow cytometry (see above). Inhibition strategies include extracellular heparin, reduced temperature (thermodynamics), 2-deoxyglucose/azide (metabolism), cytochalasin D (actin filaments), HSPG biosynthetic effects (4-nitrophenyl xylopyranoside), and surface receptor proteolysis (trypsin). Fluorescent PEC concentrations were one batch suspended in 20 ml MCDB 131 complete media. Wells received 400 μl PECs in media or media alone. In each case, at least one

well was maintained at normal cell culture conditions. Inhibitors were applied for 30 minutes at standard incubatory conditions (37°C, 5% CO_2, and 95% relative humidity), unless otherwise indicated previous to detachment by 5 mM EDTA. Flow cytometric measurements with and without TB were performed within 30 minutes using a 4-color FACSCalibur (BD Biosciences, Mountain View, CA) cytometer. For each sample, 10000 events were collected. Inhibitors did not elicit any cellular toxicity as defined by PI measurements.

To evaluate the effect of free glycosaminoglycans[24,25] on PEC association, two hours previous to PEC exposure, cultures were pre-incubated with 200 U/ml USP grade heparin (Celsus Laboratories, Cincinnati, OH) followed by a PBS wash, and a cocktail of 200 U/ml heparin, particle concentration indicated above, and growth media.

Energy dependence was assessed by 2-deoxyglucose/sodium azide[26] and reduced temperature (4°C)[27]. For temperature effects, HMVECs were pre-incubated in a refrigerator at 4°C for 1 h in complete MCDB 131. The media was then removed and PECs added followed by refrigeration. 50 mM 2-deoxyglucose (2-DOG, Sigma Chemical Co., St. Louis, MO) and 0.05% v/v sodium azide (Sigma Chemical Co., St. Louis, MO) was prepared in complete media and added to HMVEC-1 cultures 1 h previous to PEC exposure. PECs and 2-DOG/azide were then pipetted to the plate after aspiration of pre-incubatory media.

The effect of actin on PEC association was evaluated by exposure to 10 μM cytochalasin D[28,29] (Sigma Chemical Co., St. Louis, MO). Cell pre-incubation prior to PEC/cytochalasin D treatment elapsed 2 h. Cells were then treated with PECs for the time period indicated above.

24 hours after HMVEC-1 seeding to 48 well plates, cells are washed and exposed to 500 μM 4-nitrophenyl-α-xylopyranoside (α-xyl) or 4-nitrophenyl-β-xylopyranoside (β-xyl) overnight to elucidate the role of HSPG in PEC association. β-xyl at μM-mM concentrations has been found to suppress proteoglycan biosynthesis while α-xyl does not[30,31]. The overnight exposure to α-xyl or β-xyl was followed by exposure to PEC. Comparison of these two xylopyranoside isomers provided the appropriate controls.

Tryptic cleavage of PEC association was measured by detaching cells with 0.25% trypsin/0.1% EDTA and comparison to 5 mmol/l EDTA monolayer removal. PECs were added to culture for the time period indicated above. Subsequent to the washings, HMVECs are removed with either trypsin or EDTA.

Particle Counting

Particle concentration, in terms of PEC/ml, was determined by flow cytometry (FACS Aria, BD Biosciences). The FACSAria was fitted with SSC, FITC, and FSC detection lasers. In particular, the FSC laser was adapted with a photomultiplier tube to magnify the signal generated from PEC size. Firefli™ 200 nm fluorescent green (ex 468/em 530 nm) polystyrene microspheres (Duke Scientific Corporation, Palo Alto, CA) of known concentration were processed and detected using forward and side scatter lasers. The number of events recorded over fixed period of time (60s) was used to develop a standard calibration curve. This calibration curve was then used to evaluate PEC recorded events and thus concentration over four logs of arbitrary dilution for one batch of fluorescent PECs. The populations of PECs were analyzed for fluorescence by FACSDiva software (BD Biosciences, Mountain View, CA) to normalize fluorescence

units in terms of PEC/ml. Free and bound particle concentrations are defined based on ordinary linear interpretation and proportionality. Resultant PEC concentrations for direct association and inhibitor experiments were determined to be $1.54x10^9$ PEC/ml. In each case, media and cell fluorescent backgrounds were established.

PEC Effects on HMVEC-1 Proliferation

One day before PEC exposure, cells are plated to 48 well plates at a density of 25000 cell/well, successive to detachment of 2 T-75 cm^2 flasks at day 4 culture. After an ~20 h attachment and acclamation period, cells were exposed to serial dilutions of non-targeted and targeted PECs (PEGylated and EDAC/NHS coupled TSP521) for 72 h without media change. Subsequent to the 72 h exposure, media for all wells were removed and HMVEC-1 cell growth was measured using the Titer 96® Aqueous One Solution Cell Proliferation Assay (Promega, Madison, WI, USA). Each well then received 300 μl fresh MCDB 131, followed by 20 μl of dye solution, 3-(4,5-Dimethylthiazol-2-yl)-2,5-diphenyltetrazolium bromide (MTT). Incubation for 40 min at 37°C, 5% CO_2, 95% relative humidity ensued. Absorbance at 490 nm was determined by microplate reader (μQuant, Bio-Tek Instruments, Winooski, VT). All results were normalized to the control (no PECs).

Scatchard Plots

Scatchard titrations were prepared by exposing HMVEC-1 cells to serial dilutions of targeted, PEGylated and EDAC/NHS ligated TSP521, and non-targeted PEC for 3 hours at normal incubatory conditions. One day previous, 50000 cells/well were seeded

and incubated at 37°C, 5% CO_2, 95% relative humidity after detachment of 2 T-75 cm^2 flasks at approximately day 4 of culture. Separate plates were incubated at 4°C to shut down the endocytosis of PECs[32]. The exposure was followed by detachment and acquisition of MFI by FACSAria (BD Biosciences, Mountain View, CA). For each sample, 10000 events were collected by list-mode data that consisted of side scatter, forward scatter, and fluorescence emission centered at 530 nm (FITC). Bound median fluorescence indices (MFI) were determined using FACSDiva software. Free, unbound median fluorescence indices were evaluated by mass balance. These values were then converted to PEC concentration. Scatchard plots were prepared by plotting bound PEC/free PEC versus bound PEC as described classically[33].

In Vivo Imaging

Non-invasive, longitudinal, whole animal imaging of mice was performed with AF750-PMCG fluorescent PECs. Animals procedures, performed in VUMC, followed the Vanderbilt University Institutional Care and Use Committee. Male BALBc, approximately 4-6 weeks of age, were obtained from Charles River Laboratories (Cambridge, MA). Prior to injection, animals were shaved and anaesthetized. Retro-orbital injections were then administered: 100 μl AF750-PMCG PECs suspended in 1 ml 5 mM HEPES, pH=7.6 (one batch). Animals were imaged immediately after injections, 3 h, 6 h, 24 h, and 48 h with the IVIS 200 small animal imaging system fitted with an ICG filter (λ_{ex} 710-760 nm, λ_{em} 810-875 nm). Each time point was followed by animal sacrifice by cervical dislocation and organ extraction. Individual organs (bladder, kidneys, heart, lungs, liver, spleen) were transferred to 6 well plates (Nunc, Rochester,

NY) and imaged. The fluorescence of each well was extracted using the Living Image software package integrated with IgorPro 5 (Wavemetrics, Lake Oswego, OR) in terms of pixel flux.

Histology

Following animal euthanasia, sections of animal organs were prepared for delivery to the VUMC Immunohistochemistry Core (IHC). All organs were fixed overnight on 10% buffered neutral formalin. Tissue paraffin blocks were made by embedding the tissue in melted paraffin. Paraffin-tissue section were cut and mounted onto the glass slides. Sections were deparaffinized and stained with hematoxylin and eosine for staining nuclei and cytoplasmic components, respectively. Slides were then examined using an upright light microscope (Olympus BX50, Olympus, Center Valley, PA) and documented using QCapture Software (QImaging, Barnaby, BC, Canada).

Process Scale Up with Kenics Static Mixer

To evaluate the scale up ability of the PEC production process, Kenics static mixer technology was applied because it has the potential to yield large product titers as opposed to small batch volumes. The particles are created by simple stream mixing over alternating right and left hand elements. Static mixers are tubular reactors and are advantageous because they can offer high residence times, liquid phase plug flow at low Reynolds Numbers, and are adaptable to aseptic processing. These types of mixer arrays have been suggested as an alternative to traditional stirred tank reactors and preliminary evidence has been found that the static mixer can hold promise for the synthesis of

pharmaceuticals[34]. The Kenics mixer applied herein was 6.35 mm I.D., 21 cm in length, and made of stainless steel (Chemineer, North Andover, MA). Polyionic solutions were prepared as described in *PEC Chemistries* and complexed using the same stoichiometry. Solutions were pumped from reservoirs through 16 gauge polypropylene tubing (Cole Parmer, Vernon Hill, IL) using a peristaltic pump (Cole Parmer, Vernon Hills, IL). The flow rate ratios (ml/min), cation to anion, included 200:20, 160:16, 120:12, and 90:9. Aqueous particle suspensions were allowed to accumulate for 30 s in a 250 ml glass beaker (Kimble, Vineland, NJ) under moderate stirring. The process was repeated for each ratio of flows and at the outset of 30 s, a 1 ml sample is removed for size and zeta potential measurement with the Malvern ZetaSizer Nano ZS and physciochemical properties as described in *PEC Size and Zeta Potential*.

Qualitative Assessment of Static Mixer Efficiency

The mixing efficiency of the Kenics static mixer was evalulated by a parallel competing reaction scheme at various Reynolds numbers representative cation to anion stoichiometries encountered during continuous LMW and HMW PEC production. The two competing reactions, established by Fournier[35] and further applied by Fang and Lee[36], are borate neutralization and the Dushman reaction, both of which compete for hydrogen ions. Equations 2-9, 2-10, and 2-11 describe the system:

$$H_2BO_3^- + H^+ \longleftrightarrow H_3BO_3 \qquad (2\text{-}9)$$

$$5I^- + IO_3^- + 6H^+ \longleftrightarrow 3I_2 + 3H_2O \qquad (2\text{-}10)$$

$$I^- + I_2 \longleftrightarrow I_3 \qquad (2\text{-}11)$$

The amount of iodine produced depends on the efficiency of the mixer when acid is the limiting reagent. If the mixing efficiency is high, then the H^+ ions would be dissipated through 2-9, a quasi-instantaneous reaction, and no iodine would form. On the other hand, if the mixing efficiency is low, most of the injected protons would be consumed by reactions 2-10 and 2-11, orders of magnitude slower reactions than 2-9. The iodine, upon formation, goes to tri-iodide, which can be detected spectrophotometrically. The bulk solution, a mixture of $H_2BO_3/IO_3^-/I^-$, will mimic the cation while the anion will be H^+ in the form of low concentration sulfuric acid. These conditions will simulate the limiting/excess reactant conditions applied in the PEC production process.

The $H_2BO_3/IO_3^-/I$ solution was prepared by dissolution of 0.75 g H_3BO_3 in 700 ml water using a 1 L beaker. The pH was then adjusted to 9.14 with NaOH. This ensured equimolar concentrations of $H_2BO_3^-$ and H_3BO_3. In a separate beaker, 0.500 g KIO_3 and 1.93 g KI were freshly dissolved in 100 ml water. The two solutions were then combined and final volume diluted to 1 L with approximately 200 ml water. 0.005 M H_2SO_4 was used as the acid source. All chemicals were purchased from Sigma Chemical Co.

Solutions were pumped from reservoirs through 16 gauge polypropylene tubing using a peristaltic pump. The flow rate ratios (ml/min), $H_2BO_3/IO_3^-/I$ to H_2SO_4 included 200:20, 160:16, 120:12, and 90:9. Reynolds numbers were calculated by equation 2-12:

$$\mathrm{Re} = \frac{\rho V D}{\mu} \qquad (2\text{-}13)$$

where v was velocity of fluids through the mixer (m/s) and D the diameter (m). ρ (g/m^3) and μ ($g\ m^{-1}s^{-1}$) were the density and viscosity of water at room temperature.

Aqueous particle suspensions were allowed to accumulate for 20 s in a 250 ml glass beaker (Kimble Vineland, NJ) under moderate stirring. A 200 μl volume of effluent was removed and the absorbance measured at 353 nm using a microplate reader (μQuant, Bio-Tek Instruments, Winooski, VT). The concentration of tri-iodide ion was calculated by equation 2-12 (Beer's Law):

$$[I_3] = \frac{A_{353}}{\varepsilon a} \tag{2-13}$$

with an ε equal to 26.06 L $mmol^{-1}cm^{-1}$ and a, the path length, of 0.646 cm as defined by Guichardon and Falk[37].

References

1. Johnson, F. A.; Craig, D. Q. M.; Mercer, A. D. "Characterization of the block structure and molecular weight of sodium alginates" *Journal of Pharmacy and Pharmacology* **1997,** 49, 639-643.

2. Neurath, A. R.; Strick, N.; Li, Y. Y. "Anti-HIV-1 activity of anionic polymers: a comparative study of candidate microbicides" *Bmc Infectious Diseases* **2002,** 2, 27-37.

3. Echard, B. W.; Talpur, N. A.; Funk, K. A.; Bagchi, D.; Preuss, H. G. "Effects of oral glucosamine and chondroitin sulfate alone and in combination on the metabolism of SHR and SD rats" *Molecular and Cellular Biochemistry* **2001,** 225, 85-91.

4. Bachrach, U. "Polyamines and cancer: Minireview article" *Amino Acids* **2004,** 26, 307-309.

5. Loret, B.; Simoes, F. M. F. "Mechanical effects of ionic replacements in articular cartilage. Part I: The constitutive model" *Biomechanics And Modeling In Mechanobiology* **2005,** 4, 63-80.

6. Muller, M.; Brissova, M.; Rieser, T.; Powers, A. C.; Lunkwitz, K. "Deposition and properties of polyelectrolyte multilayers studied by ATR-FTIR spectroscopy" *Materials Science & Engineering C-Biomimetic And Supramolecular Systems* **1999,** 8-9, 163-169.

7. Lacik, I.; Brissova, M.; Anilkumar, A. V.; Powers, A. C.; Wang, T. "New capsule with tailored properties for the encapsulation of living cells" *Journal Of Biomedical Materials Research* **1998,** 39, 52-60.

8. Wang, T.; Lacik, I.; Brissova, M.; Anilkumar, A. V.; Prokop, A.; Hunkeler, D.; Green, R.; Shahrokhi, K.; Powers, A. C. "An encapsulation system for the immunoisolation of pancreatic islets" *Nature Biotechnology* **1997,** 15, 358-362.

9. Carlesso, G.; Kozlov, E.; Prokop, A.; Unutmaz, D.; Davidson, J. M. "Nanoparticulate system for efficient gene transfer into refractory cell targets" *Biomacromolecules* **2005,** 6, 1185-1192.

10. Prokop, A.; Holland, C. A.; Kozlov, E.; Moore, B.; Tanner, R. D. "Water-based nanoparticulate polymeric system for protein delivery" *Biotechnology and Bioengineering* **2001,** 75, 228-232.

11. Prokop, A.; Kozlov, E.; Carlesso, G.; Davidson, J. M. "Hydrogel-based colloidal polymeric system for protein and drug delivery: Physical and chemical characterization, permeability control and applications" *Advances in Polymer Science* **2002,** 160, 119-173.

12. Ito, T.; Sun, L.; Bevan, M. A.; Crooks, R. M. "Comparison of nanoparticle size and electrophoretic mobility measurements using a carbon-nanotube-based coulter counter, dynamic light scattering, transmission electron microscopy, and phase analysis light scattering" *Langmuir* **2004,** 20, 6940-6945.

13. Bacchin, P. "A possible link between critical and limiting flux for colloidal systems: consideration of critical deposit formation along a membrane" *Journal of Membrane Science* **2004,** 228, 237-241.

14. Burova, T. V.; Grinberg, N. V.; Visschers, R. W.; Grinberg, V. Y.; de Kruif, C. G. "Thermodynamic stability of porcine beta-lactoglobulin - A structural relevance" *European Journal of Biochemistry* **2002,** 269, 3958-3968.

15. Croguennec, T.; Molle, D.; Mehra, R.; Bouhallab, S. "Spectroscopic characterization of heat-induced nonnative beta-lactoglobulin monomers" *Protein Science* **2004,** 13, 1340-1346.

16. Patrickios, C. S.; Yamasaki, E. N. "Polypeptide amino-acid-composition and isoelectric point.2. comparison between experiment and theory" *Analytical Biochemistry* **1995,** 231, 82-91.

17. Huang, M.; Ma, Z. S.; Khor, E.; Lim, L. Y. "Uptake of FITC-chitosan nanoparticles by a549 cells" *Pharmaceutical Research* **2002,** 19, 1488-1494.

18. Carlesso, G.; Hartig, S. M.; Higginbotham, J. N.; Kozlov, E. A.; Roberts, D. D.; Prokop, A.; Davidson, J. M. "Enhancement of binding and gene delivery to endothelial cells by targeted nanoparticulate polyelectrolyte complexes" **2006,** In Preparation.

19. Grabarek, Z.; Gergely, J. "Zero-Length Crosslinking Procedure With The Use Of Active Esters" *Analytical Biochemistry* **1990,** 185, 131-135.

20. Nuutila, J.; Lilius, E. M. "Flow cytometric quantitative determination of ingestion by phagocytes needs the distinguishing of overlapping populations of binding and ingesting cells" *Cytometry Part A* **2005,** 65A, 93-102.

21. Rejman, J.; Oberle, V.; Zuhorn, I. S.; Hoekstra, D. "Size-dependent internalization of particles via the pathways of clathrin-and caveolae-mediated endocytosis" *Biochemical Journal* **2004,** 377, 159-169.

22. Vanamersfoort, E. S.; Vanstrijp, J. A. G. "Evaluation of a flow cytometric fluorescence quenching assay of phagocytosis of sensitized sheep erythrocytes by polymorphonuclear leukocytes" *Cytometry* **1994,** 17, 294-301.

23. Rasola, A.; Geuna, M. "A flow cytometry assay simultaneously detects independent apoptotic parameters" *Cytometry* **2001,** 45, 151-157.

24. Mislick, K. A.; Baldeschwieler, J. D. "Evidence for the role of proteoglycans in cation-mediated gene transfer" *Proceedings Of The National Academy Of Sciences Of The United States Of America* **1996,** 93, 12349-12354.

25. Wiethoff, C. M.; Smith, J. G.; Koe, G. S.; Middaugh, C. R. "The potential role of proteoglycans in cationic lipid-mediated gene delivery - studies of the interaction of cationic lipid-DNA complexes with model glycosaminoglycans" *Journal Of Biological Chemistry* **2001,** 276, 32806-32813.

26. Panyam, J.; Labhasetwar, V. "Dynamics of endocytosis and exocytosis of poly(D,L-lactide-co-glycolide) nanoparticles in vascular smooth muscle cells" *Pharmaceutical Research* **2003,** 20, 212-220.

27. Huth, U. S.; Schubert, R.; Peschka-Suss, R. "Investigating the uptake and intracellular fate of pH-sensitive liposomes by flow cytometry and spectral bio-imaging" *Journal Of Controlled Release* **2006,** 110, 490-504.

28. Nakase, I.; Niwa, M.; Takeuchi, T.; Sonomura, K.; Kawabata, N.; Koike, Y.; Takehashi, M.; Tanaka, S.; Ueda, K.; Simpson, J. C.; Jones, A. T.; Sugiura, Y.; Futaki, S. "Cellular uptake of arginine-rich peptides: roles for macropinocytosis and actin rearrangement" *Molecular Therapy* **2004,** 10, 1011-1022.

29. Suzuki, T.; Futaki, S.; Niwa, M.; Tanaka, S.; Ueda, K.; Sugiura, Y. "Possible existence of common internalization mechanisms among arginine-rich peptides" *Journal Of Biological Chemistry* **2002,** 277, 2437-2443.

30. Belting, M. "Heparan sulfate proteoglycan as a plasma membrane carrier" *Trends In Biochemical Sciences* **2003,** 28, 145-151.

31. Belting, M.; Persson, S.; Fransson, L. A. "Proteoglycan involvement in polyamine uptake" *Biochemical Journal* **1999,** 338, 317-323.

32. Wiley, H. S.; Cunningham, D. D. "A steady-state model for analyzing the cellular-binding, internalization and degradation of polypeptide ligands" *Cell* **1981,** 25, 433-440.

33. Scatchard, G. "The attractions of proteins for small molecules and ions" *Annals of the New York Academy of Sciences* **1949,** 51, 660-672.

34. Brechtelsbauer, C.; Ricard, F. "Reaction engineering evaluation and utilization of static mixer technology for the synthesis of pharmaceuticals" *Organic Process Research & Development* **2001,** 5, 646-651.

35. Fournier, M. C.; Falk, L.; Villermaux, J. "A new parallel competing reaction system for assessing micromixing efficiency - determination of micromixing time by a simple mixing model" *Chemical Engineering Science* **1996,** 51, 5187-5192.

36. Fang, J. Z.; Lee, D. J. "Micromixing efficiency in static mixer" *Chemical Engineering Science* **2001,** 56, 3797-3802.

37. Guichardon, P.; Falk, L. "Characterisation of micromixing efficiency by the iodide-iodate reaction system. Part I: experimental procedure" *Chemical Engineering Science* **2000,** 55, 4233-4243.

CHAPTER III

DEVELOPMENT OF IMPROVED NANOPARTICULATE POLYELECTROLYTE COMPLEX PHYSICOCHEMISTRY BY NON-STOICHIOMETRIC MIXING OF POLYIONS WITH SIMILAR MOLECULAR WEIGHTS

Introduction

Efficient nano- and micro-scale therapeutic vehicles are ideally, nontoxic, nonimmunogenic, and made from versatile building blocks that allow optimal delivery to specific cells and tissues. The potential of polymer nanostructures as targeted drug delivery vehicles has led to the creation of multitudes of colloidal formulations. This technology results from a collaboration of medicine and engineering for the delivery of macromolecular drugs that cannot be efficiently administered systemically[1]. Integration of pharmacological agents, vectors including peptide segments, proteins, and DNA vectors, into nanoparticulate polymer matrices, together, with both targeting and therapeutic abilities offers many benefits, including controlled drug release and protection, prolonged blood circulation times, and other tunable characteristics[2,3].

Many current research strategies in polymer drug delivery involve the use of solvent emulsion as a reaction environment leading to potential problems in final product formulations[4]. Water-soluble, biodegradable, polymeric, polyelectrolyte complex dispersions (PECs) have evolved because of the limitations of the currently available systems. The nanoparticulate architecture of PECs permits the environmentally attractive use of water as a solvent, a major advantage for products that may be used as drug delivery systems in humans. PECs result from strong electrostatic interactions between

charged microdomains of at least two oppositely charged polyelectrolytes[5]. The most predominant forces for PEC assembly are strong electrostatic interactions, but hydrogen bonding, hydrophobic interactions, and van der Waals forces complement PEC formation, and they are related to physical considerations presented previously[6].

Reaction phase environmental parameters dictate PEC physicochemical properties, and, specifically, complexation between polyelectrolytes having significantly different molecular weights leads to formation of water-insoluble aggregates[7-9]. The creation of large water-insoluble aggregates is undesirable because particles greater than 1000 nm can lead to circulatory limitations and tissue inflammation[10-12]. Conversely, particles which are too small quickly leave systemic circulation, cleared by the reticuloendthelial system (RES), without reaching target tissues[13].

Using these facts as a starting point, this study compares PEC systems with similar (LMW) and dissimilar (HMW) molecular weights to identify a suitable and controllable product for biological use. Several PEC characteristics are favorable for colloidal stability and provide the benchmarks for definition of an advantageous PEC system, including hydrodynamic diameter less than 200 nm[12,14], empirical surface charge of greater than 30 mV or less than -30 mV, spherical morphology, and a low polydispersity index indicative of a homogeneous distribution[15-17]. Maintenance of these properties, particularly size and shape, is critical for cellular uptake[18,19]. The current technology applied herein has utilized a water-based approach for producing PECs under the prevailing assembly and complexation theory. These biocompatible, non-toxic PECs are produced using a multipolymeric mixture with a minimum of two polyion pairs for

enhancement of thermodynamic stability and controlled incorporation of molecules such as proteins or targeting peptides.

Experimental Procedures

PECs were prepared per Chapter II, *PEC Fabrication*, using the LMW and HMW formulations. PECs were made with (20 kHz) and without frequency dispergation for both HMW and LMW systems followed by the evaluation of integrity as a function of pH as described in Chapter II, *Colloidal Stability.* Hydrodynamic diameter, zeta potential, PDI (*PEC Size and Zeta Potential*), and morphology by TEM provided the physicochemical markers.

Statistical Analysis

All statistical analyses were performed using JMP-IN 5.1 (SAS, Cary, NC). Reaction mixture formulations with and without dispergation were compared by two-sample t-test to evaluate the differences between sizes, zeta potentials, and polydispersity indices (PDI) within and between PEC systems. Hydrodynamic diameter and surface charge was tested for significant differences from 200 nm and +30 mV by a one-tailed t-test. TEM size distributions were tested using the Kolmolgorov-Smirnov two-sample test to determine whether the PEC populations were distributed identically as a function of frequency dispergation. Kurtosis and skewness for the TEM distributions were evaluated by one-tail t-test to evaluate deviations from normality. Colloidal stability for hydrodynamic diameter was first tested by one-way ANOVA to determine variations in the means as a function of pH. The one-way ANOVA was followed by Dunnet's Test,

which compared each mean to the reaction mixture. A one-tailed t-test was applied to determine at which pH instabilities in preparations, as measured by zeta potential, deviated from the empirical standard for stability ±30 mV[17]. Each analysis was evaluated at the 95% confidence level.

Results and Discussion

PEC Physicochemical Aspects

The components of the anionic solution were altered to determine the effect of low molecular weight polymers on the hydrodynamic diameter, surface charge, and PDI of polyelectrolyte complexes. Polyelectrolyte concentrations for non-stoichiometric addition of HMW anions into cations were established previously[1,14]. Increased polymer concentration and further anion titration lead to PEC size increase, aggregation, and precipitation as the overall complex charge nears neutrality. Lower polymer concentrations lead to significantly lower PEC yields. Thus, the chosen concentrations represent a practical compromise[1,20]. In both LMW and HMW formulations, the molar anion/cation charge ratio, 0.168, was constant, as calculated from the structures and molecular weights provided by the manufacturers. The criteria for acceptance of PEC systems for biological testing were: hydrodynamic diameter statistically less than or equal to 200 nm[12,14], surface charge >|±30 mV|[15-17], and a low PDI, indicative of a narrow size distribution. The physicochemical characteristics of both LMW and HMW PECs were studied by titrating, non-stoichiometrically, anions into a cationic bath without or with (20 kHz) frequency dispergation. The spontaneous complexation resulted in

cationic particles, regardless of PEC formulation, that exhibited a colloidal, Tyndall effect. PECs, as prepared in their native state, had a measured pH of 4.2 due to excess cations present in the reaction mixture. The complexation led to a core-shell morphology, with the excess cation dominating the corona surface and a neutralized inner phase of oppositely charged polyions.

The z-average size, PDI, and zeta potential for PEC preparations with LMW and HMW polyions are shown in Figure 3-1(A-C), respectively. LMW formulations provided PECs with superior characteristics independent of frequency dispergation, an outcome related to polymer molecular weight. Statistical differences in PDI, zeta potential, and hydrodynamic diameter of PECs were observed among the two titration conditions and chemistries. Both LMW titration conditions provided PECs with hydrodynamic diameters averaging statistically less than 200 nm, while the dispergated HMW formulation was the only dissimilar molecular weight chemistry with appropriate physicochemical properties. Frequency dispergation reduced HMW and LMW PEC hydrodynamic diameter by 25% and 12%, respectively. When comparing titration frequencies between systems, LMW PECs resulted in a 33% and 21% decrease in size for formulations without and with frequency dispergation, respectively. The PDIs measured for HMW PECs, 0.410 and 0.378, indicated very heterogeneous populations of particles within the desired size range, as well as aggregate structures with much greater diameter, while the reduced PDI for LMW PECs, 0.142 and 0.145, indicated more homogeneous preparations. For reference, a monodisperse distribution of standard latex beads yields a PDI of 0.05[21]. This reduction in polydispersity helps to minimize the possibility of *in vivo* circulatory limitations. Zeta potential was reduced for LMW PECs, but the systems

were stable. In fact, a decreased positive surface charge has shown reduced toxicity at cellular and systemic levels[22].

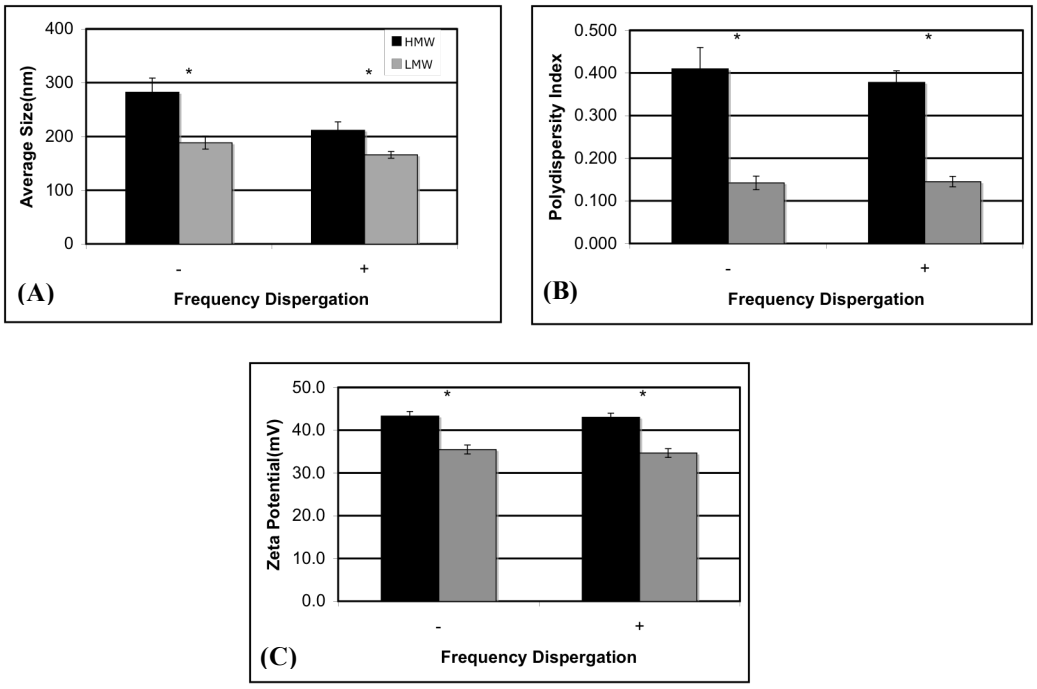

Figure 3-1. Size and zeta potential measurements for similar (LMW) and dissimilar (HMW) weight components. (A) and (B) correspond to measurements of z-average diameter and polydispersity index for PECs obtained with (+) and without (-) ultrasonic dispergation for similar and dissimilar molecular weight components. (C) describes the zeta potential for dissimilar (HMW) and similar (LMW) molecular weight components. Asterisks indicate pairs of means that differ statistically by two-sample t-test at the 95% confidence level for 10 replicates.

The improved physicochemical properties observed with and without frequency dispergation may be due to the difference in sequential addition of anion to cation. Frequency dispergation provides the anionic solution as an aerosol, upon yielding a smaller core template for subsequent cationic interactions and nucleation of the complexes. However, LMW PECs, suitable biological preparations were formed

independent of frequency dispergation. Therefore, LMW anions needed no modified titration to provide polyions in the appropriate conformation for efficient PEC creation.

PEC Morphology by TEM

TEM micrographs presented in Figure 3-2 provided verification of LMW and HMW PEC size with and without frequency dispergation. Unstained TEM specimens were used, since the PECs had enough contrast and superstructure for visualization. Observations of PEC morphology were followed by point-to-point, pixel based diameter evaluation to develop a size distribution to compare with PCS measurements. Similar structures and size for PEC structures have been reported in the literature[2,23]

Figure 3-2A(i)-(iv) showed the heterogeneity of populations created under both dispergation conditions for the HMW preparations. These images provided a physical illustration of classic PEC models dictated by the characteristics of the polyion groups, stoichiometry and molecular weights: (1) the ladder-like structure, where complex formation takes place on a molecular level via conformational adaptation, and (2) the scrambled-egg model where, a high number of chains are incorporated into the particle architecture[24]. Figure 3-2A(ii) showed the ladder-like structures formed as a result of mixing polyelectrolytes having large differences in molecular dimensions, polymer shielding, and zipperlike assembly due to adjacent polyions[24,25]. HMW PECs prepared with frequency dispergation, Figure 3-2A(iii)-(iv) showed compact, scrambled-egg architectures, which appeared to be highly aggregated. This morphology is typical for PECs formed between polyelectrolytes having different molecular weights[9]. Figure 3-2B(i-iv), for complexes formed with low molecular weight constituents, describes more

homogeneous populations of condensed, compact structures, which only displayed scrambled-egg behavior. The more uniform morphology was consistent with their lowered PDI. Again, this was likely due to more efficient interactions between polyions. The particles exhibited a condensed, opaque core, surrounded by a thick, fluffy coat. This opacity may be due to the presence of divalent cations in the formulations. Similar behavior has been previously observed for chitosan/PEO-PPO nanoparticles[26].

Instrumentation that is complementary to the TEM CCD camera was used to measure manually and estimate the diameter of the PECs for validation of the z-average mean diameter. Only spherical structures were sized, since the aggregate/filament structures provide no discernible points of reference for accurate diameter evaluation. Figure 3-3 displays the histograms for LMW and HMW PECs created with and without frequency dispergation. Number average sizes were 152.4 nm and 141.5 nm for LMW PECs without and with frequency dispergation, respectively, while HMW PECs had mean diameters of 201.5 (without) and 177.5 (with). The results correlated to measurements performed using PCS insofar as the effect of both precursor chemistry and dispergation according to two-sample Student's t-tests at the 95% confidence level. None of the distributions were normally distributed as determined by statistically testing the skewness and kurtosis of each distribution. The PDI measured by the ZetaSizer was qualitatively verified by coefficient of variance, an indication of the variabilities of the populations. Calculations performed on the distributions ranged from 34.9% (LMW without) to 49.0% (HMW with). Conversely, Kolmogorov-Smirnov tests showed that HMW and LMW size distributions were significantly different for the two frequency dispergation conditions. This result detected differences between formulations, with and

without dispergation, while this difference could not be detected by two-sample t-tests using PCS data. Although, the two statistical tests yielded different interpretations, the algorithms for evaluation of PEC diameter are quite different. PCS uses a combination of light scattering as a function of Brownian motion to derive diffusion coefficients, which can then be used to calculate hydrodynamic diameter from the Stokes-Einstein equation. The measurement of diameter via TEM was a more direct method for evaluating diameter not convoluted by the aqueous parameters that affect PCS measurements, as discussed below.

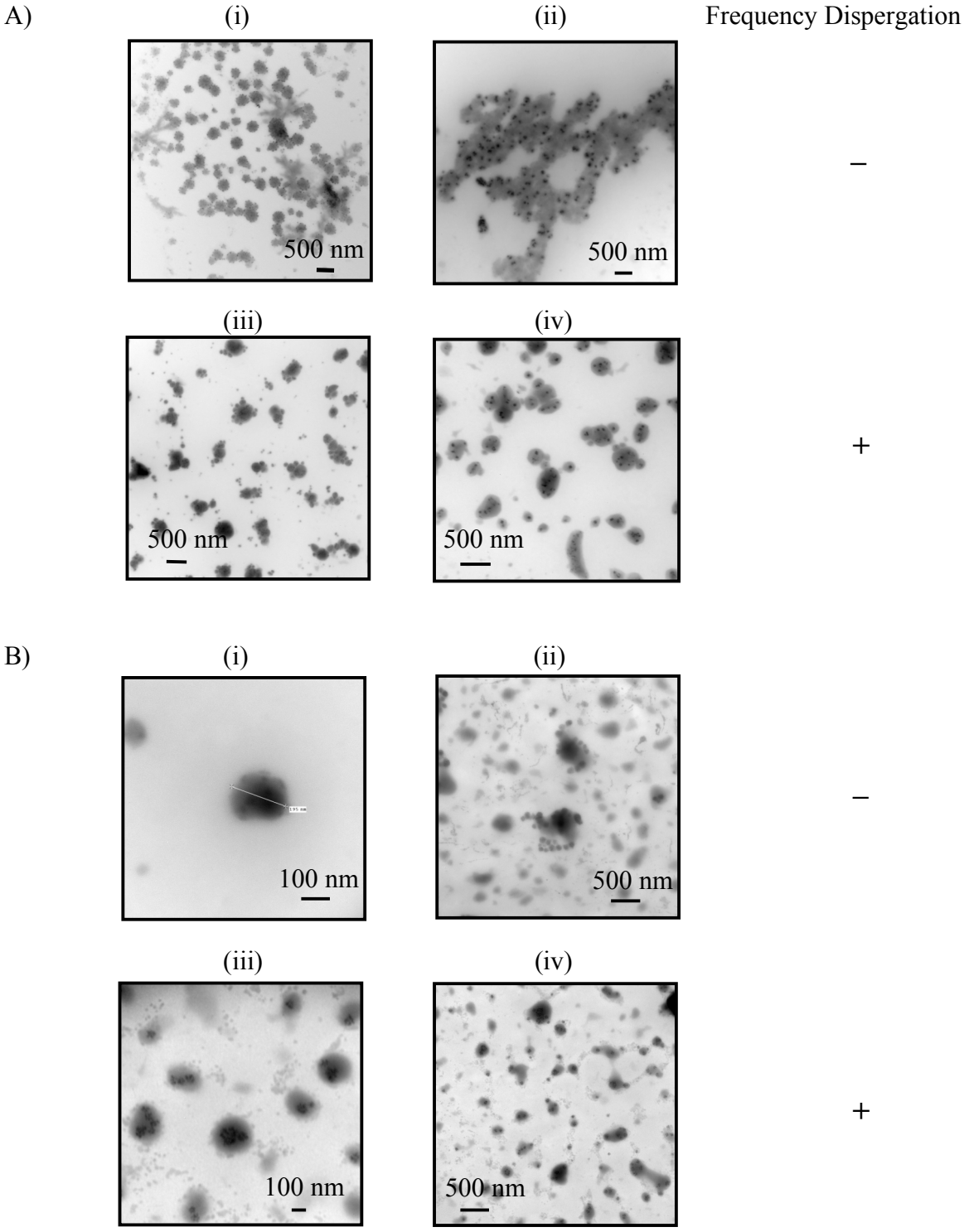

Figure 3-2. TEM micrographs for PECs prepared with and without frequency dispergation for HMW (A) and LMW (B) precursors. Images assigned (i) and (ii) are PECs created without dispergation. (iii) and (iv) represent PECs fabricated with dispergation.

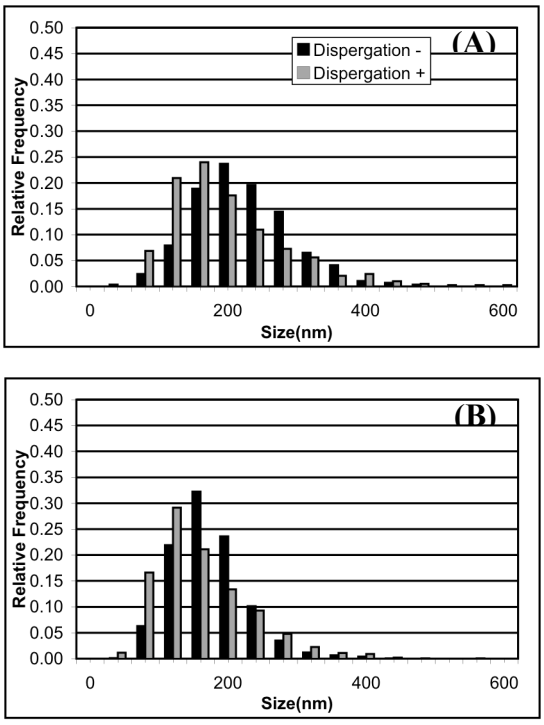

Figure 3-3. TEM PEC diameter evaluation. PEC diameter measured using TEM CCD camera software for suspensions prepared from HMW (A) and LMW (B) precursors. For HMW, 784 and 284 events were tabulated with and without dispergation settings, respectively. 1486 and 1860 observations were recorded for LMW PECs created with and without, respectively. Distribution shifts were statistically evaluated by the Kolmogorov-Smirnov test.

Figure 3-4 shows the agreement between PCS measurements and TEM diameter evaluation. TEM estimates were consistently 71%-85% lower than PCS measurements. The ZetaSizer algorithms assume that the particle population only contains spherical structures; therefore microfilaments are assumed to be large, round objects. Besides the assumption of uniform morphology, the ZetaSizer values include surface structure and electrical double layers surrounding the particle, which contributed to the increased diameter measured by PCS. Previous studies on polymeric nanoparticles show similar TEM/PCS ratios[2,27,28]. In conclusion, TEM was suitable for discerning PEC morphology

and quantitative diameters, but the ZetaSizer provides a higher throughput, unbiased method. Both types of analysis need to be considered when characterizing these types of physicochemical phenomena.

(A) (B)

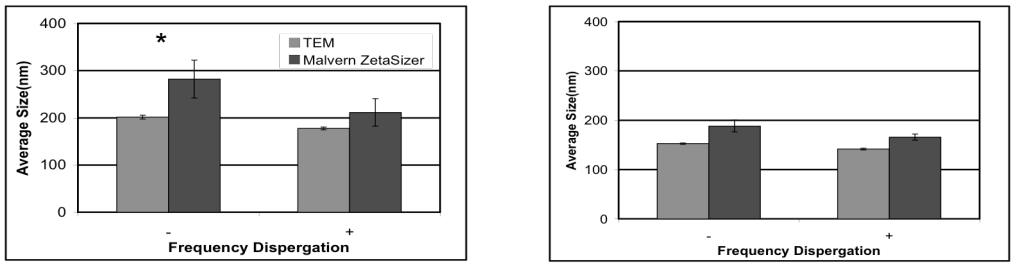

dispergation	TEM (nm)	Malvern (nm)	% TEM/Malvern
-	201.5	282.1	71.4
+	177.5	211.3	84.0

dispergation	TEM (nm)	Malvern (nm)	% TEM/Malvern
-	152.5	188.2	81.0
+	141.5	165.8	85.4

Figure 3-4. Comparison of PEC diameter measured by Malvern ZetaSizer Nano ZS and TEM for HMW (A) and LMW (B) polymer PECs. The above figure details percent agreement between the two techniques along with a side-by-side graphical comparison. Asterisks indicate pairs of means which differed according to a two-sample t-test at the 95% confidence interval, but not at 90% indicating an equivalence amongst means for the two physicochemical characterization methods.

Colloidal Stabilty as a Function of pH.

The addition of electrolytes or the change in the pH affects the colloidal stability of colloidal dispersions. These modifications are significant considerations for further use of any nanoparticulate system in biological media[29]. The alteration of surface groups in electrostatic complexes between anions and cations can lead to a large size change, dependent upon the extent of ionization[30]. Any ionizable groups in the charged domains presented at the nanovehicle periphery can act as electrostatic stabilizer, which is mediated by repulsive Coulombic interactions between particle surface charges[31,32]. As

shown in Figure 3-1, reaction mixture PECs yielded stable, positively charged structures with zeta potentials greater than +30 mV. However, this condition occurred at low pH (~4.2) and may not be a suitable suspension for in vivo or in vitro use. The cationic charge of the PECs indicated that the surface-exposed polymeric groups were in a highly protonated state, causing repulsive forces to propagate and prevent particle coalescence in solution. In addition, the delicate balance between electrostatic double layers and Van der Waals forces likely contributed to the maintenance of colloidal stability, signified by zeta potential[33].

The stability of the four PEC systems was evaluated by PEC collection and resuspension at various pH, low salt and ionic strength media. Salts can cause secondary aggregation and flocculation, as well as a disintegration of the complexes[34]. Therefore, if the salt concentration is low, the effect of pH on PEC physicochemistry is isolated. Because of the presence of positively charged, pH ionizable, primary amino groups that were present as a result of excess PMCG and spermine of the cationic shell, a pH variation should modify the electrical state and thus the stability of the complexes. Hydrodynamic diameter (z-average size) and zeta potential were used as stability indices.

Figures 3-5 and 3-6 show the variation of PEC diameter and zeta potential, respectively, as a function of pH. The two properties were directly related and consecutively measured by the ZetaSizer immediately after colloidal resuspension and pH measurement. Surface charge stabilities were empirically defined as values greater than $\left|\pm 30 \text{ mV}\right|$. For z-average, statistical stability was defined by one-way ANOVA and then by comparison of means to the reaction mixture by Dunnet's test. Figure 3-5 shows a progressive reduction in statistical stabilities moving from HMW without dispergation

to HMW with dispergation, LMW without dispergation, and LMW with dispergation. Figure 3-6 shows a similar trend, but LMW systems provided greater colloidal stability as a function of pH. In general, the behavior for Figures 3-5(A-C) and 3-6(A-C), showed a clear tendency towards aggregation as pH approached neutrality, corresponding to changes in surface charge. Therefore, the maintenance of ideal dimensions was governed by electrostatic contributions. For these particular systems, PECs coalesced, rather than swell, and the effect was irreversible. If particles aggregate, then they have reached an endpoint state. The increase in pH from 4 to 7 brought about a rapid decrease in zeta potential and colloidal stability, as shown by fusion of PECs as the repulsive surface charges were reduced. As the resuspension pH was increased beyond a transition point, (~7.8), the suspension appeared to become more stable as shown by preservation of the Tyndall effect and negative zeta potential less than -30 mV. This type of behavior, with zeta potential shoulders on either side of neutrality, indicated the possibility that these PECs exhibit zwitterionic behavior. Therefore, PECs upon assembly contain both positive and negative ionizable groups and behave as acidic or basic groups of monoacids or monobases. At low pH, pendant amino and carboxyl groups remain in a protonated state, leading to a predominance of positive charges. Following resuspension at increasing pH, the protons from the charged groups dissociate. The decreasing total surface charge depletes the PECs' ability to repel each other and they effectively coalesce. However, adequate negative charge appeared to be generated at basic conditions when sufficient protrusion and ionization of the carboxyl groups from anion may occur[35]. Figure 3-7(A-C) schematizes this phenomenon. In all cases, an experimental PEC isoelectric point (pI), the pH where dispersions carry no net charge and

is in its least stable state, was determined by fitting a line through the most linear portion of the zeta potential versus pH curve (Figure 3-6). The calculated x-intercept was designated as the experimental pI. pIs for the systems ranged from 5.76 (LMW without dispergation) to 5.90 (LMW with dispergation) and 5.79 (HMW without dispergation) to 5.89 (HMW with dispergation) . The variability in pIs between systems and/or titration conditions, including possibly two regions of instability exhibited in Figure 3-6(A,C), may be directly due to the assembly mechanisms and presentation of charged groups for complexation.

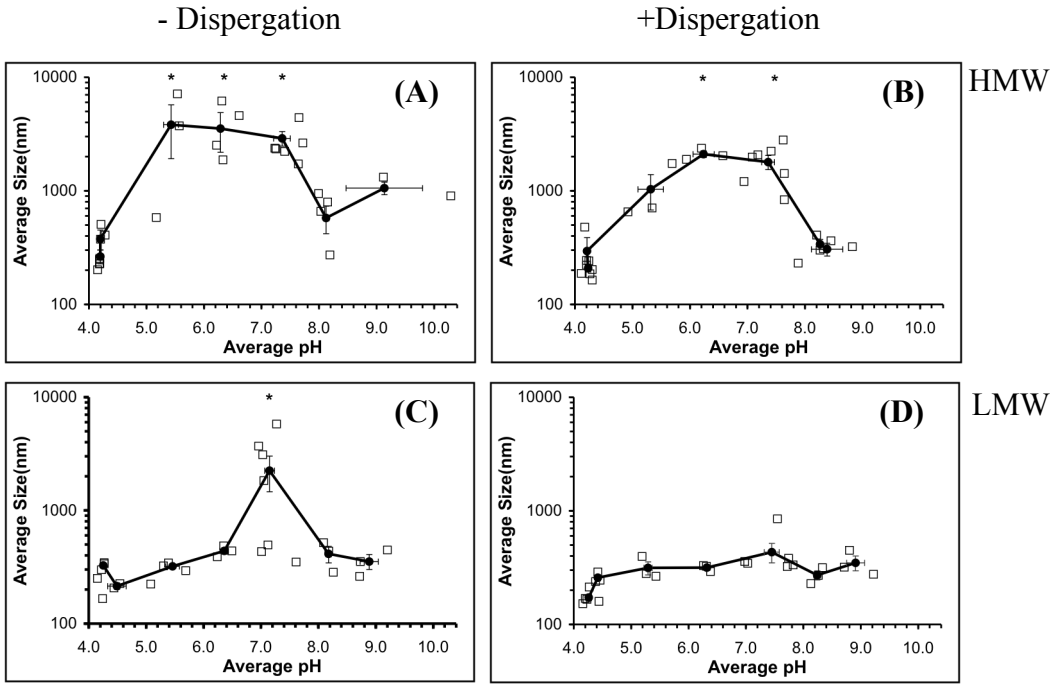

Figure 3-5. Response of PEC diameter in varied pH, low salt environments. (A) and (B) show the effect of pH on HMW PECs prepared without and with frequency dispergation, respectively, while (C) and (D) display the response of LMW PECs. Raw data are represented by squares, while the average of at least 3 replicates by circles and error bars corresponding to standard error. The asterisks indicate means which differ from the reaction mixture at the 95% confidence interval using Dunnet's Test.

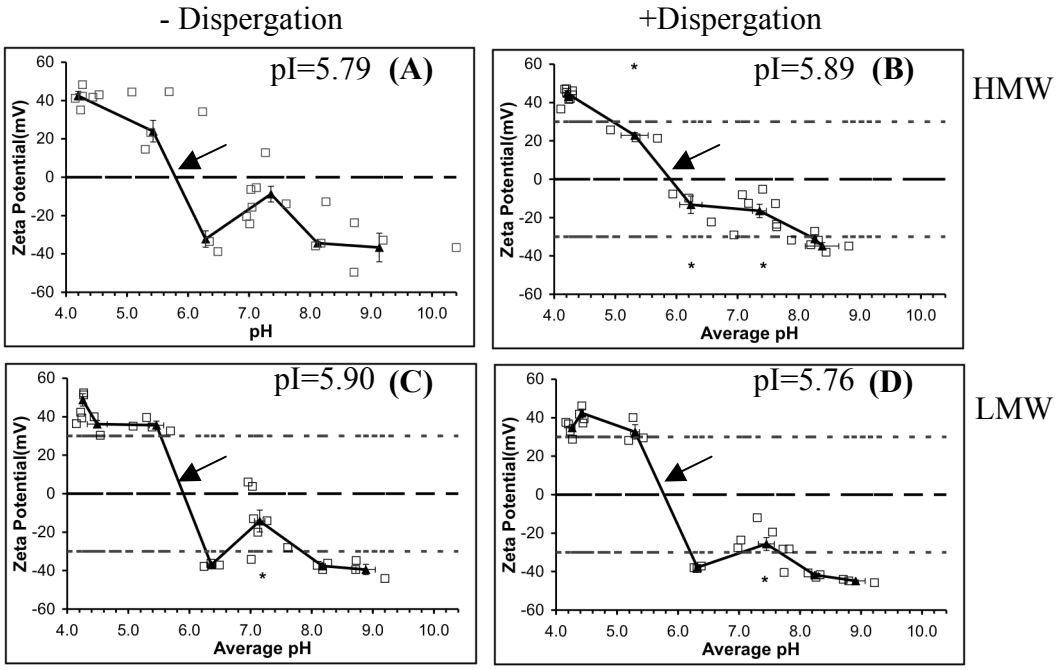

Figure 3-6. Response of PEC zeta potential in varied pH, low salt environments. (A) and (B) show the effect of pH on HMW PECs prepared at without and with frequency dispergation, respectively, while (C) and (D) display the response of LMW PECs. Raw data is represented by squares, while the average of at least 3 replicates by circles and error bars corresponding to standard error. Asterisks denote zeta potentials that deviate, statistically, from the empirical stability criterion of |30 mV|, defined by dashed lines, according to a one-tail t-test at the 95% confidence interval. Arrows indicate experimental pIs.

The most interesting results were obtained for LMW PECs prepared with dispergation, as shown in Figures 3-5D and 3-6D. Even though the zeta potential-pH curve exhibited a typical behavior, there appeared to be some intra-particle forces, which allowed the complexes to retain their dimensions even when the zeta potential neared neutrality. The maintenance of hydrodynamic diameter may also be related to the presence and incorporation of Pluronic F-68, assumed to be a steric stabilizer with no net charge[36]. The long chains of flexible tri-block copolymer polyethylene oxide/polypropylene oxide (PEO/PPO), when adsorbed to the surface, could create an osmotic and entropic barrier to particle-particle interactions induced by pH alterations[37].

Pluronic F-68 may discourage surface adhesion and conceivably inter-particle interactions. Intimate blending of PEO/PPO polymers into core-shell nanomatrices has been shown to attenuate hydrodynamic diameter and enhance structural integrity[38,39]. The electrically neutral copolymer, composed of hydrophilic and bydrophobic segments, is mechanically entrapped when present in cationic bath. The incorporation of PEO/PPO was possibly facilitated by the intermolecular bonding between electropositive amino hydrogens of the constitutive cationic polymers and the electronegative oxygens of PEO/PPO[40]. The interaction between the oxygen atom of PEO/PPO and the amino groups of the corona solution is weak, but could still have an effect on PEC stability and formation. The retention of ideal dimensions denotes the LMW dispergated formulation for biological application. Preliminary in vitro testing has shown PEC stability in endothelial cell growth media (MCDB131, pH=7.4) supplemented with 10% fetal calf serum, supporting their use for specific cell binding and internalization applications. The hydrodynamic diameter for this LMW nanoparticulate system was 235.9±30.5 nm (mean±standard error). Although the size falls outside of the benchmark of less than 200 nm, it is still expected to efficiently interact with biological systems. In fact, it was statistically equivalent to the diameter at pH=7.4 (432.6±84.1 nm), as measured in Figure 3-5(D), for a low salt buffer dispersion. This increase in size is most likely due interactions with media components[41].

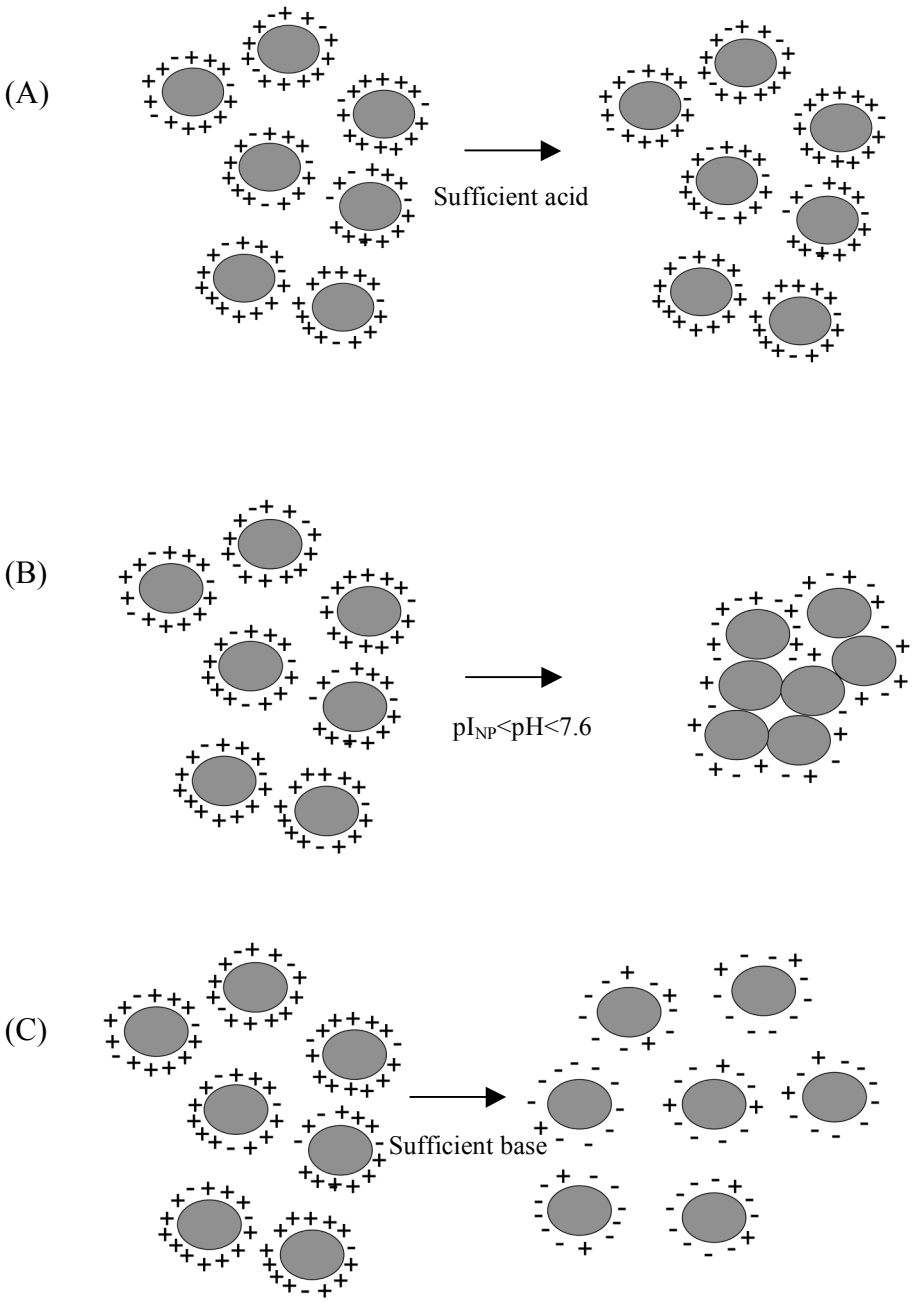

Figure 3-7. Schematic representation of PEC charge modification. The left figures are the PEC suspensions immediately after preparation. The native state has a surface dominated by excess cationic charge as shown by the significantly positive zeta potential. The presence of sufficient acid maintains a stable protonation state as shown in (A). As pH changes and nears the pI and neutrality, the ionizable states of the complexes are modified. The decreasing total surface charge depletes the complexes' ability to repel each other and they effectively coalesce, displayed by (B). But, if adequate base is present, the carboxyl groups become ionized and the colloid remains stable as denoted in (C).

Conclusions

This work, through the use of TEM and PCS technology, shows the effect of polyanion size reduction on PEC physicochemical properties that are essential for developing a biocompatible system for targeted drug delivery. As shown, the titration of nonstoichiometric amounts of HMW anions, compared to LMW anions for equivalent total molar charges, into cations formed larger complexes with marked size heterogeneity. In addition, HMW formulations resulted in decreased physicochemical stability. A system has been further optimized for size and charge properties that are pH insensitive, making it a useful system for optimal delivery to a range of tissues. The surface density of PEO/PPO may ensure sufficient steric stabilization, phagocytic resistance and prolonged systemic circulation[38,39,42,43]. This new formulation is an improvement over a previous non-toxic system[44-46] which has been shown to effectively deliver genes to cells of hematopoietic origin[14].

The pH and serum insensitivity, self-assembly, modular nature, and unique polymeric architecture of dispergated LMW PECs allows for surface groups to be independently modified to impart desired characteristics without substantial alteration of existing properties. The polycationic nature of the PEC periphery, predominantly polyamine and guanidinium moieties, may also facilitate their cellular uptake and transport via cell surface heparan sulfate proteoglycans or polyamine-based transport[47-49]. Taken together, the favorable characteristics of this system suggest that these PECs may be utilized as safe and highly efficient bioactive drug delivery systems. This system was further applied in the following chapters to evaluate biological and protein release/incorporation properties.

References

1. Prokop, A.; Kozlov, E.; Carlesso, G.; Davidson, J. M. "Hydrogel-based colloidal polymeric system for protein and drug delivery: physical and chemical characterization, permeability control and applications" *Advances in Polymer Science* **2002,** 160, 119-173.

2. Taylor, S.; Qu, L. W.; Kitaygorodskiy, A.; Teske, J.; Latour, R. A.; Sun, Y. P. "Synthesis and characterization of peptide-functionalized polymeric nanoparticles" *Biomacromolecules* **2004,** 5, 245-248.

3. Vinogradov, S. V.; Bronich, T. K.; Kabanov, A. V. "Nanosized cationic hydrogels for drug delivery: preparation, properties and interactions with cells" *Advanced Drug Delivery Reviews* **2002,** 54, 135-147.

4. Cruz, T.; Gaspar, R.; Donato, A.; Lopes, C. "Interaction between polyalkylcyanoacrylate nanoparticles and peritoneal macrophages: MTT metabolism, NBT reduction, and NO production" *Pharmaceutical Research* **1997,** 14, 73-79.

5. Schatz, C.; Lucas, J. M.; Viton, C.; Domard, A.; Pichot, C.; Delair, T. "Formation and properties of positively charged colloids based on polyelectrolyte complexes of biopolymers" *Langmuir* **2004,** 20, 7766-7778.

6. Dragan, S.; Cristea, M.; Luca, C.; Simionescu, B. C. "Polyelectrolyte complexes.1. synthesis and characterization of some insoluble polyanion-polycation complexes" *Journal of Polymer Science Part a-Polymer Chemistry* **1996,** 34, 3485-3494.

7. Dautzenberg, H. "Polyelectrolyte complex formation in highly aggregating systems. 1. Effect of salt: Polyelectrolyte complex formation in the presence of NaCl" *Macromolecules* **1997,** 30, 7810-7815.

8. Reihs, T.; Muller, M.; Lunkwitz, K. "Preparation and adsorption of refined polyelectrolyte complex nanoparticles" *Journal of Colloid and Interface Science* **2004,** 271, 69-79.

9. Schatz, C.; Domard, A.; Viton, C.; Pichot, C.; Delair, T. "Versatile and efficient formation of colloids of biopolymer-based polyelectrolyte complexes" *Biomacromolecules* **2004,** 5, 1882-1892.

10. Debuigne, F.; Cuisenaire, J.; Jeunieau, L.; Masereel, B.; Nagy, J. B. "Synthesis of nimesulide nanoparticles in the microemulsion epikuron/isopropyl myristate/water/n-butanol (or isopropanol)" *Journal of Colloid and Interface Science* **2001,** 243, 90-101.

11. Dev, V.; Eigler, N.; Fishbein, M. C.; Tian, Y. Q.; Hickey, A.; Rechavia, E.; Forrester, J. S.; Litvack, F. "Sustained local drug delivery to the arterial wall via biodegradable microspheres" *Catheterization and Cardiovascular Diagnosis* **1997,** 41, 324-332.

12. Panyam, P.; Labhasetwar, V. "Biodegradable nanoparticles for drug and gene delivery to cells and tissue" *Advanced Drug Delivery Reviews* **2003,** 55, 329-347.

13. Moghimi, S. M.; Hunter, A. C.; Murray, J. C. "Long-circulating and target-specific nanoparticles: theory to practice" *Pharmacological Reviews* **2001,** 53, 283-318.

14. Carlesso, G.; Kozlov, E.; Prokop, A.; Unutmaz, D.; Davidson, J. M. "Nanoparticulate system for efficient gene transfer into refractory cell targets" *Biomacromolecules* **2005,** 6, 1185-1192.

15. Chern, C. S.; Lee, C. K.; Chang, C. J. "Electrostatic interactions between amphoteric latex particles and proteins" *Colloid and Polymer Science* **2004,** 283, 257-264.

16. Fatouros, D. G.; Piperoudi, S.; Gortzi, O.; Ioannou, P. V.; Frederik, P.; Antimisiaris, S. G. "Physical stability of sonicated arsonoliposomes: Effect of calcium ions" *Journal of Pharmaceutical Sciences* **2005,** 94, 46-55.

17. Sugrue, S. "Predicting and controlling colloid suspension stability using electrophoretic mobility and particle size measurements" *American Laboratory* **1992,** 24, 64-71.

18. Chithrani, B. D.; Ghazani, A. A.; Chan, C. W. "Determing the size and shape dependence of gold nanoparticle uptake in mammalian cells" *Nano Letters* **2006,** 6, 662-668.

19. Desai, M. P.; Labhasetwar, V.; Walter, E.; Levy, R. J.; Amidon, G. L. "The mechanism of uptake of biodegradable microparticles in Caco-2 cells is size dependent" *Pharmaceutical Research* **1997,** 14, 1568-1573.

20. Buchhammer, H. M.; Mende, M.; Oelmann, M. "Formation of mono-sized polyelectrolyte complex dispersions: effects of polymer structure, concentration and mixing conditions" *Colloids And Surfaces A-Physicochemical And Engineering Aspects* **2003,** 218, 151-159.

21. Malvern Instruments. "What is particle size, zeta potential, and molecular weight" In *Zetasizer Nano Series User Manual*, Worcestershire, UK, 2004; pp 3-4.

22. Kabanov, A. V.; Kabanov, V. A. "DNA complexes with polycations for the delivery of genetic material into cells" *Bioconjugate Chemistry* **1995,** 6, 7-20.

23. Janes, K. A.; Calvo, P.; Alonso, M. J. "Polysaccharide colloidal particles as delivery systems for macromolecules" *Advanced Drug Delivery Reviews* **2001,** 47, 83-97.

24. Dautzenberg, H. "Light scattering studies on polyelectrolyte complexes" *Macromolecular Symposia* **2000,** 162, 1-21.

25. Muller, M.; Kessler, B.; Richter, S. "Preparation of monomodal polyelectrolyte complex nanoparticles of PDADMAC/poly(maleic acid-alt-alpha-methylstyrene) by consecutive centrifugation" *Langmuir* **2005,** 21, 7044-7051.

26. Calvo, P.; RemunanLopez, C.; VilaJato, J. L.; Alonso, M. J. "Chitosan and chitosan ethylene oxide propylene oxide block copolymer nanoparticles as novel carriers for proteins and vaccines" *Pharmaceutical Research* **1997,** 14, 1431-1436.

27. Du, J. Z.; Tang, Y. P.; Lewis, A. L.; Armes, S. P. "pH-sensitive vesicles based on a biocompatible zwitterionic diblock copolymer" *Journal Of The American Chemical Society* **2005,** 127, 17982-17983.

28. Duguid, J. G.; Li, C.; Shi, M.; Logan, M. J.; Alila, H.; Rolland, A.; Tomlinson, E.; Sparrow, J. T.; Smith, L. C. "A physicochemical approach for predicting the effectiveness of peptide-based gene delivery systems for use in plasmid-based gene therapy" *Biophysical Journal* **1998,** 74, 2802-2814.

29. Sahoo, S. K.; Panyam, J.; Prabha, S.; Labhasetwar, V. "Residual polyvinyl alcohol associated with poly (D,L-lactide-co-glycolide) nanoparticles affects their physical properties and cellular uptake" *Journal of Controlled Release* **2002,** 82, 105-114.

30. Ogawa, K.; Sato, S.; Kokufuta, E. "Formation of intra- and interparticle polyelectrolyte complexes between cationic nanogel and strong polyanion" *Langmuir* **2005,** 21, 4830-4836.

31. Einarson, M. B.; Berg, J. C. "Electrosteric stabilization of colloidal latex dispersions" *Journal Of Colloid And Interface Science* **1993,** 155, 165-172.

32. Pincus, P. "colloid stabilization with grafted polyelectrolytes" *Macromolecules* **1991,** 24, 2912-2919.

33. Ishikawa, Y.; Katoh, Y.; Ohshima, H. "Colloidal stability of aqueous polymeric dispersions: Effect of pH and salt concentration" *Colloids And Surfaces B-Biointerfaces* **2005,** 42, 53-58.

34. Dautzenberg, H.; Rother, G. "Response of polyelectrolyte complexes to subsequent addition of sodium chloride: time-dependent static light scattering studies" *Macromolecular Chemistry and Physics* **2004,** 205, 114-121.

35. Tong, W. J.; Gao, C. Y.; Mohwald, H. "Stable weak polyelectrolyte microcapsules with pH-responsive permeability" *Macromolecules* **2006,** 39, 335-340.

36. Fitch, R. M., In *Polymer Colloids: A Comprehensive Approach*, Academic Press: New York, 1997.

37. Prokop, A.; Holland, C. A.; Kozlov, E.; Moore, B.; Tanner, R. D. "Water-based nanoparticulate polymeric system for protein delivery" *Biotechnology and Bioengineering* **2001,** 75, 228-232.

38. Csaba, N.; Caamano, P.; Sanchez, A.; Dominguez, F.; Alonso, M. J. "PLGA: poloxamer and PLGA: poloxamine blend nanoparticies: new carriers for gene delivery" *Biomacromolecules* **2005,** 6, 271-278.

39. Shenoy, D.; Little, S.; Langer, R.; Amiji, M. "Poly(ethylene oxide)-modified poly(beta-amino ester) nanoparticles as a pH-sensitive system for tumor-targeted delivery of hydrophobic drugs: Part 2. in vivo distribution and tumor localization studies" *Pharmaceutical Research* **2005,** 22, 2107-2114.

40. Kim, S. S.; Lee, Y. M.; Cho, C. S. "Synthesis and properties of semiinterpenetrating polymer networks composed of beta-chitin and poly(ethylene glycol) macromer" *Polymer* **1995,** 36, 4497-4501.

41. Peracchia, M. T.; Harnisch, S.; Pinto-Alphandary, H.; Gulik, A.; Dedieu, J. C.; Desmaele, D.; d'Angelo, J.; Muller, R. H.; Couvreur, P. "Visualization of in vitro protein-rejecting properties of PEGylated stealth (R) polycyanoacrylate nanoparticles" *Biomaterials* **1999,** 20, 1269-1275.

42. Dash, P. R.; Read, M. L.; Barrett, L. B.; Wolfert, M.; Seymour, L. W. "Factors affecting blood clearance and in vivo distribution of polyelectrolyte complexes for gene delivery" *Gene Therapy* **1999,** 6, 643-650.

43. Lee, J. H.; Kopeckova, P.; Kopecek, J.; Andrade, J. D. "Surface properties of copolymers of alkyl methacrylates with methoxy (polyethylene oxide) methacrylates and their application as protein-resistant coatings" *Biomaterials* **1990,** 11, 455-464.

44. Prokop, A.; Kozlov, E.; Moore, W.; Davidson, J. M. "Maximizing the in vivo efficiency of gene transfer by means of nonviral polymeric gene delivery vehicles" *Journal Of Pharmaceutical Sciences* **2002,** 91, 67-76.

45. Prokop, A.; Kozlov, E.; Newman, G. W.; Newman, M. J. "Water-based nanoparticulate polymeric system for protein delivery: Permeability control and vaccine application" *Biotechnology and Bioengineering* **2002,** 78, 459-466.

46. Wang, T.; Lacik, I.; Brissova, M.; Anilkumar, A. V.; Prokop, A.; Hunkeler, D.; Green, R.; Shahrokhi, K.; Powers, A. C. "An encapsulation system for the immunoisolation of pancreatic islets" *Nature Biotechnology* **1997,** 15, 358-362.

47. Belting, M. "Heparan sulfate proteoglycan as a plasma membrane carrier" *Trends In Biochemical Sciences* **2003,** 28, 145-151.

48. Wadia, J. S.; Stan, R. V.; Dowdy, S. F. "Transducible TAT-HA fusogenic peptide enhances escape of TAT-fusion proteins after lipid raft macropinocytosis" *Nature Medicine* **2004,** 10, 310-315.

49. Wright, L. R.; Rothbard, J. B.; Wender, P. A. "Guanidinium rich peptide transporters and drug delivery" *Current Protein & Peptide Science* **2003,** 4, 105-124.

CHAPTER IV

ENTRAPMENT AND RELEASE PROPERTIES FOR LOW MOLECULAR WEIGHT NANOPARTICULATE POLYELECTROLYTE COMPLEXES

Introduction

Proteins are often marginally stable and consequently easily damaged during their formulation as drugs. Nanoparticle and polymer delivery systems, first introduced by Langer and Folkman[1] in 1976, have been developed which have the potential to improve protein stability, increase the duration of the therapeutic effect, and permit administration through non-parenteral, possibly oral, routes[2]. Encapsulation of proteins within biodegradable polymers has been shown to enhance the half-life in vitro[3,4] and in vivo[4-6]. It is critical to control the liberation of drugs entrapped in polymeric supports under defined pharmacological and physicological conditions. Payloads can be delivered intracellularly in two ways: internalization of the PEC followed by release inside or particle docking at the cell surface and liberation through a bystander effect[7]. The release should when and where the drug is required and in the appropriate concentration for the desired therapeutic effect[8].

Previous studies have investigated the drug releasing response from polymeric matrices as a function of pH[9], electric field[10], temperature[11], ultrasound[12], or light[13]. Several PEC systems[8,14-18] have incorporated proteins and analyzed the release kinetics and entrapment. PECs allow the loading of proteins by polyion coacervation between charged groups. The purpose of the current study was to explore the protein loading and release for multi-component LMW PECs. PECs were prepared with 3 different iodinated

proteins to trace their fate and address the effect of protein charge on entrapment and discharge in a simulated physiological environment under external sink release conditions: 100% fetal calf serum (FCS) was added after replacement of fluid at each time point. Soybean trypsin inhibitor (STI), β-lactoglobulin (BLG), and cytochrome C (Cyt C) were selected because they have high water solubilities and a fairly wide range of isoelectric points (pI). Radioactivity (I^{125}) was chosen because isotopes do not quench which is a common problem for fluorescent tracers in combination with microplate readers. The radioisotope also allowed for mass balance closure.

Experimental Procedures

The protocols applied from Chapter II were as follows: *PEC Fabrication* with LMW polyions at 20 kHz frequency dispergation, *PEC Size and Zeta Potential*, *Protein Iodination*, and *PEC Protein Loading and Release Monitoring*. Equations 2-2, 2-3, 2-4, 2-5, and 2-6 were used to analyze the release and loading measurements. Additionally, the rate of release, $Rate_{REL}$, (μg/day) was calculated by Equation 4-1:

$$Rate_{REL} = \frac{Mass_{t=n} - Mass_{t=n-1}}{t_n - t_{n-1}} \tag{4-1}$$

where $Mass_{t=n,}$ and $Mass_{t=n-1}$ were the mass of protein released over the specified time interval.

Statistical Analysis

Statistical analysis was carried out with JMP-IN 5.1 (SAS, Cary, NC). Reaction mixture formulations and final preparations in FCS were compared by two-sample t-tests to evaluate the differences between sizes, zeta potentials, polydispersity indices (PDI), loading efficiencies, and 7 d retainment percentages. All statistical tests were performed at $p<0.05$ (95% confidence level). Results are displayed as average ± standard error.

Results and Discussion

Measurement of Size, Zeta Potential, and Polydispersity Index

Sizes, polydispersity indices (PDI), and zeta potentials (ZP) of PECs with Cyt C (pI=10.8), STI (pI=4.5), and BLG (pI=5.1) loaded into the anion core were shown in Figure 4-1 for reaction (Rxn) mixtures and final formulations in FCS. Isolation and resuspension in FCS led to an increase in hydrodynamic diameter and PDI, but a decrease in ZP. Incorporation of protein and dissolution in FCS, in all cases, resulted in statistical changes for each physicochemical property. Hydrodynamic diameter increased in FCS with sizes ranging from 252.4 nm (STI) to approximately 330 nm for Cyt C and BLG. The zeta potentials for PECs in FCS were similar in absolute magnitude, but the sign was reversed. There was no visible aggregation in FCS, but these properties were likely influenced and altered due to the presence of heterogeneous serum particulates.

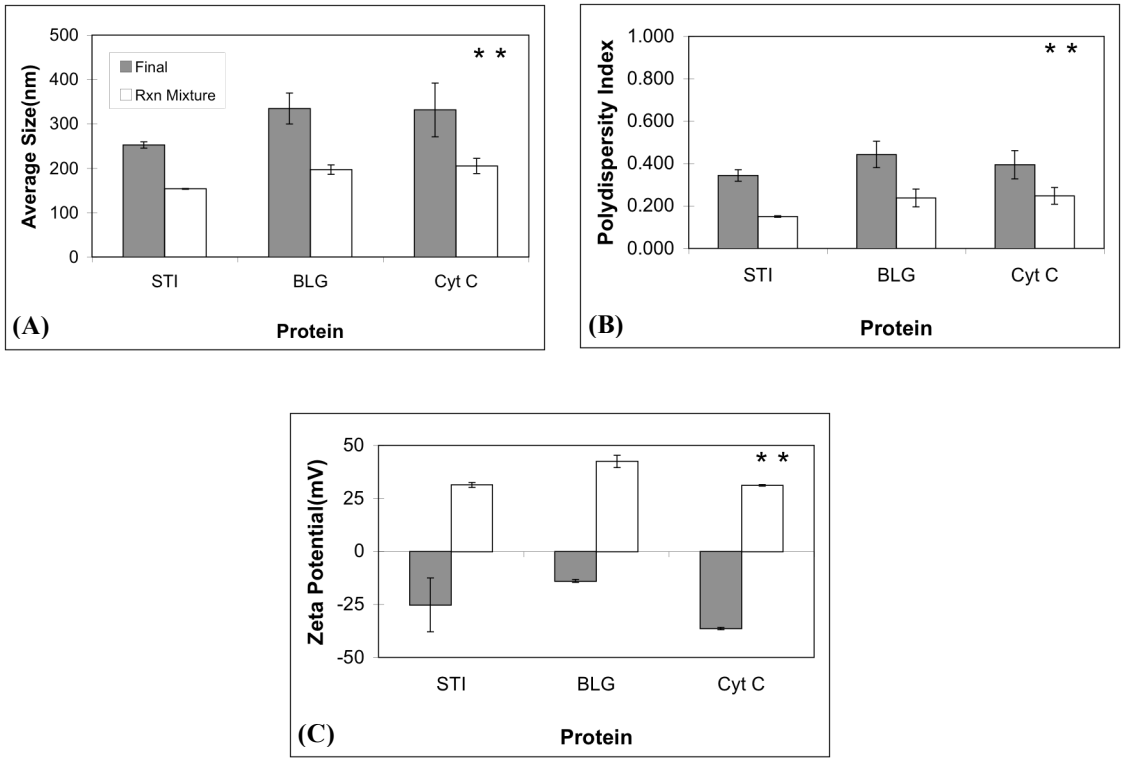

Figure 4-1. Physicochemical properties of the reaction (Rxn) mixture and final preparations, in 100% FCS, for multi-component PECs prepared with various proteins loaded into the anionic solution. (A), (B), and (C) correspond to hydrodynamic diameter, zeta potential, and polydispersity index, respectively, measured by PCS. The double asterisks indicate means (Rxn Mixture versus Final) that differ statistically by two-sample t-test at the 95% confidence interval (n=3).

Encapsulation Efficiency of STI, BLG, and Cyt C

The effect of proteins with different pIs on PEC loading is shown in Figure 4-2. The pH of the anionic solution before PEC fabrication was 6.85 meaning that STI and BLG were negatively charged, while Cyt C was net positive. Assembly of PECs resulted in a pH of 4.2 due to excess cations, which reverses the charged state of STI and BLG. The encapsulation efficiency of 15 μg I^{125}-labeled STI, BLG, and Cyt C was not dependent on the nature of the protein; all loading efficiencies were statistically

heterogeneous and ranged from 6.0% (STI) to 7.4% for Cyt C and BLG. The loading of proteins has been found to be largely dependent on several molecular and environmental parameters: amount, molecular volume, polarity, charge, and degree of ionization[19]. In this case, only the charge and degree of ionization was studied; none of which affected the incorporation.

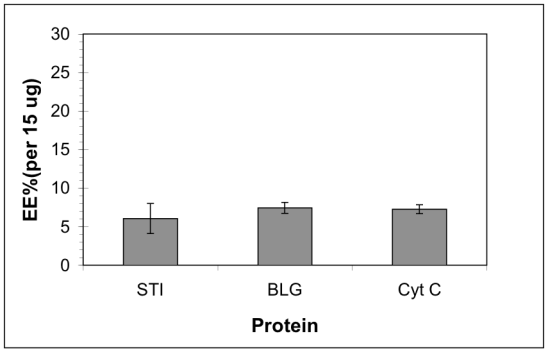

Figure 4-2. Effect of protein on the protein entrapment efficiency (EE%) for PECs. Radioactive (I^{125}) protein associated with PECs was measured after particle preparation, isolation by centrifugation and resuspension in 100% FCS, for n=3. No statististical difference was indicated at $p<0.05$.

In Vitro Release Kinetics and Protein Retainment

The ability of PECs to release the protein over a sustained period of time is critical[20]. Hence, a comparison of STI, BLG, and Cyt C loaded PEC release was carried out over the course of 1 week at room temperature (20°C), followed by the determination of the amount retained. External sink conditions were applied which involved the replacement of the solvent gradient at every day.

Figure 4-3(A,B) shows the percent cumulative release and release rate, respectively. Figure 4-3(A) indicated a 'burst' release over the first 24 h and then a plateau leading to an irreversibly bound phase. BLG-containing PECs exhibited a 43% loss of protein after 1 day, while STI and Cyt C showed 34% and 21% released over the same period. These types of initial 'bursts' have been seen widely and, again, largely controlled by environmental (temperature, pH) and molecular variables (polymer molecular weight, internal cross-linking)[20]. Protein release rates, Figure 4-3(B), showed that STI, BLG, and Cyt C demonstrated first-order release kinetics as a function of time and approached zero-order relationships at longer times (t=4d-7d). BLG displayed the largest initial rate (0.42 μg/day) and Cyt C (0.24 μg/day), the lowest, which could be a consequence of more intimate charged interactions maintained over the first 24 h.

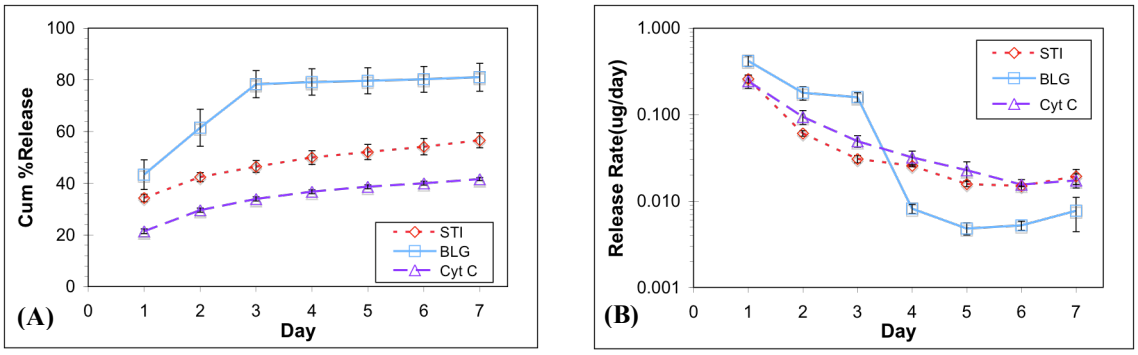

Figure 4-3. (A) In vitro, iodinated protein release from PECs and (B) rate of release, both measured over the course of 7 d (n=3).

The protein discharge was modeled with an one-dimensional, empirical equation developed by Ritger and Peppas[21] for Fickian and non-Fickian diffusional release (Equation 4-2), where M_t and M_{inf} represented the masses of total protein released at time (t) and total amount of incorporated drug, respectively. k was the correlation constant incorporating characteristics of the macromolecular network and n the diffusional constant which defined non-Fickian and Fickian activity regimes. Equation 4-2 is an expression derived from a heuristic solution of Fick's second law. Fickian diffusion would describe the change in concentration over time is equal in terms of changes in local diffusion flux[22]. The diffusing species flux will follow a square root trend until an equilibrium is reached at long times (n=0.5). Case II transport follows a zero-order kinetics where the release is independent of time and a nominal n equal to 1. Anomalous transport processes do not fit either Fickian or Case II transport, but include sigmoidal, two-stage, and pseudo-Fickian ($n \neq 1$, $n \neq 0.5$) mass transfer[23] .

$$\frac{M_t}{M_{\inf}} = kt^n \tag{4-2}$$

The constants were determined experimentally by preparing a log-log plot which yielded a linear correlation with a slope of n and y-intercept of log k. Table 4-1 shows the calculated n and k values for each protein, while Figure 4-4 the experimental and modeled data. The units of k were day^{-n}.

Table 4-1. Tabulated power law constants (average ±s.e., n=3) for STI, BLG, and Cyt C loaded PECs.

Protein	n	k
STI	0.33±0.01	0.25±0.04
BLG	0.33±0.04	0.42±0.08
Cyt C	0.20±0.03	0.32±0.03

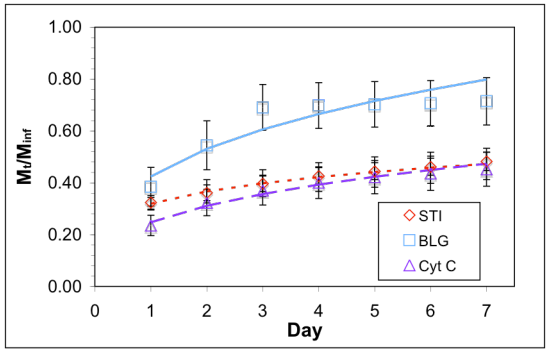

Figure 4-4. Empirical modeling of release data based on Equation 4-2. Points represented experimental data while solid lines were calculated based on the power law model.

The data modeled in Figure 4-4 confirmed that the release of protein was not controlled by strict Fickian diffusion as each n was less than 0.5 (Table 4-1). Therefore, it can be concluded that I^{125}-labeled protein does not follow a pattern which will eventually reach equilibrium. The anomalous diffusion in this system may be confounded by polyelectrolyte exchange reactions between serum macromolecules and the loaded proteins or PEC degradation. Regardless, the model appears to fit the data appropriately.

Further evidence that the amount of protein released does not reach M_{inf} was seen in Figure 4-5. Figure 4-5 displayed the amount of bound protein after 7 d. Because the rates of release reached 0.02 μg/day, 0.01 μg/day, 0.02 μg/day for STI, BLG, and Cyt C, respectively, the formulations became a more controlled release depot, following the burst regime. After 7 d, a significant amount of protein persisted: 54.77% (Cyt C), 28.59% (BLG), and 44.33% (STI).

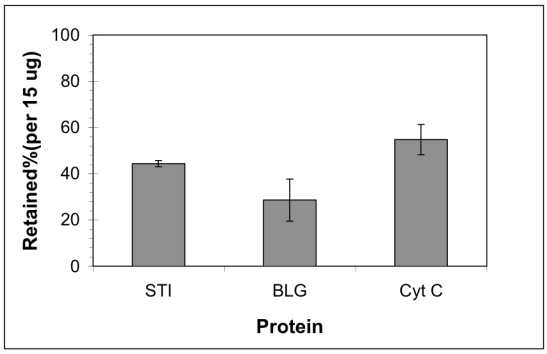

Figure 4-5. Percent protein remaining after 7 d release experiments. No statistical difference was detected ($p<0.05$, $n=3$).

Conclusions

Depending on their design, in vitro entrapment and release studies may be used to simulate the mechanistic release behavior and carrier-drug physicochemical relationship in vivo[24]. The PECs in this study (LMW 20 kHz) showed interesting features as protein delivery systems. PECs maintained appropriate physicochemical parameters for biological applications in physiological media (100% FCS), although charge reversal and some increase in hydrodynamic diameter were observed. The complexes incorporate the

proteins, independent of their nature, under mild conditions in a water-soluble preparation. The networks formed by PECs could entrap the proteins through intermolecular interactions and electrostatic forces between the proteins and the polyions. Unfortunately, the incorporation was relatively low due to the weak amphipathic nature of the proteins. STI, BLG, and Cyt C cannot compete with stronger electotrolytes (PMCG, chondroitin sulfate, alginate, spermine) for sites in the complex, leading to eventual washout upon centrifugation. According to the literature, alginate and chondroitin sulfate, constituents of the PEC core, are highly hydrophilic, owing to the presence of –OH, –COOH, and SO_4 groups on the polysaccharide chains[8], while spermine and PMCG comprise a hydrophilic outer shell. Therefore, the entrapped proteins became sequestered outside of the inner core, but inside of the corona. The incorporations were consistent with chitosan/PPO PECs developed by Calvo, et. al.[14]. The application of a more highly charged drug or protein would likely lead to higher entrapment levels[19].

It was shown, through a simple power law model, that the release of STI, BLG, and Cyt C into 100% FCS exhibited anomalous, non-Fickian diffusion behavior. This was not surprising since the PECs are multi-phase structures, whereby there could be release followed by re-adsorption to the surface or liberation into the external sink. Recently, Kamiya and Klibanov[15], made an argument for PEC size and extent of release: larger complex diameter led to slower release. PECs did not appear to adhere to that finding as the release profiles were independent of the hydrodynamic diameter. Additionally, because the PECs exhibited a burst release profile, they do not provide a good delivery system upon intravenous administration. Further PEC processing, before

or after complexation, would have to be performed to further retain the protein to prevent the loss of the cargo. In spite of the low entrapment efficiency and burst release, PECs are a still a promising candidate for drug delivery via a local application where the vehicles would be taken up by cells. The drug could then be released by changes in the intracellular concentration gradients or through intrinsic enzymatic degradation of the PEC.

References

1. Langer, R.; Folkman, J. "Polymers for sustained-release of proteins and other macromolecules" *Nature* **1976,** 263, 797-800.

2. Tiyaboonchai, W.; Woiszwillo, J.; Sims, R. C.; Middaugh, C. R. "Insulin containing polyethylenimine-dextran sulfate nanoparticles" *International Journal of Pharmaceutics* **2003,** 255, 139-151.

3. Niwa, T.; Takeuchi, H.; Hino, T.; Kunou, N.; Kawashima, Y. "Preparations of biodegradable nanospheres of water-soluble and insoluble drugs with D,L-lactide glycolide copolymer by a novel spontaneous emulsification solvent diffusion method, and the drug release behavior" *Journal Of Controlled Release* **1993,** 25, 89-98.

4. Tabata, Y.; Gutta, S.; Langer, R. "Controlled delivery systems for proteins using polyanhydride microspheres" *Pharmaceutical Research* **1993,** 10, 487-496.

5. Johnson, O. L.; Cleland, J. L.; Lee, H. J.; Charnis, M.; Duenas, E.; Jaworowicz, W.; Shepard, D.; Shahzamani, A.; Jones, A. J. S.; Putney, S. D. "A month-long effect from a single injection of microencapsulated human growth hormone" *Nature Medicine* **1996,** 2, 795-799.

6. Cohen, S.; Yoshioka, T.; Lucarelli, M.; Hwang, L. H.; Langer, R. "Controlled delivery systems for proteins based on poly(lactic glycolic acid) microspheres" *Pharmaceutical Research* **1991,** 8, 713-720.

7. Allen, T. M. "Ligand-targeted therapeutics in anticancer therapy" *Nature Reviews Cancer* **2002,** 2, 750-763.

8. Cruz, M. C. P.; Ravagnani, S. P.; Brogna, F. M. S.; Campana, S. P.; Trivino, G. C.; Lisboa, A. C. L.; Mei, L. H. I. "Evaluation of the diffusion coefficient for controlled release of oxytetracycline from alginate/chitosan/poly(ethylene glycol) microbeads in simulated gastrointestinal environments" *Biotechnology And Applied Biochemistry* **2004,** 40, 243-253.

9. Sahoo, S. K.; De, T. K.; Ghosh, P. K.; Maitra, A. "pH- and thermo-sensitive hydrogel nanoparticles" *Journal Of Colloid And Interface Science* **1998,** 206, 361-368.

10. Kwon, I. C.; Bae, Y. H.; Kim, S. W. "Electrically erodible polymer gel for controlled release of drugs" *Nature* **1991,** 354, 291-293.

11. Huang, S. K.; Stauffer, P. R.; Hong, K. L.; Guo, J. W. H.; Phillips, T. L.; Huang, A.; Papahadjopoulos, D. "Liposomes and hyperthermia in mice - increased tumor uptake and therapeutic efficacy of doxorubicin in sterically stabilized liposomes" *Cancer Research* **1994,** 54, 2186-2191.

12. Kost, J.; Leong, K.; Langer, R. "Ultrasound-enhanced polymer degradation and release of incorporated substances - controlled Release Drug Delivery Systems" *Proceedings Of The National Academy Of Sciences Of The United States Of America* **1989,** 86, 7663-7666.

13. Gerasimov, O. V.; Boomer, J. A.; Qualls, M. M.; Thompson, D. H. "Cytosolic drug delivery using pH- and light-sensitive liposomes" *Advanced Drug Delivery Reviews* **1999,** 38, 317-338.

14. Calvo, P.; RemunanLopez, C.; VilaJato, J. L.; Alonso, M. J. "Chitosan and chitosan ethylene oxide propylene oxide block copolymer nanoparticles as novel carriers for proteins and vaccines" *Pharmaceutical Research* **1997,** 14, 1431-1436.

15. Kamiya, N.; Klibanov, A. M. "Controling the rate of protein release from polyelectrolyte complexes" *Biotechnology And Bioengineering* **2003,** 82, 590-594.

16. Shi, X. W.; Du, Y. M.; Sun, L. P.; Zhang, B. Z.; Dou, A. "Polyelectrolvte complex beads composed of water-soluble chitosan/alginate: Characterization and their protein release behavior" *Journal Of Applied Polymer Science* **2006,** 100, 4614-4622.

17. Wang, Y. J.; Jiang, H. L.; Hu, Y. Q.; Zhu, K. J. "Biodegradable heparin/ampholytic chitosan complexes for pH-sensitive release of proteins" *Acta Polymerica Sinica* **2005**, 524-528.

18. Zezin, A.; Rogacheva, V.; Skobeleva, V.; Kabanov, V. "Controlled uptake and release of proteins by polyelectrolyte gels" *Polymers for Advanced Technologies* **2002,** 13, 919-925.

19. Allen, C.; Maysinger, D.; Eisenberg, A. "Nano-engineering block copolymer aggregates for drug delivery" *Colloids and Surfaces B-Biointerfaces* **1999,** 16, 3-27.

20. Fu, K.; Harrell, R.; Zinski, K.; Um, C.; Jaklenec, A.; Frazier, J.; Lotan, N.; Burke, P.; Klibanov, A. M.; Langer, R. "A potential approach for decreasing the burst effect of protein from PLGA microspheres" *Journal of Pharmaceutical Sciences* **2003,** 92, 1582-1591.

21. Ritger, P. L.; Peppas, N. A. "A simple equation for description of solute release II. Fickian and anamolous release from swellable devices" *Journal Of Controlled Release* **1987,** 5, 37-42.

22. Deen, W. M., *Analysis of Transport Phenomena*. 1st ed.; Oxford University Press: New York City, 1998.

23. Siepmann, J.; Gopferich, A. "Mathematical modeling of bioerodible, polymeric drug delivery systems" *Advanced Drug Delivery Reviews* **2001,** 48, 229-247.

24. Chorny, M.; Fishbein, I.; Danenberg, H. D.; Golomb, G. "Study of the drug release mechanism from tyrphostin AG-1295-loaded nanospheres by in situ and external sink methods" *Journal Of Controlled Release* **2002,** 83, 401-414.

CHAPTER V

FLOW CYTOMETRIC DETERMINATION OF NANOPARTICULATE POLYELECTROLYTE COMPLEX NON-SPECIFIC INTERACTIONS WITH ENDOTHELIAL CELLS

Introduction

Detailed mechanistic studies on binding and internalization of PECs, and nanoparticles for that manner, by cells have not been well characterized. Multi-component PECs, combined with Pluronic F-68 as a steric stabilizer, have been fabricated as a generic scaffold for incorporation of drugs and targeting moieties. We have developed a fluorescent approach, by application of a visible fluorophore, to describe the non-specific adsorptive mechanisms of nanoparticulate polyelectrolyte complex association in an endothelial cell (EC) model.

EC were chosen as the model because of their importance in disease and pathlogical significance[1]. EC line vascular systems: capillary, vein, and artery networks through which the blood carries nutrients. They are critical players in a number of pathological processes, many of which carry unique markers for targeted delivery: cancer (dysregulated angiogenesis), inflammation, oxidative stress, and thrombosis[2,3]. Moreover, and specifically related to cancer, solid tumors require access to blood vessels for growth and metastasis[4].

The use of fluorescently or radioactively labeled NP is the most common experimental approach found in the literature[5-7]. Fluorescent labeling and fluorescence activated cell sorting (FACS) was chosen for the recent study to avoid radioactivity;

radioactive PEC components in this study were not currently available or the incorporation of an isotope was too cumbersome. The limited toxicity and mechanisms of association are shown in the form of inhibitor studies. A novel, flow cytometric Scatchard analysis was used to define the yield of the PEC production, nature of the binding and internalization, components ignored in all studies to date. LMW PECs prepared with dispergation were applied because they met the engineering criteria defined in Chapter III.

Experimental Procedures

Various protocols were applied as defined in Chapter II. LMW PECs were fabricated as described in *PEC Fabrication*, with 20 kHz frequency dispergation. FITC was incorporated for fluorescence studies as per *Polymer Labeling* and *Fluorescent PEC Preparation*. Physicochemical characteristics were characterized by *TEM* and *PEC Size and Zeta Potential*. HMVECs were cultured as defined in *Cell Line and Maintenance.* Cytotoxicity was evaluated by *PEC Effects on HMVEC-1 Proliferation.* Subsequent to fluorescent PEC preparation, various methodologies were applied: *Confocal Microscopy, Flow Cytometric (FACS) Detection of PEC/Cell Interactions*, *Saturation PEC-Cell Association Kinetics*, *PEC Acute Toxicity by Propidium Iodide (PI)*, *Treatment of Cells with Various Inhibitors*, *Particle Counting*, and *Scatchard Plots*.

Statistical Analysis

Statistical analysis was performed using JMP-IN 5.1 (SAS, Cary, NC). Reaction mixture formulations and final preparations in cell growth media were compared by two-sample t-test to evaluate the differences between sizes, zeta potentials, and polydispersity indices (PDI). One-way ANOVA was used to compare cell proliferation data with controls (PEC-free exposures) while one-tail t-tests were applied to analyze statistical deviations of inhibitor responses from controls. All statistical tests were performed at $p<0.05$ (95% confidence level). Results are displayed as average ± standard error.

Results and Discussion

PEC Physicochemistry

The non-stoichiometric titration, under 20 kHz frequency dispergation, of the anions chondroitin sulfate and sodium alginate into a multi-component cation bath, containing Pluronic F-68, led to the spontaneous assembly of cationic nanoparticulate complexes. Physicochemical attributes, hydrodynamic diameter and zeta potential, were assessed by photon correlation spectroscopy (PCS), while morpohological properties by TEM. As shown in Figure 5-1(A-C), particles in their native reaction (Rxn) mixture had a mean diameter, of 164.6 nm, a polydispersity index of 0.199, and were positively charged (34.7 mV). The significant zeta potential was indicative of a stable colloidal suspension as has been pragmatically defined[8-10]. TEM images, represented in Figure 5-1(D), showed that the complexes were spherical in nature and had a mean diameter of 141.5 nm, averaged over several separate micrographs and observations (n=1484),

resulting in an 86% agreement (TEM/Malvern). This finding was consistent with results from Chapter III.

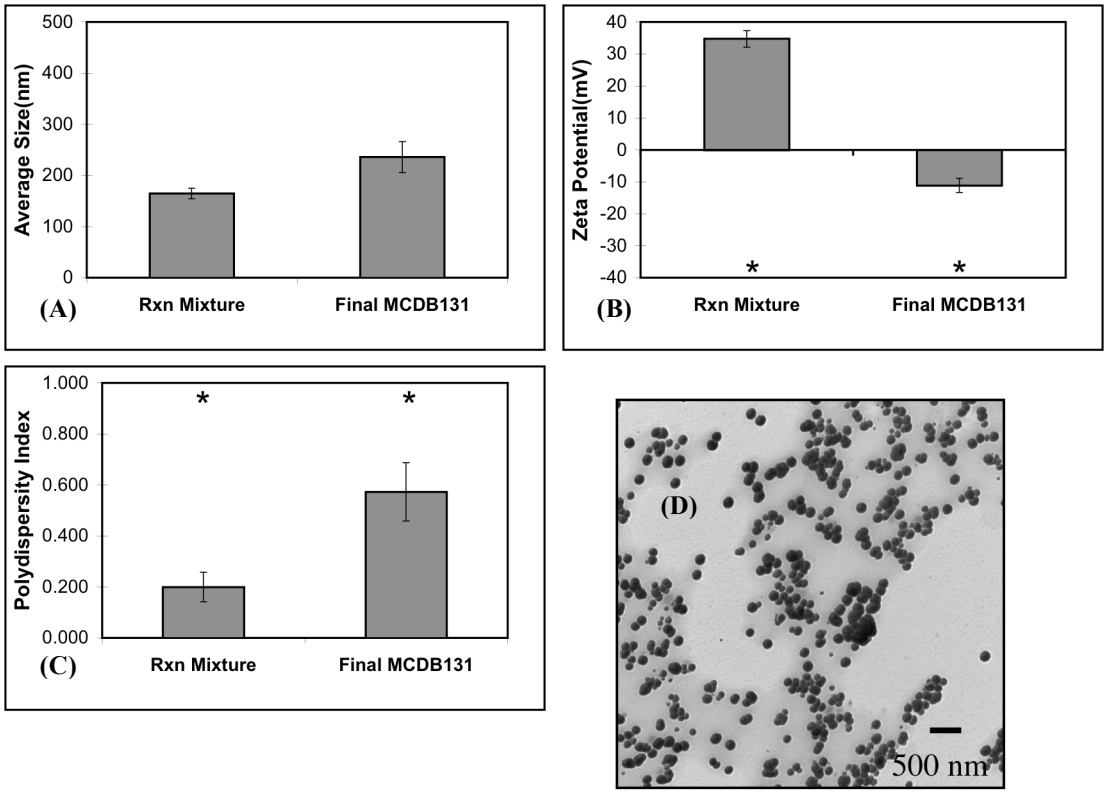

Figure 5-1. Physicochemical properties of the reaction (Rxn) mixture and final preparations, in EC media, for multi-component PECs. (A), (B), and (C) correspond to hydrodynamic diameter, zeta potential, and polydispersity index, respectively, measured by PCS. (D) is a representative TEM image. Asterisks indicate means that differ statistically by two-sample t-test at the 95% confidence interval.

PEC isolation and resuspension in endothelial cell growth media (MCDB 131), before HMVEC-1 exposure, led to an increase in size and PDI, and a decrease in zeta potential as shown in Figure 5-1(A-C). Two-sample t-tests did not indicate a statistical difference in size, but did for surface charge and PDI ($p<0.05$). In addition, a one-way t-test did not show any significant difference between the measured hydrodynamic

diameter and 200 nm, the empirical benchmark for efficient cellular uptake[11-13]. The change in PDI was likely due to the presence of serum particles and proteins, which have intrinsic light scattering properties detected by PCS. Alterations in PEC surface charge were attributed to changes in the extent of ionization of surface groups[14] and the protrusion of ionized, core hydroxyl groups[15]. Contributions to electrophoretic mobility were also due to the presence of serum particulates. The preservation of hydrodynamic diameter may be related to the presence and passive entrapment of Pluronic F-68, added to provide steric stabilization[16], but has also been found to improve PEC-mediated gene transfer. When adsorbed to surface the polymer could create osmotic and entropic barriers to particle-particle interactions and discourage adhesion of electronegatively charged serum molecules resulting in maintenance of structural integrity[17,18].

Determination of PEC Number by Flow Cytometry

Flow cytometry was used to evaluate the concentration of PECs. This method was used for Scatchard analysis and for toxicity titration by MTT reduction. Such a method would be less intensive and more accurate than an electron microscope-based technique where extrapolations based on Poisson distributions are necessary. Therefore, serial dilutions of NIST traceable fluorescent nanospheres (stock=2.3×10^{12} beads/ml, 200 nm nominal diameter) were prepared, diluted and processed using a FACSAria cytometer. This was important so that free PECs could be delineated from cell bound. As beads moved at a constant flow rate through the detector (SSC and FSC PMT), events were counted and recorded until 60 s passed. Dot plots of FSC versus SSC showed very little overlapping populations between 200 nm beads, FITC-labeled PECs, and HMVECs

as exhibited by Figure 5-2(A-C). The number of events was then divided by the time elapsed comprising the ordinate of the calibration. The quantity, threshold events per second, was then plotted against bead concentration, as in Figure 5-2(D). In an analogous approach, one batch of FITC-PECs was prepared and suspended in 1 ml of standard MCDB 131. This suspension was then diluted, arbitrarily, over 4 logs of concentration and the number of PECs was collected for 60 s. This allowed a linear range from concentrations 1.54×10^9 to 9.80×10^6 PEC/ml, corresponding to a 1:20 and 1:10000 dilutions, respectively, as shown in Figure 5-2(E,F). Suspensions at lower dilutions (1:10, 1:5) resulted in concentrations, which were less than 1.54×10^9 PEC/ml related to saturation of the detector or aggregation due to a decrease in particle interstitial space. Similar behavior was observed for the bead standards after an upper level of 2.30×10^9 bead/ml was reached.

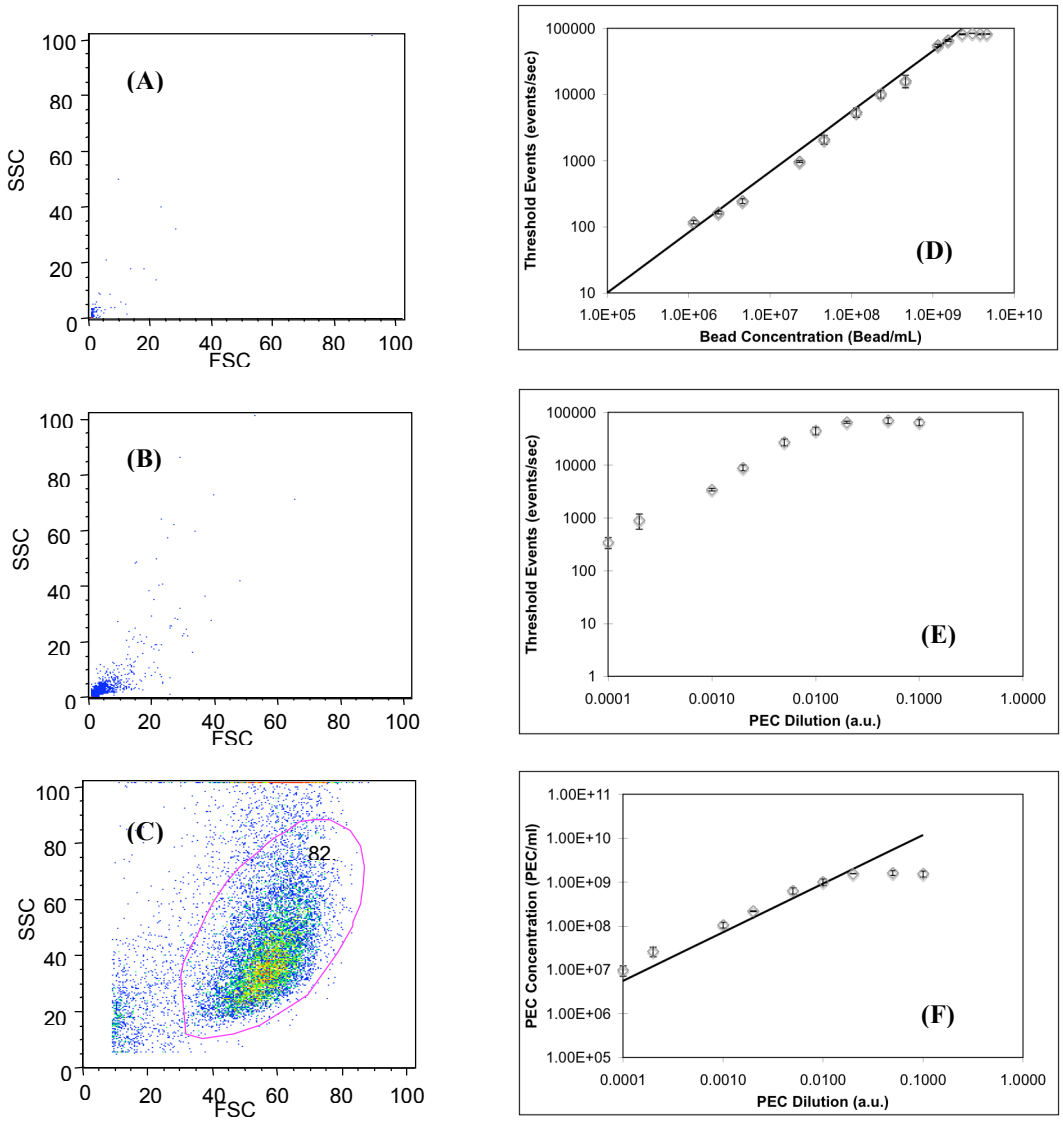

Figure 5-2. Evaluation of PEC concentrations by flow cytometry. FACS anlysis of (A) NIST traceable fluorescent green beads and (B) multi-component PECs suspended in HMVEC growth media; (C) gating of HMVECs showed little or no overlap between cellular and PEC gates, while PECs and 200 nm bead share similar FSC and SSC scattering. (D) was the calibration (detected events v. bead concentration) generated for various dilutions of NIST beads. (E) measured detected events versus arbitrary PEC dilutions per batch, while (F) calculated the concentration of PECs based on the bead standardization. Error bars are the standard error for n=3.

Cytotoxicity

Multi-component PEC system biocompatibility was tested by MTT reduction and propidium iodide (PI) internalization. Confluent HMVECs were seeded to 48 well plates (25000 cell/well) 24 h previous to PEC exposure. Responses to PEC doses were compared to cells cultured in the absence of particles (untreated control=100%). As shown in Figure 5-3(A), concentrations ranging from 400 to 60000 PEC/cell did not cause any statistical changes in MTT reduction as verified by one-way ANOVA and Dunnet's Test. For PI staining, Figure 5-3(B), HMVECs were exposed to $1.54x10^9$ PEC/ml, detached, and, over two hours, no change in viability was detected. The wide span of limited cytotoxicity validated this PEC system as a candidate for drug delivery to endothelial cells.

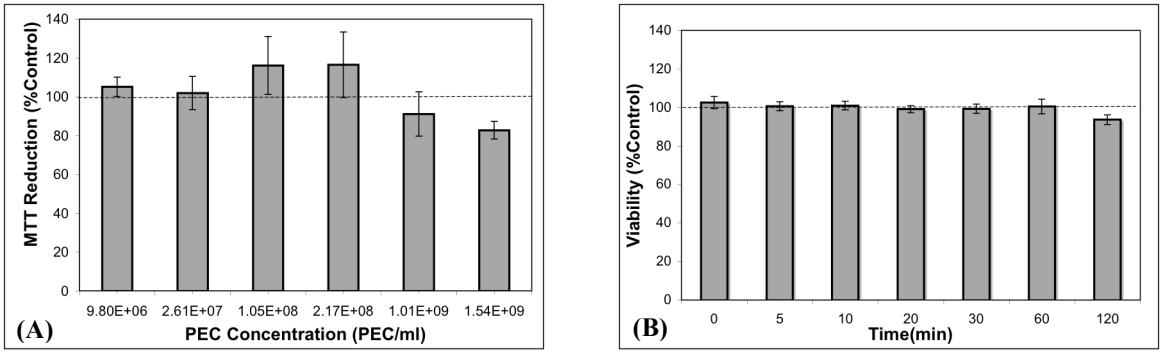

Figure 5-3. Relative toxicity profiles, chronic and acute, for multi-component PECs by (A) MTT reduction after 72 h incubation over various serial dilutions and (B) PI staining at a fixed concentration of particles ($1.54x10^9$ PEC/ml). Statistical testing by one-way ANOVA showed no difference amongst samples, while Dunnet's test showed that each mean was statistically the same as the control (no PECs), $p<0.05$. Data are means of at least 3 experiments (mean±s.e.)

Suppression of Extracellular Fluorescence by Trypan Blue

The ability of trypan blue to abolish free FITC was evaluated by addition to a suspension of FITC-PMCG PECs. This was critical to define intracellular fluorescence by FACS and has been previously applied[19-23], as trypan blue is excluded from viable cells. Figure 5-4(A) displayed the decrease in FITC distribution and complete shift from before (blue) and after (red) addition of trypan blue to a 200 µl suspension of 1.54×10^9 PEC/ml in a 1:1 volumetric ratio. Figure 5-4(B) represented the mean of three separate FITC PECs before and after trypan blue. The mixing of trypan blue with the suspension of FITC PECs resulted in a 98% suppression in median fluorescence. In terms of fluorescence, the medians dropped from 6142 a.u. (TB+) to 130 a.u. (TB-). These experiments validated the use of trypan blue to characterize compartmentalization (surface versus inside) of multi-component PECs.

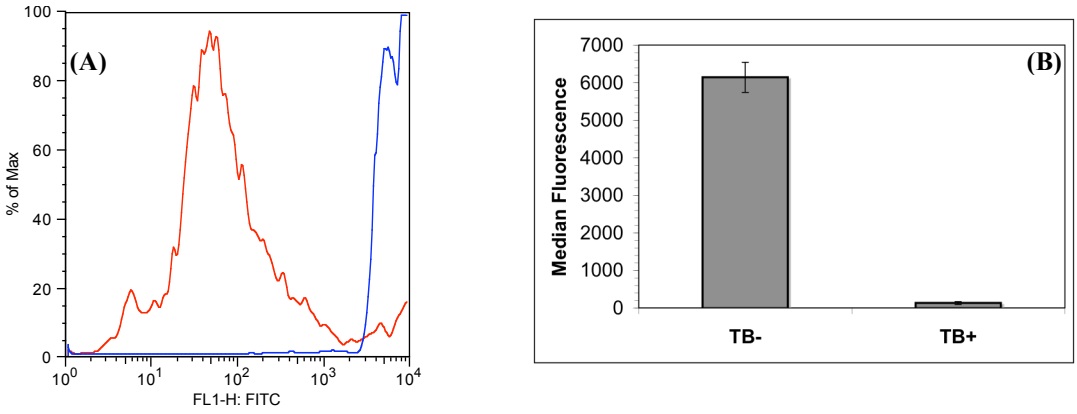

Figure 5-4. Suppression of free FITC via addition of trypan blue. (A) and (B) establish the concept of using trypan blue to quench extracellular fluorescence. Addition of 0.4 mg/ml trypan blue completely abolished the fluorescence (A) of free PECs in suspension in the absence of cells where blue and red were the distributions of fluorescent events before and after exposure to trypan blue, respectively. Histograms (B) and distribution (A), are the means ±standard error for three independent experiments and PEC preparations.

Kinetics of PEC Binding and Uptake: Tryptic Degradation of Interactions

FACS tracked the binding and uptake of FITC-containing PECs in HMVECs, cultured in serum-containing media, at various intervals up to 2 h. Exposure was followed by detachment by EDTA and the signals were expressed as median fluorescence in Figure 5-5(A,B) for both compartments (surface and internal). The surface bound phase was calculated by, first, measuring the total fluorescence bound, followed by subtraction of the trypan blue quenched signal. Figure 5-5(A) and 5-5(B) both indicated that particle binding and uptake was rapid and increased with the incubation time, despite the negative measured zeta potential in MCDB 131; shifts in fluorescence were seen as early as addition of PECs and immediate removal and washing (t=0). However, both curves showed a plateau effect, due, possibly, to limited saturation[24,25]. PEC association was also observed in mouse fibroblast (CRL-10225 and NIH3T3), CHO, CT26 colon carcinoma, primary human endothelial, macrophage, and hepatocyte cells.

Because the attachment and internalization appeared to reach saturation, the process was speculated to be receptor-mediated to some extent[26,27]. The particles are not likely to be phagocytosed due to the hydrodynamic diameter[28]. Even though the bulk surface charge was negative, microdomains of positive charge largely contribute to the attachment of PECs. PECs, in the absence of any targeting ligand, likely interacted with HMVEC through electrostatic interactions, particularly through PMCG. PMCG, guandinium rich, induced PEC electrostatic adsorption via cell surface bidentate hydrogen bonding to distal polyanionic residues[29,30]. Visual evidence of PEC/cell interactions, FITC-PECs were incubated with HMVECs for 2 h and observed by confocal laser scanning microscopy (CLSM). Figure 5-5(D,E) showed evidence of perinuclear

accumulation of PECs (green), while CLSM z-sectioning indicated that PECs were in the same plane as cells.

Figure 5-5(C) indicated the tryptic degradation of PEC association, necessitating the use of EDTA as the cell monolayer removal method. This type of study is commonly ignored in the literature that considers nanovehicle interactions with cells[5,21,31-35]. The tryptic proteolysis of the PEC association was analyzed by exposing HMVEC to FITC-labeled complexes for 30 min followed by either detachment by 0.25% trypsin/0.1% EDTA or 5 mM EDTA in HBSS, pH=7.6. Trypsin decreased the total amount of surface bound and internalized PECs, compared to cells detached by EDTA. PECs showed a 60% reduction in surface attachment and a 40% decrease in internalization, both statistically significant ($p<0.05$) to cells removed by EDTA. The result suggested that cellular surface proteins were involved in binding and uptake. This treatment, which strips HSPG[36], showed evidence that PEC associative properties may depend partially on HSPG, but does not address the dependence on calcium.

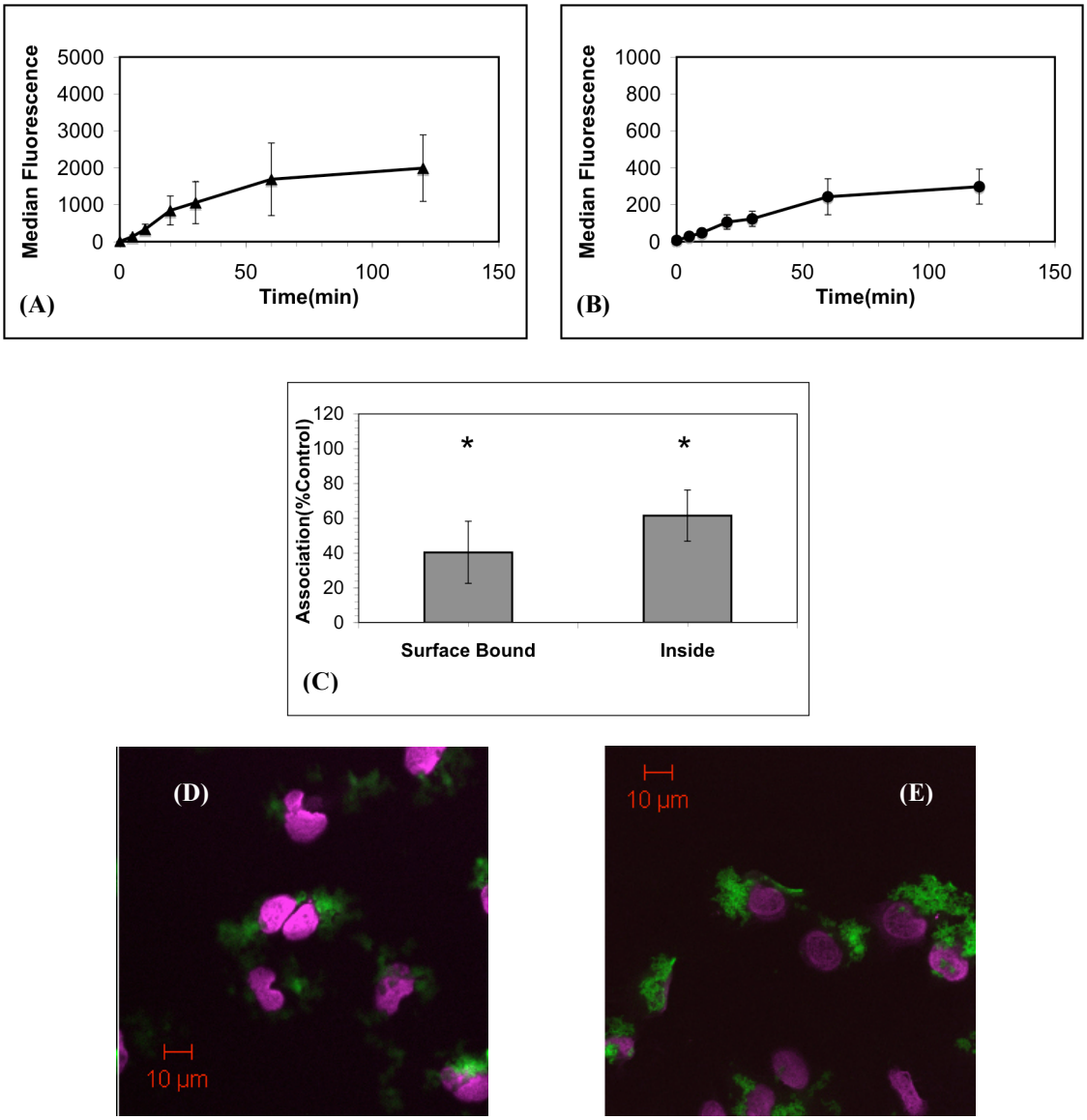

Figure 5-5. Overall PEC association kinetics and trypsin sensitivity for HMVECs. Kinetics of rapid binding (A) and internalization (B) for 2 h PEC exposure measured by FACS showed a phenomena which appeared to be saturable (n=3). The 30 min binding and uptake (C) were also sensitive to tryptic detachment ($p<0.05$, n=3) necessitating the use of EDTA in all *in vitro* experiments. A one-sample t-test was applied to compare trypsinized samples to EDTA treated (control). Confocal laser scanning microscopy imaging of PECs (green) incubated with HMVEC-1 for 2 h. (D) and (E) represented two separate fields of view. Complexes were incubated with HMVECs for 2 h and a perinuclear accumulation was observed qualitatively verifying FACS experiments. Nuclei were stained with TOPRO-3 (violet).

PEC Association and Energy Requirement

The involvement of energy, both thermodynamic and metabolic, was probed by incubation at reduced temperature (4°C) and media addition of 0.05% sodium azide/50 mM 2-deoxyglucose, respectively. Prior to addition of PECs, cultures were pre-incubated at 4°C for 1 h. PECs were then dispensed and further incubation at 4°C proceeded for 30 min. Exposure to 0.05% sodium azide/50 mM 2-deoxyglucose in MCDB 131 also elapsed 1 h previous to PEC exposure, followed by addition of particles in the presence of inhibitor for 30 min. In both cases, cells were detached following the 30 min exposure level by EDTA and analyzed by FACS; controls were HMVECs with PECs at normal incubatory conditions. Incubation with these two inhibitors resulted in the largest decreases in uptake signifying energy's important role in PEC intracellular transport.

Incubation of PECs at 4°C, (Figure 5-6, black) showed significant, statistical reduction in both binding and internalization after 30 min, compared to the control. Reduced temperature is a classical endocytosis and active transport inhibitor, where only passive PEC membrane fusion occurs. Therefore, the results indicated the dependence of thermodynamic energy for dynamic PEC uptake[6]. Additionally, decreased temperature reduces the motility of surface protein groups and the diffusion of PECs to the cell boundary. There was not a complete shutdown in the endocytosis; internalization decreased 80%. This was due to the presence of the basic surface molecule PMCG; integration of PECs into the plasma membrane and the cytosol was different than the process that occurs at 37°C, consistent with data on the internalization of arginine-rich peptides[37].

Further evidence of an energy-dependent adsorptive process was shown by incubation of cells with sodium azide/2-deoxyglucose, an inhibitor of glycolysis, (Figure 5-6, gray) both before and during PEC exposure. The decrease in bound (-55%) and internalized (-70%) PECs was statistically significant ($p<0.05$) through a mechanism mediated by depletion of ATP and membrane potential[27,30]. This response provided further proof that PEC attachment and endocytosis was a dynamic process that begins with adsorptive fusion with the cell membrane[38].

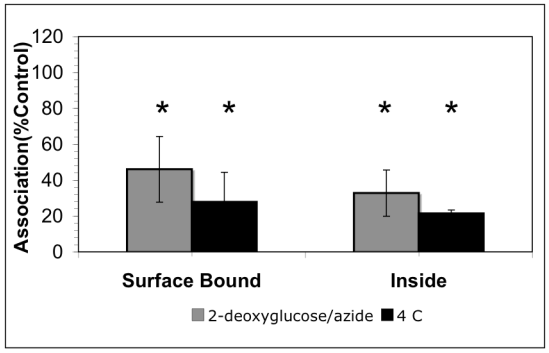

Figure 5-6. Energy mediated PEC internalization and binding. The dependence on metabolic and thermodynamic conditions was evaluated by incubation with 2-deoxyglucose (gray) and reduced temperature (black), respectively. Statistically significant differences were seen at the 95% confidence interval for surface attachment and uptake (n=3).

Actin Disruption

The role of filament networks in binding and endocytosis was studied by addition of 10 μM cytochalasin D, found to sufficiently inhibit actin polymerization, thus blocking phagocytosis and pinocytosis[37]. Cells were pre-treated with cytochalasin D for 2 h, at standard incubatory conditions, followed by PEC exposure for 30 min. Figure 5-7 showed statistical effects for (-58%, $p<0.05$) only the internalization of PECs. This result would indicate the role of the actin cytoskeleton during endocytosis and was consistent with other studies[5,23,37].

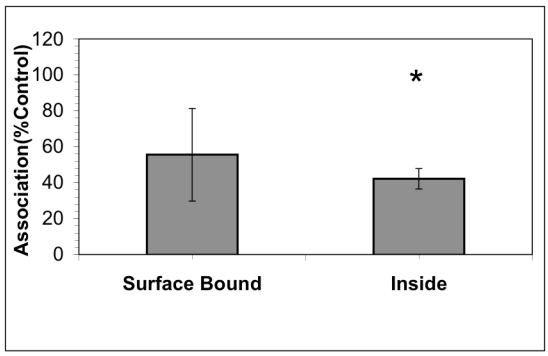

Figure 5-7. Actin facilitates the internalization of PECs. Preincubation of HMVEC with 10 μM cytochlasin D for 2 h statistically inhibited particle uptake, but not binding (one-sample t-test $p<0.05$). Data are the average of 3 replicates with error bars corresponding to standard error.

Heparin and Heparan Sulfate Proteoglycans (HSPG) Affect PEC Transport

The function of HSPG in PEC transport was characterized by two methods. The first approach was competitive inhibition of PEC binding by adding the exogenous, anionic glycosaminoglycan heparin to the media before (2 h) and during (30 min) PEC exposure. Biosynthesis of HSPG was perturbed by the 24 h incubation with 500 μM 4-

nitrophenyl-α-xylopyranoside (α-xyl) or 4-nitrophenyl-β-xylopyranoside (β-xyl) overnight, where β-xyl disrupts HSPG elongation[39,40]. The overnight treatment was followed by PEC introduction for 30 min.

Addition of heparin, 200 U/ml, to the media containing PECs almost completely abolished cellular interactions, Figure 5-8(A), consistent with previous data using lipo- and polyplexes[41]. Surface binding was reduced (93%), while internalization diminished by 58%. Both effects were statistically significant. Heparin, because of its highly anionic nature and as a HSPG mimetic, non-specifically adhered to the complexes, causing the neutralization of positively charged groups on the PEC corona; prospective cell binding sites were masked. The neutralization was possibly followed by destabilization of complexes in solution preventing cell binding and entry[42]. The destabilization simultaneously could have caused an increase in size, another obstacle for efficient PEC delivery[43].

Incubation with a HSPG biosynthesis inhibitor, β-xyl, supported the hypothesis that membrane-associated HSPG partly mediated the attachment and internalization of PECs, as shown in Figure 5-8(B). HMVECs were incubated with either 500 μM β-xyl or α-xyl 24 h previous to PEC exposure. After which, the cells are washed and PECs were added for 30 min. The two xylosides have the same molecular weight, but only the beta isomer competes with the proteoglycan core protein xylosyl residues for the galactosyltransferase I, inhibiting the construction of glycosaminoglycans. The depleted HSPG by, addition of β-xyl, led to a 47% reduction in surface PEC binding compared to the control. Exposure to the α-xyl isoform led to no statistical deviation in binding and uptake compared to the control, as expected. Internalization was not statistically affected

for either xylopyranoside, although β-xyl did show an obvious decrease and possible HSPG role in endocytosis. The remaining portion of binding may be non-specific and electrostatic, but also due to sufficient amount of HSPG that persisted. This result was in agreement with results published for cationic polyamines[40] and DNA-loaded liposomes[44].

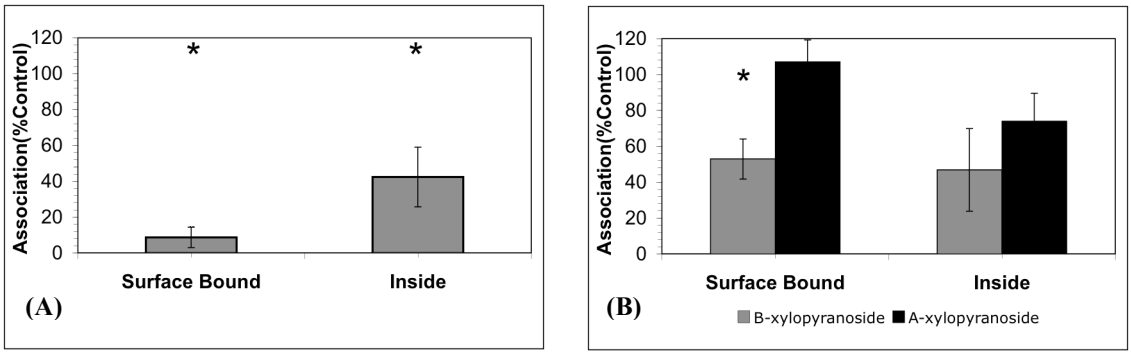

Figure 5-8. HSPG dependence on cell binding. (A) shows the competitive inhibition of attachment and binding by incubation of cells with PECs and 200 U/ml heparin. (B) displays the role of HSPG in PEC binding. HMVEC were 24 h pre-incubated with either 4-nitrophenyl-α-xylopyranoside (α-xyl, black) or 4-nitrophenyl-β-xylopyranoside (β-xyl, gray), where the α-isomer does not inhibit HSPG biosynthesis. Only the surface binding differed statististically from the control ($p<0.05$, $n=3$).

Non-Specific Binding Verified by Scatchard Plots

Using FITC-labeled PECs, a FACS-based Scatchard equilibrium experiment for the detection and characterization of non-specific binding was developed for titrations performed at 37°C and 4°C. The conventional binding curves are shown in Figure 5-9(A,B). Scatchard titrations were prepared by exposing HMVEC-1 cells to serial PEC dilutions over 3 orders of magnitude, over the concentration range tested for toxicity by MTT, for 3 hours at 37°C and 4°C. Efforts were made to cover as wide a range of PEC concentrations as possible and to carry the measurements to the highest allowable

concentrations by solubility and practical circumstances, i.e. PEC aggregation. The ratio of PECs added to initial cell density ranged from 32000:1 down to 200:1; proportion of PEC bound to initial cell density varied from 30000:1 to 5:1, both of which were calculated experimentally. The time was defined by the kinetic experiments, Figure 5-5(A,B), and the FACS acquisition performed on a FACSAria system fitted with a photomultiplier tube on the forward scattering laser for more sensitive detection of cell bound PECs. The exposure was followed by detachment, acquisition of MFI, and conversion of bound (total associated fluorescence) indices to particle concentrations. This was possible after calibration of our ~200 nm PECs with known concentrations of NIST-traceable beads. The approach allowed the Scatchard transformation (bound/free versus bound) and also provided a verification of non-specific, adsorptive binding seen in kinetic experiments shown in Figures 5-9(C,D) for incubations at 37°C and 4°C, respectively. Also it was the first such FACS based Scatchard representation of non-specific interactions of a polymeric drug delivery system.

In both cases, the binding isotherms, Figure 5-9(A,B) form the lower half of the standard S-curve saturation seen in steady-state experiments; there was no apparent saturation of cell surface receptors interacting with PECs. However, the curves never approach saturation. The data transformations for Figure 5-9(C,D) showed an inverse relationship for the apparent binding constant due to extensive cooperativity, an atypical response in Scatchard plots. In many documented in vitro binding experiments, the initial positive slope goes to a maxima followed by a monotonic decrease in slope as the total ligand increases in concentration[45-48]. Similar behavior to Figure 5-9(A,B) has been

observed in human serum albumin binding[49,50], but no inflection point was observed in this study.

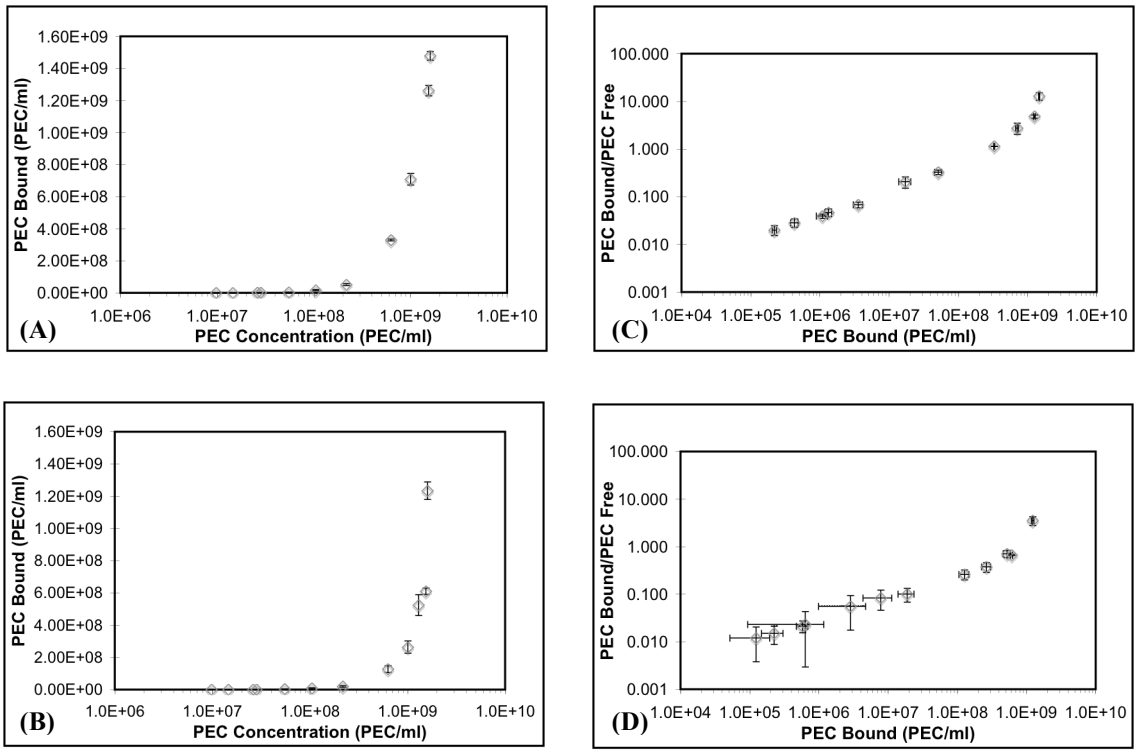

Figure 5-9. PECs exhibit non-saturable binding and positive cooperativity for 3 h at 37°C and 4°C. Incubations for (A) and (C) were performed at 37°C, while (B) and (D) at 4°C. (A) and (B) are dose-dependent binding curves. (C) and (D) represented Scatchard plot analysis. Curves were determined by flow cytometry (n=3). The ratios of bound and free PECs for each concentration were determined based on the MFI of each dose in the absence of cells, followed by correlation to calibration curves determined as in Figure 5-2. Y-error bars represent the average ± s.e. in calculated bound PECs, while X-error bars are the free PEC concentration ± s.e. by difference between initial dose and bound.

Conclusions

This study provides a comprehensive study of naked PEC interactions with endothelial cells in vitro through the use of applications ideally suited for nanoscale system: PCS and FACS. Effective delivery of PECs is of paramount significance for the development of systems that target the vascular endothelium, the nutrient supply line for tumor environments[2]. While many of the current PEC delivery systems have focused and reported on gene delivery[51-54], there has been little focus on the process of PEC interactions that occur before the expression of DNA. Therefore, in order to improve polyelectrolyte drug delivery systems, it is critical to understand the mechanisms and barriers for successful interactions with target cells.

The architectures described herein provide a media-stable, core-shell nanoparticulate structure with physicochemical properties ideal for use in vitro. PCS measurements provided proof that instantaneous complexation of oppositely charged polyelectrolytes led to nanoparticle structures with ~200 nm hydrodynamic diameter and robust serum stability, verified by no statistical change in size after isolation and resuspension, appropriate for systemic delivery. Moreover, the presentation of outer shell amine groups may allow the presentation of ligands for targeted accumulation in disease sites. A lack of long term cytoxicity was first demonstrated by MTT, while short term effects diagnosed by no intercalation of PI with DNA for concentrations of PECs that were orders of magnitude larger than the cell population.

The incorporation of a fluorescently-labeled polymer constituent allowed the use of flow cytometry to evaluate cellular interactions. Through the use of trypan blue, flow cytometry can distinguish between surface associated and internalized PECs. This

facilitated the understanding cellular compartmentalization of PECs without cell lysis, a method commonly used in other studies[25,38,55,56]. Initial binding and internalization studies showed that the associative phenomena were saturable and sensitive to proteolytic enzymes.

The mechanisms of PEC attachment and entry were further probed through the use of various inhibitors at concentrations and levels prescribed in the literature: cytochalasin D[37,57], azide/2-deoxyglucose[27], reduced temperature[5], exogenous heparin[42,43], and two xylopyranoside enantiomers[39]. No data exists to date on the specific mechanisms of PEC uptake, although liposomes have been found to be endocytosed[5,58,59].

The use of reduced temperature and depletion of cellular ATP by azide/2-deoxyglucose slowed uptake and binding. This would indicate that both active processes are energy-dependent. However, some residual attachment and internalization persisted in an energy-independent manner, indicative of a process other than endocytosis. Transduction, or direct PEC entry, may contribute to this portion of the internalization after diffusion of complexes to the cell surface[60]. PMCG, a polymer with repeating guandinium residues and structural similarity to arginine resides likely facilitated penetration across the plasma membrane[61,62]. This result was consistent with a previous finding for DNA complexed with a sequence of the HIV-Tat protein[63].

The inhibition of uptake by cytochalasin D identified the role of macropinocytosis and non-clathrin, non-caveolae dependent endocytosis in the trafficking of PECs to the cell interior. Macropinocytosis is lipid raft-mediated with macropinosomes often larger than 1 μm and dependent on cytoskeletal rearrangements[64]. Clathrin and caveolae dependent endocytosis rely on clathrin coated pits (~120 nm) or caveolae invaginations

(~60 nm), respectively[65]. The PEC system applied in this study had hydrodynamic diameters consistently around 200 nm making them too large for the latter processes.

There is increasing evidence that HSPGs play a role as cellular entry gateways for positively charged molecules and synthetic delivery vehicles. It has already been reported that HSPG facilitate the entry of polyamines and cationic liposomes[7,42]. HSPG biosynthetic inhibition of cell-associative properties by 4-nitrophenyl-β-xylopyranoside further verified the role of macropinocytosis[66]. Interactions between HSPG and PECs carrying very cationic chemical groups are inevitable because the anionic cell surface proteoglycans encompass the entire cell surface[67]. The remaining amount of PECs bound suggests that, apart from HSPG, there are other cell surface receptors, possibly sialylated glycoproteins or glycolipids, that may account for PEC attachment.

Because HSPGs, in the form of syndecans and glypicans, are involved in adhesion, migration, and cytoskeletal organization, it was no surprise that the inhibition of HSPG binding coordinated with actin microfilament affected uptake. Cytoplasmic tails and actin filaments are connected inside the cell through linker proteins. Therefore, binding to adhesion receptors provides the initial step for particle engulfment mediated by membrane rufflings caused by networks of cortical actin fibers[29].

The evaluation of nanoparticle concentrations, in terms of PEC/ml, allowed the determination of binding isotherms and Scatchard transformations for multi-component PECs. Scatchard plots are largely ignored for polymeric drug delivery systems, but characterizations of the type of binding occurring in biological systems is critical for the development of target-specific nanovehicles. Non-specific PEC binding was further verified by the shape of the Scatchard plots. Independent of temperature, the curves have

positive slopes, where PECs bind to a heterogeneous group of receptors with cooperativity. Because PECs are not hard objects, their amorphous nature leads to conformational flexibility and adaptability, further facilitating the cell association. The positive slopes have been interpreted to indicate possible cooperativity and interaction with multiple binding sites and do not lend themselves to the analyses generally performed with typical Scatchard curves in terms of calculation of binding parameters[68]. The positive cooperativity would suggest that the binding of one PEC to any receptor on the cell surface created an energetically favorable site for another PEC.

Mathematically, the total concentration of bound PEC, [Bound], to a single class of receptors can be defined by the Michaelis-Menten equation below:

$$[Bound] = \frac{[R_{total}] * [L_{Free}]}{K_d + [L_{Free}]} \tag{5-1}$$

where $[L_{Free}]$, $[R_{total}]$, and K_d the concentration of free PEC (ligand), total receptor concentration (constant), and equilibrium binding constant, respectively. In the case of the naked PECs, the free ligand was at concentrations much lower than the K_d, leading to a linear relationship between bound and free PECs with a slope of R_{total}/K_d. Breakdown in mass action laws may also be a contributing factor to PEC binding: receptor heterogeneity, cooperativity, and irreversible binding. PECs bind promiscuously to any receptor on the cell surface, as shown by PECs in the presence of depleted HSPG.

Brodersen and coworkers[49] argue that if the interactions were saturable, the binding isotherm should have an inflexion point indicating the existence of such a limit. PECs appeared to bind cells without the possibility of displaceability, likely until effective charge neutralization between the anionic cell surface (functioning only as a

charged entity) and cationic microdomains of the PEC, but saturation does not appear to be possible.

In conclusion, when considering the binding and internalization mechanisms of PECs, the particular types of interactions must be considered for developing effective targeting approaches. Additionally, systems must be non-toxic both in cell culture and upon systemic administration and have physicochemical characteristics to facilitate cellular uptake. For multi-component PECs, HMVECs showed no appreciable toxicity and are internalized through non-specific macropinocytosis. The binding and association was deemed totally non-specific by a combinatorial FACS and Scatchard design. The system presented in this study further provided a platform which can be subsequently modified for a targeted delivery approach due to its favorable physical attributes and rapid intra- and extracellular accumulation. Classical methods, like the Scatchard plots, combined with more current technologies, FACS, are critical for the further design and application of nanoscale delivery architectures. Meeting requirements such as low cytoxicity and significant uptake into a target cell line, this system provides a promising candidate for further development and study. Moreover, the chemical nature and presence of common functional groups (carboxyls and amines) allows for simple incorporation of small drugs or non-viral payloads and targeting vectors.

References

1. Simionescu, M.; Gafencu, A.; Antohe, F. "Transcytosis of plasma macromolecules in endothelial cells: a cell biological survey" *Microscopy Research And Technique* **2002,** 57, 269-288.

2. Hood, J. D.; Bednarski, M.; Frausto, R.; Guccione, S.; Reisfeld, R. A.; Xiang, R.; Cheresh, D. A. "Tumor regression by targeted gene delivery to the neovasculature" *Science* **2002,** 296, 2404-2407.

3. Hallahan, D.; Geng, L.; Qu, S. M.; Scarfone, C.; Giorgio, T.; Donnelly, E.; Gao, X.; Clanton, J. "Integrin-mediated targeting of drug delivery to irradiated tumor blood vessels" *Cancer Cell* **2003,** 3, 63-74.

4. Jain, R. K. "Normalization of tumor vasculature: an emerging concept in antiangiogenic therapy" *Science* **2005,** 307, 58-62.

5. Huth, U. S.; Schubert, R.; Peschka-Suss, R. "Investigating the uptake and intracellular fate of pH-sensitive liposomes by flow cytometry and spectral bio-imaging" *Journal Of Controlled Release* **2006,** 110, 490-504.

6. Kessner, S.; Krause, A.; Rothe, U.; Bendas, G. "Investigation of the cellular uptake of E-Selectin-targeted immunoliposomes by activated human endothelial cells" *Biochimica Et Biophysica Acta-Biomembranes* **2001,** 1514, 177-190.

7. Marty, C.; Meylan, C.; Schott, H.; Ballmer-Hofer, K.; Schwendener, R. A. "Enhanced heparan sulfate proteoglycan-mediated uptake of cell-penetrating peptide-modified liposomes" *Cellular And Molecular Life Sciences* **2004,** 61, 1785-1794.

8. Chern, C. S.; Lee, C. K.; Chang, C. J. "Electrostatic interactions between amphoteric latex particles and proteins" *Colloid and Polymer Science* **2004,** 283, 257-264.

9. Fatouros, D. G.; Piperoudi, S.; Gortzi, O.; Ioannou, P. V.; Frederik, P.; Antimisiaris, S. G. "Physical stability of sonicated arsonoliposomes: Effect of calcium ions" *Journal of Pharmaceutical Sciences* **2005,** 94, 46-55.

10. Sugrue, S. "Predicting and controlling colloid suspension stability using electrophoretic mobility and particle size measurements" *American Laboratory* **1992,** 24, 64-71.

11. Carlesso, G.; Kozlov, E.; Prokop, A.; Unutmaz, D.; Davidson, J. M. "Nanoparticulate system for efficient gene transfer into refractory cell targets" *Biomacromolecules* **2005,** 6, 1185-1192.

12. Panyam, P.; Labhasetwar, V. "Biodegradable nanoparticles for drug and gene delivery to cells and tissue" *Advanced Drug Delivery Reviews* **2003,** 55, 329-347.

13. Wood, K. C.; Little, S. R.; Langer, R.; Hammond, P. T. "A family of hierarchically self-assembling linear-dendritic hybrid polymers for highly efficient targeted gene delivery" *Angewandte Chemie-International Edition* **2005,** 44, 6704-6708.

14. Ogawa, K.; Sato, S.; Kokufuta, E. "Formation of intra- and interparticle polyelectrolyte complexes between cationic nanogel and strong polyanion" *Langmuir* **2005,** 21, 4830-4836.

15. Tong, W. J.; Gao, C. Y.; Mohwald, H. "Stable weak polyelectrolyte microcapsules with pH-responsive permeability" *Macromolecules* **2006,** 39, 335-340.

16. Fitch, R. M., In *Polymer Colloids: A Comprehensive Approach*, Academic Press: New York, 1997.

17. Csaba, N.; Caamano, P.; Sanchez, A.; Dominguez, F.; Alonso, M. J. "PLGA: poloxamer and PLGA: poloxamine blend nanoparticies: New carriers for gene delivery" *Biomacromolecules* **2005,** 6, 271-278.

18. Shenoy, D.; Little, S.; Langer, R.; Amiji, M. "Poly(ethylene oxide)-modified poly(beta-amino ester) nanoparticles as a pH-sensitive system for tumor-targeted delivery of hydrophobic drugs: part 2. in vivo distribution and tumor localization studies" *Pharmaceutical Research* **2005,** 22, 2107-2114.

19. Hed, J.; Hallden, G.; Johansson, S. G. O.; Larsson, P. "The use of fluorescence quenching in flow cytofluorometry to measure the attachment and ingestion phases in phagocytosis in peripheral blood without prior cell separation" *Journal Of Immunological Methods* **1987,** 101, 119-125.

20. Jevprasesphant, R.; Penny, J.; Attwood, D.; D'Emanuele, A. "Transport of dendrimer nanocarriers through epithelial cells via the transcellular route" *Journal Of Controlled Release* **2004,** 97, 259-267.

21. Rejman, J.; Oberle, V.; Zuhorn, I. S.; Hoekstra, D. "Size-dependent internalization of particles via the pathways of clathrin-and caveolae-mediated endocytosis" *Biochemical Journal* **2004,** 377, 159-169.

22. Sahlin, S.; Hed, J.; Rundquist, I. "Differentiation between attached and ingested immune-complexes by a fluorescence quenching cytofluorometric assay" *Journal Of Immunological Methods* **1983,** 60, 115-124.

23. Voinea, M.; Manduteanu, I.; Dragomir, E.; Carpraru, M.; M., S. "Immunoliposomes directed toward VCAM-1 interact specifically with activated endothelial cells-a potential tool for specific drug delivery" *Pharmaceutical Research* **2005,** 22, 1906-1917.

24. Desai, M. P.; Labhasetwar, V.; Walter, E.; Levy, R. J.; Amidon, G. L. "The mechanism of uptake of biodegradable microparticles in Caco-2 cells is size dependent" *Pharmaceutical Research* **1997,** 14, 1568-1573.

25. Win, K. Y.; Feng, S. S. "Effects of particle size and surface coating on cellular uptake of polymeric nanoparticles for oral delivery of anticancer drugs" *Biomaterials* **2005,** 26, 2713-2722.

26. Catizone, A.; Albani, L. M.; Reola, F.; Alescio, T. "A quantitative assessment of nonspecific pinocytosis by human endothelial-cells surviving in-vitro" *Cellular And Molecular Biology* **1993,** 39, 155-169.

27. Panyam, J.; Labhasetwar, V. "Dynamics of endocytosis and exocytosis of poly(D,L-lactide-co-glycolide) nanoparticles in vascular smooth muscle cells" *Pharmaceutical Research* **2003,** 20, 212-220.

28. Rupper, A.; Cardelli, J. "Regulation of phagocytosis and endo-phagosomal trafficking pathways in Dictyostelium discoideum" *Biochimica Et Biophysica Acta-General Subjects* **2001,** 1525, 205-216.

29. Kopatz, I.; Remy, J. S.; Behr, J. P. "A model for non-viral gene delivery: through syndecan adhesion molecules and powered by actin" *Journal Of Gene Medicine* **2004,** 6, 769-776.

30. Rothbard, J. B.; Jessop, T. C.; Wender, P. A. "Adaptive translocation: the role of hydrogen bonding and membrane potential in the uptake of guanidinium-rich transporters into cells" *Advanced Drug Delivery Reviews* **2005,** 57, 495-504.

31. Kim, S. H.; Jeong, J. H.; Chun, K. W.; Park, T. G. "Target-specific cellular uptake of PLGA nanoparticles coated with poly(L-lysine)-poly(ethylene glycol)-folate conjugate" *Langmuir* **2005,** 21, 8852-8857.

32. Lorenz, M. R.; Holzapfel, V.; Musyanovych, A.; Nothelfer, K.; Walther, P.; Frank, H.; Landfester, K.; Schrezenmeier, H.; Mailander, V. "Uptake of functionalized, fluorescent-labeled polymeric particles in different cell lines and stem cells" *Biomaterials* **2006,** 27, 2820-2828.

33. Suh, H.; Jeong, B. M.; Liu, F.; Kim, S. W. "Cellular uptake study of biodegradable nanoparticles in vascular smooth muscle cells" *Pharmaceutical Research* **1998,** 15, 1495-1498.

34. Thomas, T. P.; Majoros, I. J.; Kotlyar, A.; Kukowska-Latallo, J. F.; Bielinska, A.; Myc, A.; Baker, J. R. "Targeting and inhibition of cell growth by an engineered dendritic nanodevice" *Journal Of Medicinal Chemistry* **2005,** 48, 3729-3735.

35. Weissenbock, A.; Wirth, M.; Gabor, F. "WGA-grafted PLGA-nano spheres: preparation and association with Caco-2 single cells" *Journal Of Controlled Release* **2004,** 99, 383-392.

36. Gill, P. J.; Silbert, C. K.; Silbert, J. E. "Effects of heparan-sulfate removal on attachment and reattachment of fibroblasts and endothelial-cells" *Biochemistry* **1986,** 25, 405-410.

37. Nakase, I.; Niwa, M.; Takeuchi, T.; Sonomura, K.; Kawabata, N.; Koike, Y.; Takehashi, M.; Tanaka, S.; Ueda, K.; Simpson, J. C.; Jones, A. T.; Sugiura, Y.; Futaki, S. "Cellular uptake of arginine-rich peptides: roles for macropinocytosis and actin rearrangement" *Molecular Therapy* **2004,** 10, 1011-1022.

38. Behrens, I.; Pena, A. I. V.; Alonso, M. J.; Kissel, T. "Comparative uptake studies of bioadhesive and non-bioadhesive nanoparticles in human intestinal cell lines and rats: The effect of mucus on particle adsorption and transport" *Pharmaceutical Research* **2002,** 19, 1185-1193.

39. Belting, M. "Heparan sulfate proteoglycan as a plasma membrane carrier" *Trends In Biochemical Sciences* **2003,** 28, 145-151.

40. Belting, M.; Persson, S.; Fransson, L. A. "Proteoglycan involvement in polyamine uptake" *Biochemical Journal* **1999,** 338, 317-323.

41. Ruponen, M.; Ronkko, S.; Honkakoski, P.; Pelkonen, J.; Tammi, M.; Urtti, A. "Extracellular glycosaminoglycans modify cellular trafficking of lipoplexes and polyplexes" *Journal Of Biological Chemistry* **2001,** 276, 33875-33880.

42. Mislick, K. A.; Baldeschwieler, J. D. "Evidence for the role of proteoglycans in cation-mediated gene transfer" *Proceedings Of The National Academy Of Sciences Of The United States Of America* **1996,** 93, 12349-12354.

43. Wiethoff, C. M.; Smith, J. G.; Koe, G. S.; Middaugh, C. R. "The potential role of proteoglycans in cationic lipid-mediated gene delivery - studies of the interaction of cationic lipid-DNA complexes with model glycosaminoglycans" *Journal Of Biological Chemistry* **2001,** 276, 32806-32813.

44. Mounkes, L. C.; Zhong, W.; Cipres-Palacin, G.; Heath, T. D.; Debs, R. J. "Proteoglycans mediate cationic liposome-DNA complex-based gene delivery in vitro and in vivo" *Journal Of Biological Chemistry* **1998,** 273, 26164-26170.

45. Clegg, L. S.; Lindup, W. E. "Scatchard plots with a positive slope - dependence upon ligand concentration" *Journal Of Pharmacy And Pharmacology* **1984,** 36, 776-778.

46. Nesbitt, W. E.; Doyle, R. J.; Taylor, K. G.; Staat, R. H.; Arnold, R. R. "Positive Cooperativity in the binding of Streptococcus sanguis to hydroxylapatite" *Infection And Immunity* **1982,** 35, 157-165.

47. Thaler, C. D.; Cardullo, R. A. "The initial molecular interaction between mouse sperm and the zona pellucida is a complex binding event" *Journal Of Biological Chemistry* **1996,** 271, 23289-23297.

48. Thom, D.; Cox, D. S.; Safford, R.; Rees, D. A. "Co-operativity of lectin binding to fibroblasts and its relation to cellular actomyosin" *Journal Of Cell Science* **1979,** 39, 117-136.

49. Brodersen, R.; Honore, B.; Larsen, F. G. "Serum albumin - a non-saturable carrier" *Acta Pharmacologica Et Toxicologica* **1984,** 54, 129-133.

50. Paal, K.; Muller, J.; Hegedus, L. "High affinity binding of paclitaxel to human serum albumin" *European Journal Of Biochemistry* **2001,** 268, 2187-2191.

51. Dash, P. R.; Read, M. L.; Barrett, L. B.; Wolfert, M.; Seymour, L. W. "Factors affecting blood clearance and in vivo distribution of polyelectrolyte complexes for gene delivery" *Gene Therapy* **1999,** 6, 643-650.

52. Kabanov, A. V.; Vinogradov, S. V.; Suzdaltseva, Y. G.; Alakhov, V. Y. "Water-soluble block polycations as carriers for oligonucleotide delivery" *Bioconjugate Chemistry* **1995,** 6, 639-643.

53. Chittimalla, C.; Zammut-Italiano, L.; Zuber, G.; Behr, J. P. "Monomolecular DNA nanoparticles for intravenous delivery of genes" *Journal Of The American Chemical Society* **2005,** 127, 11436-11441.

54. Oupicky, D.; Ogris, M.; Seymour, L. W. "Development of long-circulating polyelectrolyte complexes for systemic delivery of genes" *Journal Of Drug Targeting* **2002,** 10, 93-98.

55. Panyam, J.; Dali, M. A.; Sahoo, S. K.; Ma, W. X.; Chakravarthi, S. S.; Amidon, G. L.; Levy, R. J.; Labhasetwar, V. "Polymer degradation and in vitro release of a model protein from poly(D,L-lactide-co-glycolide) nano- and microparticles" *Journal of Controlled Release* **2003,** 92, 173-187.

56. Panyam, J.; Sahoo, S. K.; Prabha, S.; Bargar, T.; Labhasetwar, V. "Fluorescence and electron microscopy probes for cellular and tissue uptake of poly(D,L-lactide-co-glycolide) nanoparticles" *International Journal of Pharmaceutics* **2003,** 262, 1-11.

57. Suzuki, T.; Futaki, S.; Niwa, M.; Tanaka, S.; Ueda, K.; Sugiura, Y. "Possible existence of common internalization mechanisms among arginine-rich peptides" *Journal Of Biological Chemistry* **2002,** 277, 2437-2443.

58. Finkelstein, M.; Weissmann, G. "Introduction of enzymes into cells by means of liposomes" *Journal Of Lipid Research* **1978,** 19, 289-303.

59. Simoes, S.; Slepushkin, V.; Pires, P.; Gaspar, R.; de Lima, M. C. P.; Duzgunes, N. "Human serum albumin enhances DNA transfection by lipoplexes and confers resistance to inhibition by serum" *Biochimica Et Biophysica Acta-Biomembranes* **2000,** 1463, 459-469.

60. Zaro, J. L.; Shen, W. C. "Quantitative comparison of membrane transduction and endocytosis of oligopeptides" *Biochemical And Biophysical Research Communications* **2003,** 307, 241-247.

61. Koch, A. M.; Reynolds, F.; Kircher, M. F.; Merkle, H. P.; Weissleder, R.; Josephson, L. "Uptake and metabolism of a dual fluorochrome tat-nanoparticle in HeLa cells" *Bioconjugate Chemistry* **2003,** 14, 1115-1121.

62. Richard, J. P.; Melikov, K.; Vives, E.; Ramos, C.; Verbeure, B.; Gait, M. J.; Chernomordik, L. V.; Lebleu, B. "Cell-penetrating peptides -a reevaluation of the mechanism of cellular uptake" *Journal Of Biological Chemistry* **2003,** 278, 585-590.

63. Ignatovich, I. A.; Dizhe, E. B.; Pavlotskaya, A. V.; Akifiev, B. N.; Burov, S. V.; Orlov, S. V.; Perevozchikov, A. P. "Complexes of plasmid DNA with basic domain 47-57 of the HIV-1 Tat protein are transferred to mammalian cells by endocytosis-mediated pathways" *Journal Of Biological Chemistry* **2003,** 278, 42625-42636.

64. Swanson, J. A.; Watts, C. "Macropinocytosis" *Trends In Cell Biology* **1995,** 5, 424-428.

65. Conner, S. D.; Schmid, S. L. "Regulated portals of entry into the cell" *Nature* **2003,** 422, 37-44.

66. Wadia, J. S.; Stan, R. V.; Dowdy, S. F. "Transducible TAT-HA fusogenic peptide enhances escape of TAT-fusion proteins after lipid raft macropinocytosis" *Nature Medicine* **2004,** 10, 310-315.

67. Yanagishita, M.; Hascall, V. C. "Cell-surface heparan-sulfate proteoglycans" *Journal Of Biological Chemistry* **1992,** 267, 9451-9454.

68. Judis, J. "Binding of codeine, morphine, and methadone to human serum proteins" *Journal Of Pharmaceutical Sciences* **1977,** 66, 802-806.

CHAPTER VI

ENHANCED BINDING TO ENDOTHELIAL CELLS BY TARGETED NANOPARTICULATE POLYELECTROLYTE COMPLEXES

Introduction

The site-specific delivery to cells or organs is a potentially attractive mode of treatment for increasing the therapeutic efficiency of drugs and reducing their toxicity[1]. Several strategies have been developed to employ specific ligands that interact with the endothelial cell (EC) surface to mediate delivery of drugs selectively to the tumor microenvironment without affecting normal tissue[2-4]. Tumor vasculature targeting is a promising strategy, as both primary tumor maturation and metastasis depend on the survival and growth of new blood vessels, termed angiogenesis. Additionally, intimate contact with the blood makes the tumor endothelial cell a uniquely accessible target within the tumor[5]. Extensive research has led to the identification and isolation of several regulators of angiogenesis, some of which represent therapeutic targets[6,7].

EC in the angiogenic vessels are known to overexpress several markers, which are either barely detectable or entirely absent in normal blood vessels[8-11]. A number of extracellular matrix molecules possess sites that interact with the tumor endothelium and play key roles in the regulation of angiogenesis[12]. Anti-angiogenic strategies have evolved that utilize this strategy, but the affinity and specificity of this interaction can be used as part of a targeting approach[13,14]. One such molecule, thrombospondin-1 (TSP-1) is a large glycoprotein composed of three identical subunits, which are covalently linked by interchain disulfide bonds and has intrinsic antiangiogenic activity[15].

TSP-1 has been proposed to play a role in numerous biological processes including embryonic development, angiogenesis, and hemostasis[16,17]. The ability of TSP-1 to regulate these processes has been attributed to its capacity to bind to matrix proteins, proteinases, growth factors, and cell surface receptors through specific domains. The receptor-mediated binding and endocytosis of TSP-1 is controlled by heparan sulfate proteoglycans (HSPGs)[18], cell surface receptors which are recognized by metastatic tumor cells upon their binding[19], and overexpressed in tumor milieu[20-23]. Further clinical use of TSP-1 is inhibited by the inability to synthesize large quantities of pharmaceutical grade protein and potentially off target side effects[12]. However, peptide sequences derived from certain TSP-1 domains show antiangiogenic activity and mimic the function of the intact macromolecule with high affinity binding. One such peptide (TSP521) specifically binds HSPGs and has been shown to target the vasculature of an experimental glioma model[24]. It also has been shown to impede the translocation of fibroblast growth factor-2 (FGF-2) to its tyrosine kinase receptor, resulting in inhibition of cell proliferation[25]. These properties led to the selection of TSP521 as a potential neovascular targeting platform.

Significant effort has been devoted to develop novel, nanoparticulate polymeric carriers for targeted drug delivery to specific cells and especially the tumor vasculature[26], many of which were listed in Chapter I. The development of pH and serum stable LMW PECs, prepared with frequency dispergation, in Chapter III, followed by their biological characterization and rapid cellular uptake (Chapter V), lend themselves as candidates for incorporation of TSP521. Two methods of incorporation of TSP521 were applied

followed by fluorescence techniques to evaluate peptide loading and study the cellular interactions with human microvascular endothelial cells (HMVECs):

- passive entrapment after TSP521 conjugation to polyethylene glycol (PEG) to achieve both a geometric and flexible presentation[27], decreased susceptibility to circulatory proteolytic enzymes, and improved phamacokinetic properties[28]
- direct, covalent coupling by 1-ethyl-3-(3-dimethyl-aminopropyl) carbodiimide (EDAC)/N-hydroxysuccinimide (NHS) two-step, zero-length cross-linking[29] of the aspartic acid carboxylic acid to surface PEC amines.

Experimental Procedures

Many procedures were applied as defined in Chapter II. LMW PECs were fabricated as described in *PEC Fabrication*, with 20 kHz frequency dispergation. FITC was incorporated for fluorescence studies as per *Polymer Labeling* and *Fluorescent PEC Preparation*. Physicochemical characteristics were characterized by *PEC Size and Zeta Potential*. HMVECs were cultured as defined in *Cell Line and Maintenance.* Cytotoxicity was evaluated by *PEC Effects on HMVEC-1 Proliferation.* Subsequent to fluorescent PEC preparation and *Incorporation of TSP521: Direct Surface Coupling and Passive Entrapment,* various methodologies were applied: *Flow Cytometric (FACS) Detection of PEC/Cell Interactions*, *Saturation PEC-Cell Association Kinetics*, *Treatment of Cells with Various Inhibitors*, and *Scatchard Plots*. Compartmentalization (surface bound versus internalized) was analyzed by extracellular FITC quenching with trypan blue.

Statistical Analysis

Statistical analysis was performed using JMP-IN 5.1 (SAS, Cary, NC). Final preparations, with and without TSP521, in cell growth media were compared by two-sample t-test to evaluate the differences between sizes, zeta potentials, and polydispersity indices (PDI). One-way ANOVA was used to compare cell proliferation data with controls (PEC-free exposures) while one-tail t-tests were applied to analyze statistical deviations of inhibitor responses from controls. All statistical tests were performed at $p<0.05$ (95% confidence level). Results are displayed as average ± standard error.

Results and Discussion

Synthesis and Characterization of TSP521-Loaded PECs

PEC self-assembly led to the spontaneous incorporation of PEGylated TSP521 (PEGp521), which was loaded (750 μg) into the anionic solution pre-fabrication. The other strategy involved TSP521 (100 μg), without PEG, linkage to the PEC corona post-production and isolation by centrifugation. The loading efficiency for PEGylated peptide entrapment was 2% (15 μg), verified isotopically and with fluorescence, whereas surface engineering by EDAC/NHS led to 10% immobilization (10 μg). Suspension of the two strategies in MCDB 131 (EC growth media) led to stable suspensions and showed no statistical difference ($p<0.05$) in size and zeta potential compared to non-targeted PECs (Table 6.1). The improved properties, reduced PDI, exhibited by PECs containing PEGylated TSP521 was due to the presence of PEG which increases the resistance to salt induced aggregation and provided a steric stabilization[30]. The residual increase in size shown by EDAC/NHS treated PECs was due to a small amount of cross-linking between PECs that may have occurred between protruding anionic carboxyl groups and amines.

Table 6-1. Targeted and non-Targeted PEC physicochemistry in EC growth media.

Platform	Size (nm)	PDI	Zeta Potential (mV)
non-Targeted	192.3±16.6	0.393±0.186	-18.4±4.3
Targeted PEGp521	194.2±23.6	0.167±0.024	-25.2±5.6
Targeted EDAC/NHS	240.0±17.1	0.287±0.033	-27.4±1.6

Cytotoxicity of Targeted and non-Targeted PECs

Cytoxicity of targeted and non-targeted PECs was investigated using the MTT assay on HMVECs over the same conditions applied in Chapter V. Experimental observations, PEC doses, were compared to cells without PEC. One-way ANOVA was first applied to determine the heterogeneity in means while Dunnet's test evaluated the statistical response of each observation in comparison to the control. As shown in Figure 6-1, no statistical effect ($p<0.05$) on 72 h HMVEC cell viability was detected for serial PEC concentrations over three orders of magnitude. Additionally, the PEC to initial cell density ratio ranged from approximately 60000:1 down to 400:1. The wide span of limited cytotoxicity validated this PEC system as a candidate for targeted delivery to endothelial cells.

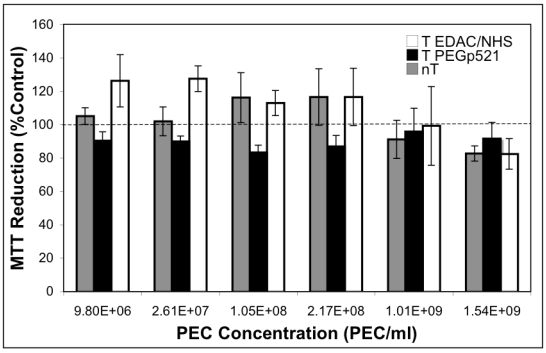

Figure 6-1. Relative viability of HMVEC-1 cells incubated 72 h with various concentrations of non-targeted (nT, gray), Targeted, PEGylated TSP521-containing (T PEGp521, black), and TSP521 coupled by EDAC/NHS PECs (T EDAC/NHS, white). Control cells are untreated. All results are given as the average ± standard error (n=3). No statistical differences in MTT reduction ($p>0.05$) were seen by one-way ANOVA (deviations amongst experimental means) and Dunnet's Test (experimental reductions compared to control).

Tryptic Effects on Targeted and non-Targeted PEC Interactions

Analogous to Chapter V, tryptic effects on PEC association was analyzed by exposing HMVEC to FITC-labeled complexes followed by either detachment by 0.25% trypsin/0.1% EDTA or 5 mM EDTA in HBSS, pH=7.6. Trypsin decreased the total amount of surface bound and internalized PECs, compared to cells detached by EDTA (Figure 6-2). Coincidentally, for non-targeted and targeted PECs (EDAC/NHS and PEGp521), an approximately 75% reduction in surface attached PECs and a 50% decrease in internalization, both statistically significant ($p<0.05$) to cells removed by EDTA, were effects independent of the targeting strategy. The result suggested that extracellular matrix proteins were involved in PEC binding and internalization. Trypsin, which strips HSPG[31], showed evidence that PEC associative properties may depend partially on surface proteoglycans, but, again, does not address the dependence on calcium.

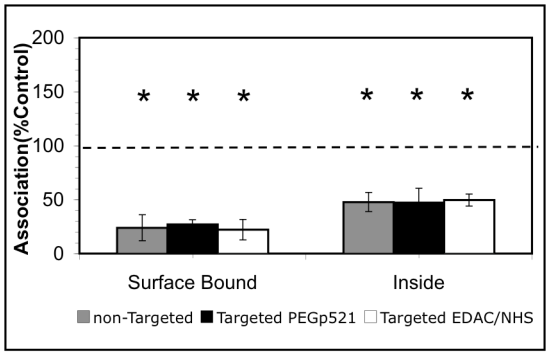

Figure 6-2. PEC binding and internalization sensitivity to trypsin exposure. The percent inhibition was defined as the ratio of $MFI_{trypsin}/MFI_{EDTA}$. Error bars represent the standard error for n=3. Asterisks indicate statistical effects at $p<0.05$ on both PEC internalization and surface binding.

Binding and Internalization Kinetics

Flow cytometry provided evidence of upregulated HMVEC binding and internalization for PECs with TSP521 loaded by both strategies (Figure 6-3). PECs ($1.54x10^9$ PEC/ml) were incubated with cells for up to 2 h. At the outset of the exposure, cells were detached using EDTA and analyzed by FACS for binding and internalization by trypan blue[32,33]. The level of binding for non-targeted PECs was relatively low while targeted PECs showed a 10 and 40 fold increase for EDAC/NHS and PEGp521 approaches, respectively. Uptake exhibited a 5 fold upregulation for both targeting platforms compared to non-targeted complexes. The enhanced binding and internalization kinetics of PEGylated and EDAC/NHS TSP521 PECs may be due to specific interactions with HSPG robustly expressed on endothelial cells[20-23], consistent with the activity of the free peptide[34]. Both PEC-containing compartments, surface and internal, appeared to reach saturation for platforms with and without targeting after an initial 20 min linear increase in the two compartments. This phenomenon indicated that both uptake mechanisms, non-targeted and targeted, were receptor-mediated[35,36]. Non-targeted PECs likely interacted with HMVEC through electrostatic interactions, particularly through PMCG[37], as described in Chapter V.

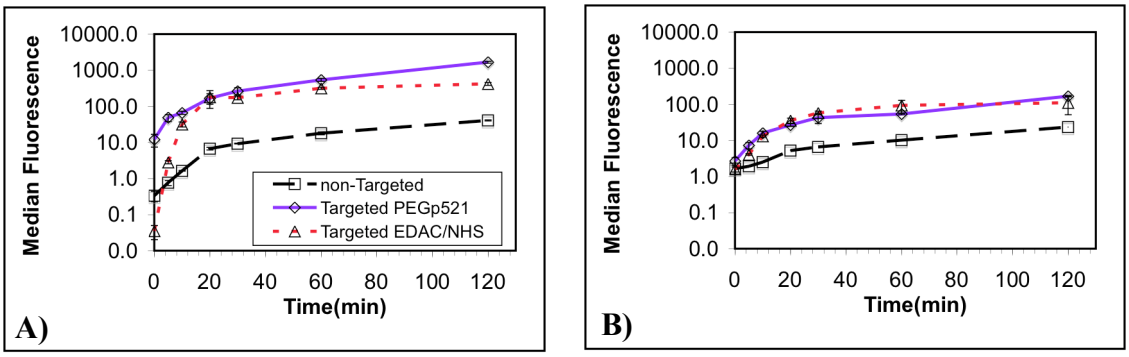

Figure 6-3. TSP521 incorporation enhances PEC association with endothelial cells. Kinetics of A) surface binding and B) internalization for PECs with and without the two TSP521 incorporation strategies were obtained by incubating HMVEC-1 cells with $1.54x10^9$ PEC/ml for up to two hours, detachment, and acquisition by FACS. All median fluorescent indices are the average ± standard error (n=3).

Exogenous Heparin Abolishes PEC Interactions

Recent studies have shown that extracellular glycosaminoglycans (heparin, chondroitin sulfate, dermatan sulfate) are a barrier to successful gene delivery via polymeric, cationic carrier vehicles[38-40]. The effects of extracellular glycosaminoglycans, 200 U/ml heparin, on binding and uptake on targeted and non-targeted PECs were clear and independent of TSP521 loading as shown in Figure 6-4(A,B), where Figure 6-4(B) displays the data with an expanded abscissa. Heparin blocked the interactions of PECs with HMVECs. Surface binding was reduced for non-targeted (97%), targeted PEGp521 PECs (95%), and targeted EDAC/NHS (88%) while internalization diminished by 69%, 86%, and 85%, respectively. No statistical effect was observed for comparisons between naked and TSP521-containing PECs. As detailed in Chapter V, heparin non-specifically adhered to the PECs causing the saturation and neutralization of positively charged

groups on the PEC corona and complex destabilization[40]. The presence of TSP521 also contributed to this effect as TSP-1 and the peptide have an affinity for heparin[19,41].

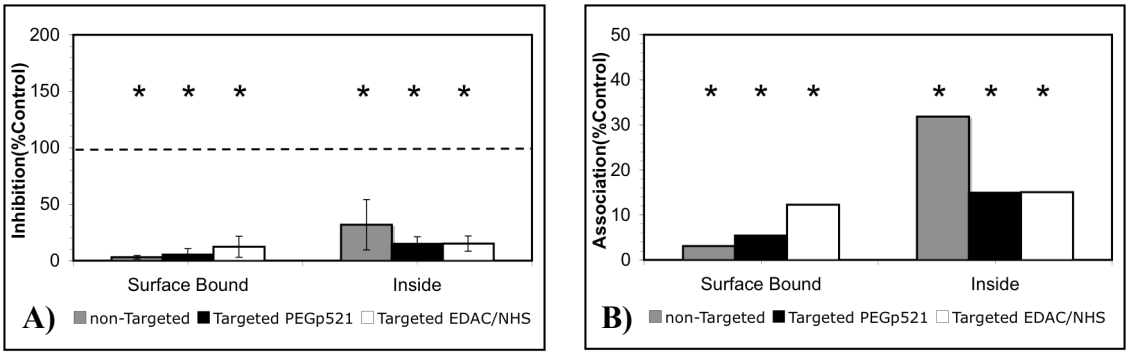

Figure 6-4. Exogenous heparin eliminated PEC/cell interactions. Incubation of PECs in the presence of 200 U/ml heparin completely inhibited surface binding and internalization of PECs (average±standard error, $p<0.05$).

Perturbation of HSPG Biosynthesis

Incubation with a HSPG biosynthesis inhibitor, 4-nitrophenyl-β-D-xylopyranoside (β-xyl), supported the hypothesis that membrane-associated HSPG partly mediated the attachment of PECs, as shown in Figure 6-5(B). β-xyl competes with xylose-substituted core proteins as a substrate for galactosyltransferases leading to inhibition of HSPG elongation whereas the α isomer has no inhibitory activity[42,43]. Figure 6(A) showed no statistical changes in PEC binding or internalization for HMVECs pre-incubated with 4-nitrophenyl-α-D-xylopyranoside (α-xyl). The inhibition of HSPG biosynthesis caused a 54%, 69%, and 42% decrease in surface PEC binding compared to the control for non-targeted, targeted PEGp521, and targeted EDAC/NHS PECs,

respectively. The 15% difference in surface binding between non-targeted and targeted PEGp521, although not statistically different, does show a higher dependence on the HSPG cell surface presentation. Internalization was not statistically affected for any system, although decreased in all cases, indicating that uptake of PECs may share a common endocytic pattern (macropinocytosis), a surprising finding since the internalization of TSP-1 has been found to be inhibited by overnight β-xyl treatment[18]. The remaining portion of binding may be non-specific and electrostatic, but also due to a sufficient amount of HSPG that persisted.

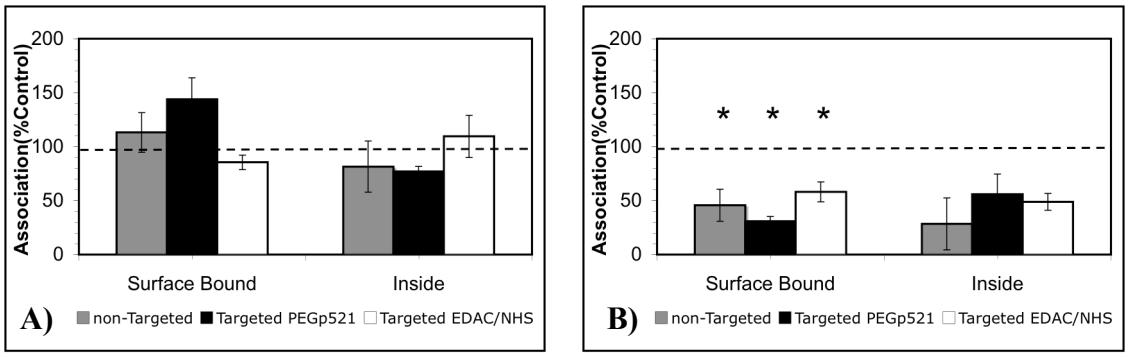

Figure 6-5. HSPG partly mediated PEC association. 24 h pre-incubation with A) inactive and B) active xylopyranoside isomers followed by 2 h PEC exposure led to inhibition of surface binding for n=3 (average ± standard error, $p<0.05$)

Detection of Targeting by FACS-based Scatchard Plots

The FACS-based Scatchard equilibrium experiment developed in Chapter V was applied to detect receptor-mediated binding for ligand-functionalized PECs. Scatchard titrations were prepared by exposing HMVEC-1 cells to serial PEC dilutions, over the concentration range tested for toxicity by MTT, for 3 hours at 37°C and 4°C. The

exposure was followed by detachment, acquisition of MFI, and conversion of bound indices to particle concentrations. This was, again, possible after calibration of our ~200 nm PECs with known concentrations of NIST-traceable beads. The approach also provided a verification of upregulated binding seen in kinetic experiments (Figure 6-3) and the first such FACS based Scatchard representation. Figure 6-6(A,B) represented the binding isotherms at 37°C and 4°C, while (C) and (D) Scatchard transformations at the same temperatures, respectively. Experiments at 4°C were performed to look at only binding, as discussed in Chapter V. These particular figures did not represent any saturable binding or receptor-mediated activity correlating to data represented in Figure 5-9.

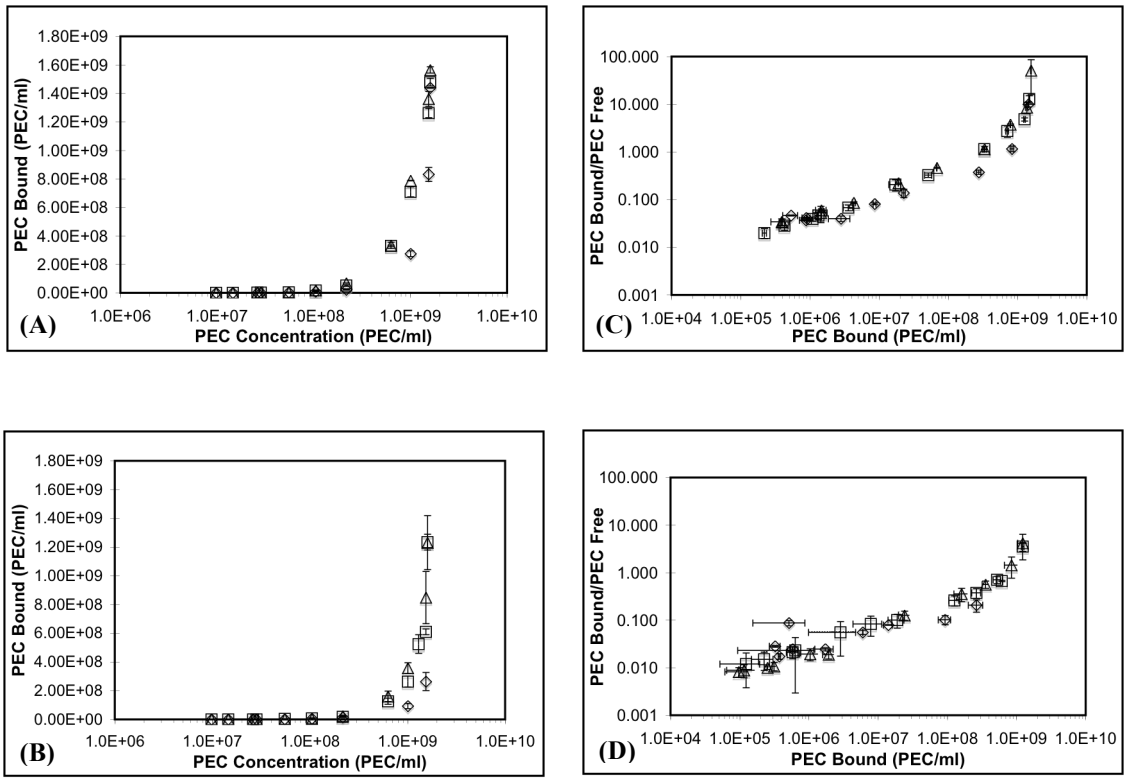

Figure 6-6. Targeted EDAC/NHS(△), Targeted PEGp521(◇), and non-targeted PECs(□) exhibit non-saturable binding and positive cooperativity for 3 h at 37°C and 4°C when displayed over all concentrations tested. Incubations for (A) and (C) were performed at 37°C, while (B) and (D) at 4°C. (A) and (B) are dose-dependent binding curves. (C) and (D) represented Scatchard plot analysis. Curves were determined by flow cytometry (n=3). The ratios of bound and free PECs for each concentration were determined based on the MFI of each dose in the absence of cells, followed by correlation to calibration curves determined as in Figure 5-2. Y-error bars represent the average ± s.e. in calculated bound PECs.

Further analysis of Figure 6-6 by isolation of the low concentration data, showed receptor mediated activity at 37°C and 4°C, upon Scatchard transformation as displayed in Figure 6-7(A,B). Through this limited concentration range, targeted PEGp521 PECs follow the laws of mass action. Algebraic rearrangement of equation 5-1 leads to equation 6-1:

$$[Bound] = \frac{[R_{total}]*[L_{Free}]}{K_d + [L_{Free}]} \tag{5-1}$$

$$\frac{[Bound]}{[L_{Free}]} = -\frac{[Bound]}{K_d} + \frac{[R_{total}]}{K_d} \tag{6-1}$$

The single monotonic transformation observed at both temperatures indicated a single class of binding sites[44], correlating to the weak affinity HSPG receptor for fibroblast growth factor-2 (FGF-2) binding[45]. This transformation allowed the calculation of an equilibrium dissociation binding constant, in terms of PEC/ml for 37°C ($1.00x10^8$ PEC/ml) and 4°C ($2.00x10^8$ PEC/ml). This verified the enhanced binding activity of targeted PEGp521 PECs seen in Figure 6-3(A,B) and limited saturation binding inside of this region shown in Figure 6-7(C,D). Further titration of the PEGylated TSP521 PECs showed positive cooperativity and no receptor-mediated binding, identical to the non-targeted system and targeted EDAC/NHS complexes. This indicated that as PECs were titrated to a 'breakthrough' concentration, the electrostatic nature of the PEC dominated the binding and effectively reduced the ability of TSP521 to interact specifically with HSPG. A breakdown in the mass action assumptions resulted, further verifying the electrostatic interaction between the anionic cell surface and PECs in the absence of a

ligand. Interestingly, direct zero-length ligation of TSP521 to amines on the PEC corona showed Scatchard plots with a positive slope, similar to the non-targeted system. This would imply, over the concentration range for Figure 6-7(A,B), that the presentation of PEGylated TSP521 was important, that possibly the peptide was sufficiently arranged on the surface to minimize electrostatic interactions. The behavior of non-targeted (all concentrations), targeted EDAC/NHS (all concentrations) and PEGp521 PECs (after [Bound]=$2x10^6$ PEC/ml at 37°C and [Bound]=$7x10^5$ PEC/ml at 4°C) denoted that concentrations never approached the equilibrium binding constant for a second regime of binding. Figure 6-7(C,D) showed that there was a limited range The limitation of that consequence was high concentrations resulted in PEC aggregation, and therefore, deviation from a nanoscale delivery system.

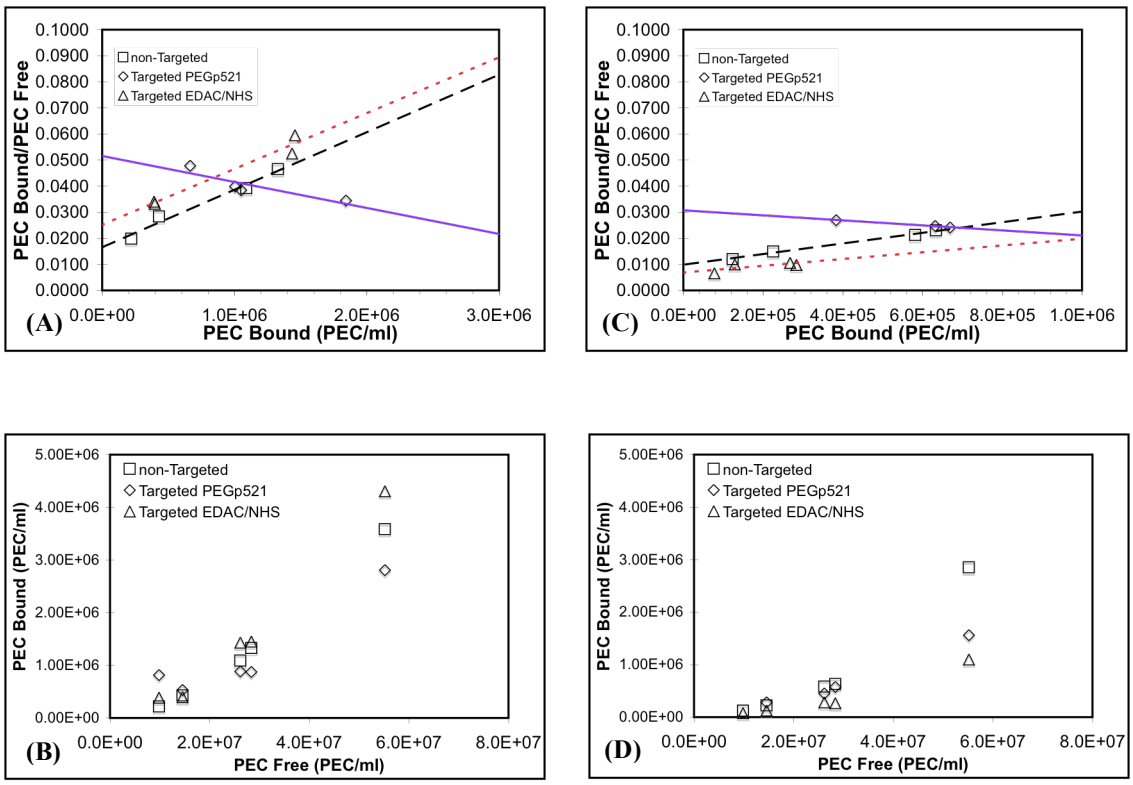

Figure 6-7. Scatchard representations for low concentration binding at A) 37°C and B) 4°C. Linear regressions were fitted to validate receptor-mediated activity for n=3. Targeted and non-targeted PECs were incubated with HMVECs for 3 h at 37°C, 5% CO_2, and 95% relative humidity. After washing steps, cell-bound PECs were analyzed by FACS. The ratios of bound and free PECs for each concentration was based on the MFI PECs in the absence of cells. C) and D) indicated a limited region where saturation binding occurred for targeted PEGp521 PECs at 37°C and 4°C, respectively.

Conclusions

TSP521, a HSPG binding peptide derived from TSP-1, was associated with the PEC by two different loading methods. It was found that these PECs had binding and internalization mechanisms that can be abolished by extracellular heparin that and were affected by trypsin exposure. Surface attachment was found to be controlled partially by HSPGs.

This study was undertaken primarily to confirm the theoretical expectation that Scatchard analysis could be performed satisfactorily with fluorescent PECs after incorporation of two targeting approaches. This was the first study that not only applied Scatchard transformations in PEC binding, but also the first to detect receptor-mediated activity of a surface engineered system. It was critical to derive the linear parameters after expansion of low concentrations of TSP521-containing PECs. The demonstration by FACS that binding was enhanced was not enough to establish a true single receptor interaction as the coupling of TSP521 by EDAC/NHS direct ligation did not demonstrate a classical Scatchard transformation; equation 6-1 could not be used to calculate a K_d or $[R_{total}]$.

The need for spacing that presents a molecule's active binding region away from a nanoparticle surface has been shown to effectively target liposomes with folic acid[46,47]. PEGylation of polypeptides and proteins is a widely used method of prolonging their biological half-life[28]; however, in this application conjugation was designed to modulate the presentation of the peptide by increasing its molecular mass and flexibility. The results showed that a key biochemical property of the peptide, HSPG affinity, was fully retained by PEGylated TSP521 conjugate. This may be a steric effect mediated by

anchoring the peptide chain to the PEG polymer. This would indicate that the peptide or targeting moiety must be at a length that can allow the molecule to interact specifically with its constitutive receptor and minimize the ubiquitous surface PEC electrostatic contributions. This conclusion evolved due to the fact that, by mass, the loading of TSP521 was similar: 10 μg (EDAC/NHS) and 15 μg (PEGp521), therefore the cell was able to interface properly with the active region of the peptide through elongation with PEG. The passive loading of TSP521, subsequent to its elongation with 4000 PEG molecules, permitted the docking of PECs through an assumed HSPG interface. This type of finding should lead to the development of better PEC targeting strategies that would display higher affinity binding activities.

References

1. Kessner, S.; Krause, A.; Rothe, U.; Bendas, G. "Investigation of the cellular uptake of E-Selectin-targeted immunoliposomes by activated human endothelial cells" *Biochimica Et Biophysica Acta-Biomembranes* **2001,** 1514, 177-190.

2. Hood, J. D.; Bednarski, M.; Frausto, R.; Guccione, S.; Reisfeld, R. A.; Xiang, R.; Cheresh, D. A. "Tumor regression by targeted gene delivery to the neovasculature" *Science* **2002,** 296, 2404-2407.

3. Kolonin, M.; Pasqualini, R.; Arap, W. "Molecular addresses in blood vessels as targets for therapy" *Current Opinion In Chemical Biology* **2001,** 5, 308-313.

4. Ruoslahti, E. "Targeting tumor vasculature with homing peptides from phage display" *Seminars In Cancer Biology* **2000,** 10, 435-442.

5. Neri, D.; Bicknell, R. "Tumour vascular targeting" *Nature Reviews Cancer* **2005,** 5, 436-446.

6. Ferrara, N.; Kerbel, R. S. "Angiogenesis as a therapeutic target" *Nature* **2005,** 438, 967-974.

7. Folkman, J. "Tumor angiogenesis: therapeutic implications" *New England Journal of Medicine* **1971,** 285, 1182-1186.

8. Burg, M. A.; Pasqualini, R.; Arap, W.; Ruoslahti, E.; Stallcup, W. B. "NG2 proteoglycan-binding peptides target tumor neovasculature" *Cancer Research* **1999,** 59, 2869-2874.

9. Friedlander, M.; Brooks, P. C.; Shaffer, R. W.; Kincaid, C. M.; Varner, J. A.; Cheresh, D. A. "Definition of 2 angiogenic pathways by distinct alpha(V) integrins" *Science* **1995,** 270, 1500-1502.

10. Schlingemann, R. O.; Rietveld, F. J. R.; Kwaspen, F.; Vandekerkhof, P. C. M.; Dewaal, R. M. W.; Ruiter, D. J. "Differential expression of markers for endothelial cells, pericytes, and basal lamina in the microvasculature of tumors and granulation tissue" *American Journal Of Pathology* **1991,** 138, 1335-1347.

11. Schlingemann, R. O.; Rietveld, F. J. R.; Dewaal, R. M. W.; Ferrone, S.; Ruiter, D. J. "Expression of the high molecular weight melanoma-associated antigen by pericytes during angiogenesis in tumors and in healing wounds" *American Journal Of Pathology* **1990,** 136, 1393-1405.

12. Clamp, A. R.; Jayson, G. C. "The clinical potential of antiangiogenic fragments of extracellular matrix proteins" *British Journal Of Cancer* **2005,** 93, 967-972.

13. Sato, H.; Takino, T.; Miyamori, H. "Roles of membrane-type matrix metalloproteinase-1 in tumor invasion and etastasis" *Cancer Science* **2005,** 96, 212-217.

14. Vihinen, P.; Ala-aho, R.; Kahari, V. M. "Matrix metalloproteinases as therapeutic targets in cancer" *Current Cancer Drug Targets* **2005,** 5, 203-220.

15. Reiher, F. K.; Volpert, O. V.; Jimenez, B.; Crawford, S. E.; Dinney, C. P.; Henkin, J.; Haviv, F.; Bouck, N. P.; Campbell, S. C. "Inhibition of tumor growth by systemic treatment with thrombospondin-1 peptide mimetics" *International Journal Of Cancer* **2002,** 98, 682-689.

16. Good, D. J.; Polverini, P. J.; Rastinejad, F.; Lebeau, M. M.; Lemons, R. S.; Frazier, W. A.; Bouck, N. P. "A tumor suppressor-dependent inhibitor of angiogenesis is immunologically and functionally indistinguishable from a fragment of thrombospondin" *Proceedings Of The National Academy Of Sciences Of The United States Of America* **1990,** 87, 6624-6628.

17. Mikhailenko, I.; Krylov, D.; Argraves, K. M.; Roberts, D. D.; Liau, G.; Strickland, D. K. "Cellular internalization and degradation of thrombospondin-1 is mediated by the amino-terminal heparin binding domain (HBD) - high affinity interaction of dimeric HBD with the low density lipoprotein receptor-related protein" *Journal Of Biological Chemistry* **1997,** 272, 6784-6791.

18. Godyna, S.; Liau, G.; Popa, I.; Stefansson, S.; Argraves, W. S. "Identification of the low-density-lipoprotein receptor-related protein (Lrp) as an endocytic receptor for thrombospondin-1" *Journal Of Cell Biology* **1995,** 129, 1403-1410.

19. Engelberg, H. "Actions of heparin that may affect the malignant process" *Cancer* **1999,** 85, 257-272.

20. Su, G.; Meyer, K.; Nandini, C. D.; Qiao, D. H.; Salamat, S.; Friedl, A. "Glypican-1 is frequently overexpressed in human gliomas and enhances FGF-2 signaling in glioma cells" *American Journal Of Pathology* **2006,** 168, 2014-2026.

21. Barbareschi, M.; Maisonneuve, P.; Aldovini, D.; Cangi, M. G.; Pecciarini, L.; Mauri, F. A.; Veronese, S.; Caffo, O.; Lucenti, A.; Palma, P. D.; Galligioni, E.; Doglioni, C. "High syndecan-1 expression in breast carcinoma is related to an aggressive phenotype and to poorer prognosis" *Cancer* **2003,** 98, 474-483.

22. Qiao, D. H.; Meyer, K.; Mundhenke, C.; Drew, S. A.; Friedl, A. "Heparan sulfate proteoglycans as regulators of fibroblast growth factor-2 signaling in brain endothelial cells" *Journal Of Biological Chemistry* **2003,** 278, 16045-16053.

23. Bernfield, M.; Gotte, M.; Park, P. W.; Reizes, O.; Fitzgerald, M. L.; Lincecum, J.; Zako, M. "Functions of cell surface heparan sulfate proteoglycans" *Annual Review Of Biochemistry* **1999,** 68, 729-777.

24. Bogdanov, A. A.; Marecos, E.; Cheng, H. C.; Chandrasekaran, L.; Krutzsch, H. C.; Roberts, D. D.; Weissleder, R. "Treatment of experimental brain tumors with trombospondin-1 derived peptides: an in vivo imaging study" *Neoplasia* **1999,** 1, 438-445.

25. Vogel, T.; Guo, N. H.; Krutzsch, H. C.; Blake, D. A.; Hartman, J.; Mendelovitz, S.; Panet, A.; Roberts, D. D. "Modulation of endothelial cell proliferation, adhesion, and motility by recombinant heparin-binding domain and synthetic peptides from the type-I repeats of thrombospondin" *Journal Of Cellular Biochemistry* **1993,** 53, 74-84.

26. Park, J. H.; Kwon, S. G.; Nam, J. O.; Park, R. W.; Chung, H.; Seo, S. B.; Kim, I. S.; Kwon, I. C.; Jeong, S. Y. "Self-assembled nanoparticles based on glycol chitosan bearing 5 beta-cholanic acid for RGD peptide delivery" *Journal of Controlled Release* **2004,** 95, 579-588.

27. Lu, J.; Jeon, E.; Lee, B. S.; Onyuksel, H.; Wang, Z. J. J. "Targeted drug delivery crossing cytoplasmic membranes of intended cells via ligand-grafted sterically stabilized liposomes" *Journal Of Controlled Release* **2006,** 110, 505-513.

28. Harris, J. M.; Chess, R. B. "Effect of pegylation on pharmaceuticals" *Nature Reviews Drug Discovery* **2003,** 2, 214-221.

29. Grabarek, Z.; Gergely, J. "Zero-length crosslinking procedure with the use of active esters" *Analytical Biochemistry* **1990,** 185, 131-135.

30. Oupicky, D.; Ogris, M.; Seymour, L. W. "Development of long-circulating polyelectrolyte complexes for systemic delivery of genes" *Journal Of Drug Targeting* **2002,** 10, 93-98.

31. Gill, P. J.; Silbert, C. K.; Silbert, J. E. "Effects of heparan sulfate removal on attachment and reattachment of fibroblasts and endothelial cells" *Biochemistry* **1986,** 25, 405-410.

32. Jevprasesphant, R.; Penny, J.; Attwood, D.; D'Emanuele, A. "Transport of dendrimer nanocarriers through epithelial cells via the transcellular route" *Journal Of Controlled Release* **2004,** 97, 259-267.

33. Rejman, J.; Oberle, V.; Zuhorn, I. S.; Hoekstra, D. "Size-dependent internalization of particles via the pathways of clathrin-and caveolae-mediated endocytosis" *Biochemical Journal* **2004,** 377, 159-169.

34. Guo, N. H.; Krutzsch, H. C.; Inman, J. K.; Roberts, D. D. "Thrombospondin 1 and type I repeat peptides of thrombospondin 1 specifically induce apoptosis of endothelial cells" *Cancer Research* **1997,** 57, 1735-1742.

35. Catizone, A.; Albani, L. M.; Reola, F.; Alescio, T. "A quantitative assessment of nonspecific pinocytosis by human endothelial cells surviving in vitro" *Cellular And Molecular Biology* **1993,** 39, 155-169.

36. Panyam, J.; Labhasetwar, V. "Dynamics of endocytosis and exocytosis of poly(D,L-lactide-co-glycolide) nanoparticles in vascular smooth muscle cells" *Pharmaceutical Research* **2003,** 20, 212-220.

37. Rothbard, J. B.; Jessop, T. C.; Wender, P. A. "Adaptive translocation: the role of hydrogen bonding and membrane potential in the uptake of guanidinium-rich transporters into cells" *Advanced Drug Delivery Reviews* **2005,** 57, 495-504.

38. Ruponen, M.; Ronkko, S.; Honkakoski, P.; Pelkonen, J.; Tammi, M.; Urtti, A. "Extracellular glycosaminoglycans modify cellular trafficking of lipoplexes and polyplexes" *Journal Of Biological Chemistry* **2001,** 276, 33875-33880.

39. Mounkes, L. C.; Zhong, W.; Cipres-Palacin, G.; Heath, T. D.; Debs, R. J. "Proteoglycans mediate cationic liposome-DNA complex-based gene delivery in vitro and in vivo" *Journal Of Biological Chemistry* **1998,** 273, 26164-26170.

40. Mislick, K. A.; Baldeschwieler, J. D. "Evidence for the role of proteoglycans in cation-mediated gene transfer" *Proceedings Of The National Academy Of Sciences Of The United States Of America* **1996,** 93, 12349-12354.

41. Yu, H. N.; Tyrrell, D.; Cashel, J.; Guo, N. H.; Vogel, T.; Sipes, J. M.; Lam, L.; Fillit, H. M.; Hartman, J.; Mendelovitz, S.; Panel, A.; Roberts, D. D. "Specificities of heparin-binding sites from the amino-terminus and type 1 repeats of thrombospondin-1" *Archives Of Biochemistry And Biophysics* **2000,** 374, 13-23.

42. Belting, M.; Persson, S.; Fransson, L. A. "Proteoglycan involvement in polyamine uptake" *Biochemical Journal* **1999,** 338, 317-323.

43. Belting, M. "Heparan sulfate proteoglycan as a plasma membrane carrier" *Trends In Biochemical Sciences* **2003,** 28, 145-151.

44. Klotz, I. M. "Numbers of receptor sites from scatchard graphs - facts and fantasies" *Science* **1982,** 217, 1247-1249.

45. Kan, M.; Disorbo, D.; Hou, J. Z.; Hoshi, H.; Mansson, P. E.; McKeehan, W. L. "High and low affinity binding of heparin binding growth factor to a 130-Kda receptor correlates with stimulation and inhibition of growth of a differentiated human hepatoma cell" *Journal Of Biological Chemistry* **1988,** 263, 11306-11313.

46. Lee, R. J.; Low, P. S. "Delivery of liposomes into cultured KB cells via folate receptor-mediated endocytosis" *Journal Of Biological Chemistry* **1994,** 269, 3198-3204.

47. Gabizon, A.; Horowitz, A. T.; Goren, D.; Tzemach, D.; Mandelbaum-Shavit, F.; Qazen, M. M.; Zalipsky, S. "Targeting folate receptor with folate linked to extremities of poly(ethylene glycol)-grafted liposomes: in vitro studies" *Bioconjugate Chemistry* **1999,** 10, 289-298.

CHAPTER VII

IN VIVO IMAGING AND BIOCOMPATIBILITY OF MULTICOMPONENT POLYELECTROLYTE COMPLEXES

Introduction

The ability to localize PECs in vivo and monitor tissue distribution is critical to understanding their biocompatibility and behavior[1]. Common techniques have involved radionuclide or magnetic resonance imaging (MRI). These methods have several advantages including high sensitivity, capability of quantitation, and clinical translation. Unfortunately, they suffer from relatively low spatial resolution and high cost. For radionuclide administration, positron emission tomography (PET), an on-site cyclotron and radiochemistry laboratory to produce short half-life tracers and radiolabeled agents are a prerequisite. Therefore, optical imaging (bioluminescence and fluorescence imaging) has emerged as an attractive alternative approach to study biological and molecular events in both cell culture and small animals.

Optical imaging modalities do not require ionizing radiation and are inexpensive[2]. Additionally, bioluminescence and fluorescence approaches are highly sensitive and allow for high throughput screening because the acquisition for obtaining an image can be as short as seconds[3]. Because of the strong tissue penetration ability of light in the near-infrared region (NIR), near-infrared fluorescence (NIRF) imaging has emerged as a powerful tool for small animal imaging. These fluorescence tracers emit or absorb light in the 650 nm-900 nm wavelengths. NIRF imaging has a great potential for clinical use

in providing both real-time surgical, functional, and molecular information on disease states. Water and biological tissues have minimal absorbance and autofluorescence in the NIR window, thus allowing efficient photon penetration into, and out of tissue with low intra-tissue scattering. NIRF probes are therefore under active investigation and has been demonstrated as a viable method to noninvasively monitor disease states at the molecular level, localize cancer, and even assess the antitumor efficacy of new therapeutics[4-6].

The extension of PECs as a drug delivery system must be proven in animal models where very few studies actually exist. It is necessary to assess the biocompatibility to validate PEC suitability for systemic administration. Standard histological sections can be examined to verify the presence or absence of inflammation in tissues. If PECs induce an inflammatory response, cells such as neutrophils, lymphocytes, and macrophages would be recruited and indicated by nuclei staining around the site. The NIRF probes have reactive groups for functionalization of amines, aldehydes, and other active chemical moieties on polymers and proteins. Therefore, AlexaFluor 750 (AF750), an NIRF probe carrying an N-hydroxysuccimidyl ester groups for linkage to amines, was incorporated into LMW PECs created with dispergation for further examination of biodistribution by state-of-the art imaging technology. The imaging further established the feasibility of LMW PECs as a template for nanoparticle-mediated targeted drug delivery.

Experimental Procedures

Chapter II defines all protocols applied in this section. Incorporation of AF750 PMCG was performed using *Polymer Labeling*, followed by *PEC Fabrication* of fluorescent PECs (*Fluorescent PEC Preparation)*. One batch was made, isolated by centrifugation, suspended in 1 ml of isotonic buffer. 100 μl was then injected retro-orbitally into male BALBc mice (n=3 per time point) and biodistribution tracked before and after sacrifice as described in *In Vivo Imaging.* Tissue inflammation was investigated by examination of histological slides (*Histology)* for liver, spleen, kidney, lungs, and heart. Additionally intramuscular and subcutaneous injections were performed followed by histological sectioning.

Statistical Analysis

Excised organs were used to measure the biodistribution of the fluorescent PECs. All data are given as the mean ± standard error (n=3 mice per time point for PBS and AF750 PECs). Statistical significance was determined by a two-sample t-test (PECs versus PBS per organ) where a critical t was calculated to determine when the fluorescence signal diminished enough to agree with the null hypothesis. For determining organ PEC distribution, fluorescence intensities (pixel/s), fluxes of light collected by the imaging instrument after excitation and emission, were calculated by the region of interest (ROI) function of the Living Image software integrated with Igor Pro (Wavemetrics, Lake Oswego, OR). ROIs were drawn for each organ and a section of the image (for background subtraction) outside of the 6-well plate; the same size ROIs were

copied and applied in each animal at every time point. All statistical analyses were performed using JMP-IN 5.1 (SAS, Cary, NC).

Results and Discussion

PEC Fluorescent and Physical Properties.

After incorporation of AF750 PMCG and fabrication of fluorescent PECs, physicochemical properties were assessed by PCS. Size, zeta potential, and PDI (average ± s.e., n=3) were 185.78 nm ± 63.34 nm, -30.9±1.00, and 0.247 ± 0.081, respectively. These results were statistically consistent with previous findings. One batch was concentrated to 1 ml of isotonic buffer for injection into animals. Figure 7-1 showed verification of fluorescent signal for AF750, indicating that AF750 PMCG was successfully incorporated into PECs.

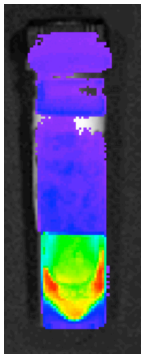

Figure 7-1. Detection of NIR fluorescence in PECs containing AF750 PMCG. PECs are imaged using the ICG filter (λ_{ex} 710-760 nm, λ_{em} 810-875 nm) on the Xenogen IVIS 200 Imaging System. Fluorescent and photographic images are overlapped after a 1 s exposure.

Whole Animal Optical Imaging

The ability to detect AF750 PMCG-containing PECs was accomplished by retro-orbital injection of 100 μl of the above suspension (~$3x10^9$ PECs) and imaging at various time points up to 48 h in mice. The mice were first shaved to prevent signal dampening. There was no acute reaction after intravenous administration, indicating bulk PEC biocompatibility. Intrajugular, tail vein, intraperitoneal, and direct heart injections were tested with no ill effects. Figure 7-2 (A-D) shows the PECs in circulation, but rapidly cleared to the bladder, as shown in the strongest signal. No fluorescence was detected in animals injected with PBS. Images for Figure 7-2(A-B) showed that this process happened between the time of injection and imaging (~10 min). Significant bladder fluorescence persisted at 3 h, but some signal was localized to the upper chest cavities (liver, lungs, spleen, kidneys). The signal completely disappeared at 24 h. This was indicative of a partial destabilization of PECs by polyelectrolyte exchange reactions leading to fast clearance of PMCG and AF750 PMCG from the bloodstream. The low molecular weight of PMCG (5000 Da) is well below the kidney clearance limits[7], but the fluorescent signal also could be indicative of the clearance of other PEC components. Following intravenous administration, naked PECs are exposed to a variety of factors that may have compromised their integrity and caused partial decomplexation, including interactions with proteoglycan-containing extracellular matrices and high concentrations of very anionic serum proteins or other molecules present in blood plasma (opsonization)[8,9]. Suspensions of AF750 PECs in 100% fetal calf serum verified these results as 40% of the fluorophore conjugated PMCG was released in the first 30 min.

AF750 PEC PBS Time (h)

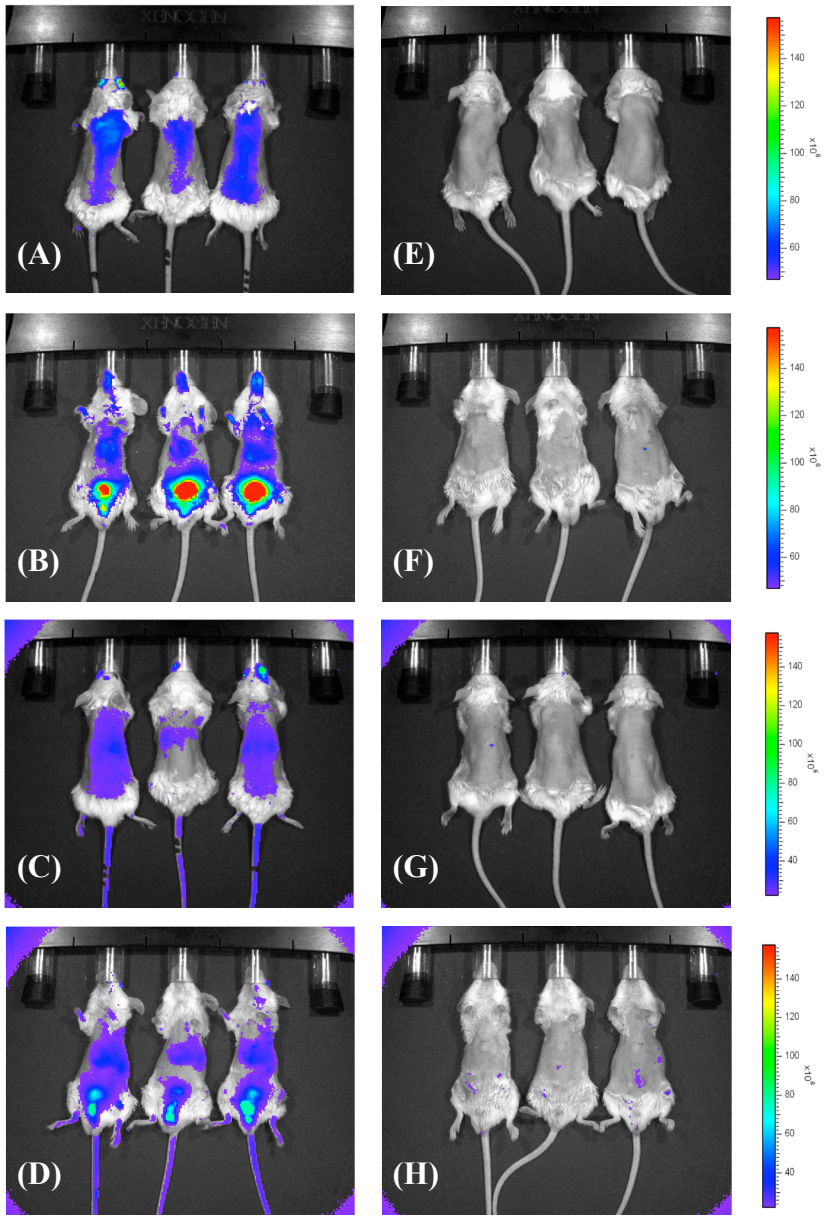

Figure 7-2. In vivo fluorescence imaging of retro-orbitally injected AF750 PECs (A-D) or PBS (E-H) immediately after injection and 3 h later in male BALBc mice. Dorsal imaging was performed in (A), (C), (E), (G) while ventral in (B), (D), (F), (H). The intensity of the signals, light flux, is denoted by the respective color bars in terms of pixels/second. 10 s exposures were applied followed by the overlay of photographic and fluorescence images.

Biocompatibility Assessed by Tissue Histology

PEC biocompatibility was assessed by several types of administration, after which animals were sacrificed and histological slides prepared. Animals were either injected intramuscularly (directly into muscle) or subcutaneously (under the skin) with AF750 PMCG PECs or PBS (50 μl, $1.5x10^9$ PECs). Three days later, the animals were sacrificed and muscle and skin extracted. The histological slides comprise Figure 7-3. The hematoxylin and eosine staining of nuclei and cytoplasmic components, respectively, showed no distinguishable differences.

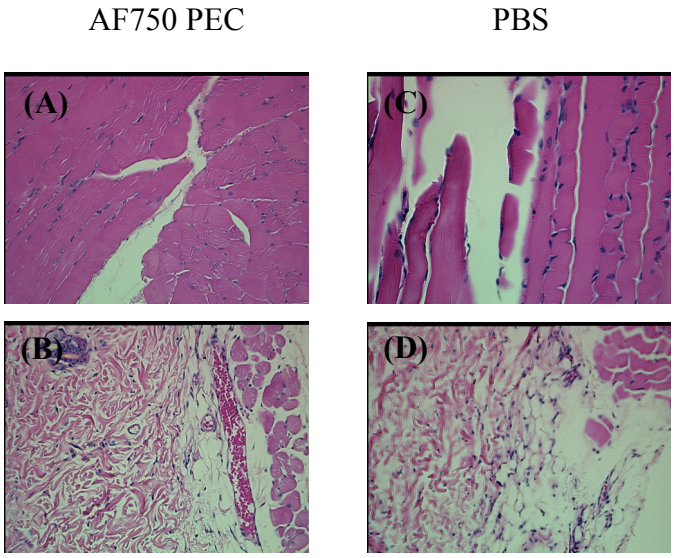

Figure 7-3. Histological examination of intramuscularly (A,C) and subcutaneously (B,D) injected AF750 PECs and PBS 3 d after administration.

Further biocompatibility was characterized by sectioning of organs for mice kept 5 days post-injection. Liver, kidney, spleen, lungs, and heart stained with hematoxylin and eosine showed no morphological differences between PBS and AF750 PMCG PECs (Figure 7-4). These two studies showed no inflammatory reactions, due to a lack of punctate blue staining, following PEC administration, and preparation of histologies.

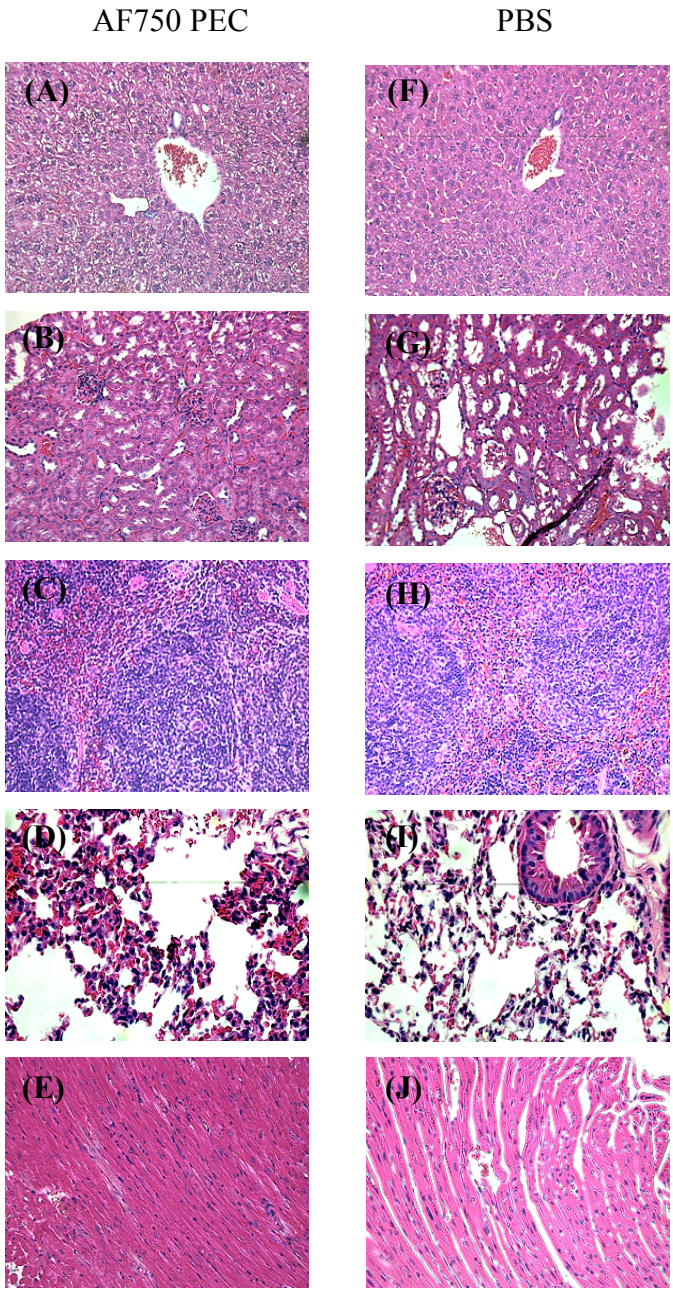

Figure 7-4. Histological sectioning of AF750 PEC and PBS injected BALBc mice 5 days post administration for liver (A,F), kidney (B,G), spleen (C,H), lungs (D,I), and heart (E,J).

Organ Biodistribution

The remaining intact complexes became rapidly sequestered into highly perfused and vascularized organs: liver, lungs, and spleen. This localization was followed by degradation of signals over a 48 h period as shown in Figure 7-5. PBS treated animals provided the fluorescence background. Each time interval involved the euthanasia of 3 AF750 PEC and PBS animals and organ extraction. The fluorescence of each organ was immediately imaged and the fluorescence extracted.

It was not surprising that the fluorescence was contained in the liver, lungs, and spleen, after initial time points showed bladder localization. The liver, lungs, and spleen contain highly vascularized networks composed of highly anionic endothelial cells facilitating PEC sequestration in these organs. Specifically, the liver has open fenestrations that control the transfer of molecules from blood vessels to tissue, which are on the order of 150 nm. These openings may also contribute to the extensive endothelial filtration of PECs in the liver. Intravenous injection of colloidal carriers, such as liposomes and polymeric nanospheres, are recognized by the reticuloendothelial system (RES) as they circulate in the blood and bind opsoninizing macromolecules[10]. The RES, a component of the immune system, consists of phagocytic (greek for cell eating) cells, primarily monocytes and macrophages i.e. Kupffer cells. These cells accumulate and line the spleen, liver, and lungs and capture foreign substances and eventually clear them from the bloodstream, as is displayed in Figure 7-5(A-D).

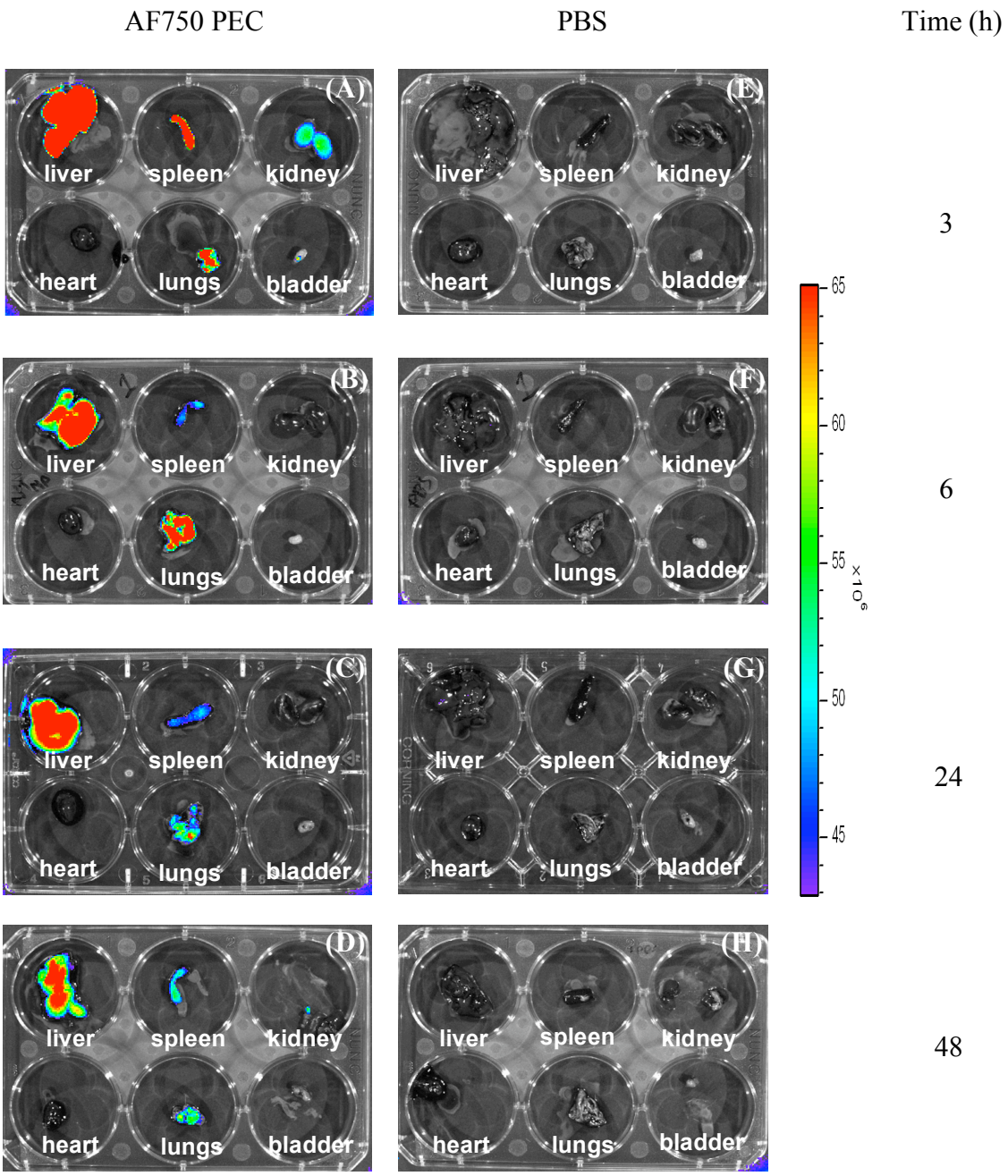

Figure 7-5. Representative ex vivo images of organs extracted from male BALBc mice at the indicated time points after retro-orbital injection. Either AF750 PECs (A-D) or PBS (E-H) was injected. 10 s exposures were applied followed by the overlay of photographic and fluorescence images. Three animals were used in each time group.

Furthermore, the NIR fluorescence, up to 48 h, was quantified by measurement of the light flux induced after excitation of the fluorochrome for both PBS and AF750 PECs treated mice, as shown in Figure 7-6(A,B). The figure shows a rapid clearance of PECs from organs, eventually washing them out after 48 h. The short circulation time verified the RES response discussed previously. To provide added evidence of the clearance of PECs, statistical tests between treatments were performed for every organ compared at each time point. In Figure 7-6(C), the calculated test statistic (t_{test}) was plotted as a function of time. The test statistic was calculated by equation 7-1:

$$t_{test} = \frac{\mu_{AF750\,PEC} - \mu_{PBS}}{\sqrt{\frac{s_1^2 + s_2^2}{n}}} \tag{7-1}$$

where $\mu_{AF750\ PEC}$ and μ_{PBS} were the mean fluxes, s_1^2 and s_2^2 the standard deviations, respectively, and n the sample size (3 mice). The critical t for 4 degrees of freedom was 2.776. Any calculated test statistic less than 2.776 met the null hypothesis, $\mu_{AF750\ PEC}=\mu_{PBS}$; the PEC signal does not differ statistically from PBS and defined by the dashed line in Figure 7-6C. Therefore, Figure 7-6C shows a steady, monotonic decrease in t_{test} for all organs. AF750 PECs showed statistically significant signals for liver, lungs, kidney and spleen at t=3, but after 24 h, only lungs and liver show statistically unique fluxes. As time further elapsed, only the liver had a t_{test}, which resulted in rejection of the null hypothesis.

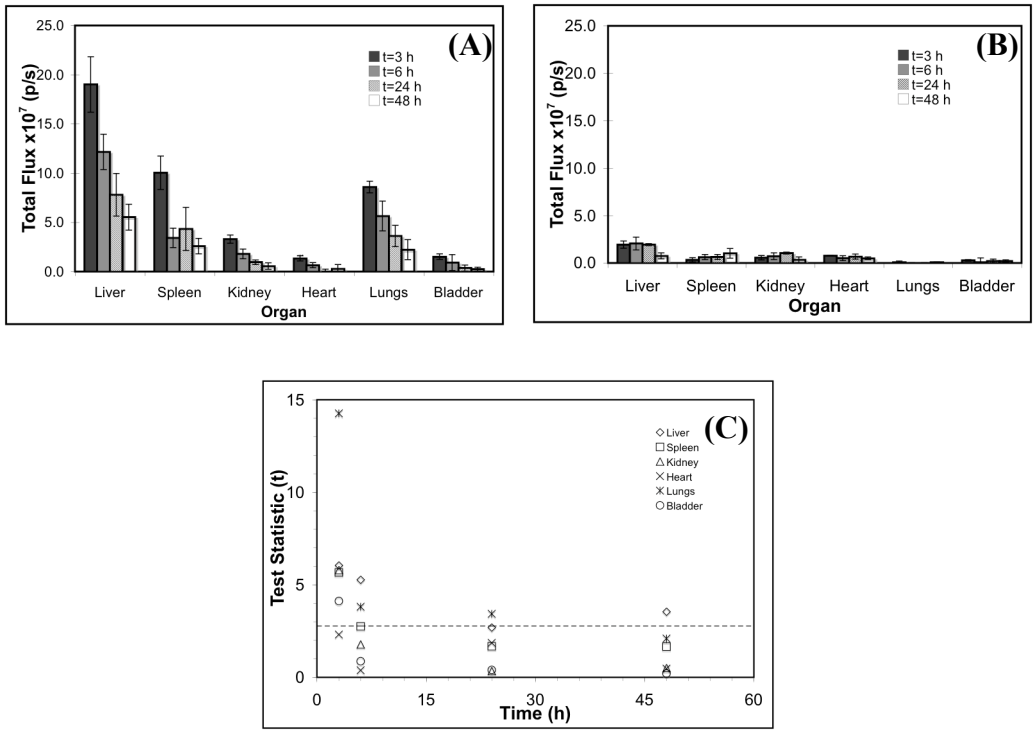

Figure 7-6. Quantification of ex vivo organ distribution for (A) AF750 PECs and (B) PBS injected animals. The fluorescence was recorded as photons/second after creation of a region of interest for each organ. The background was subtracted by creating a region of interest away from the organ signals. The statistical significance of each fluorescence measurement (n=3) was tested against its PBS counterpart. The test statistic for each two-way comparison was plotted (C) as a function of time (n=3, $p<0.05$).

Conclusions

A NIR probe was successfully incorporated into the PEC matrix and biodistribution followed by non-invasive longitudinal imaging. Additionally, the biocompatibility was verified when indistinguishable tissue histologies were observed. Unfortunately, LMW PECs were rapidly cleared from circulation as seen by whole

animal imaging, excised organ fluorescence, and statistical analysis of the measured light fluxes.

Studies have shown that the association of plasma proteins and opsonins, such as immunoglobulin G, fibrinogen, and fibronectin, with liposomes and other colloidal carriers contributed to circulatory clearance or non-specific accumulation in pulmonary capillary beds and the liver[8,9,11]. Moreover, the extent of binding increases the likelihood of recognition by the RES[12]. After intravenous injection of AF750 PECs, the cationic groups can react with plasma proteins, resulting in modified coronal chemistry and decreased adherence to anionic cell surfaces. Opsonins may come into contact typically by Brownian motion, but when sufficiently close, van der Wals, ionic, hydrophilic/hydrophobic and other attractive forces dominate the interactions. After opsonization has occurred the complex may destabilize through exchange reactions or phagocytic cells will recognize and bind this ternary PEC/opsonin structure. In the absence of opsonins, phagocytes will not bind polymeric carriers. Phagocytes will then ingest PECs and inherent secretory enzymes and oxidative-reductive agents leading to degradation of individual components and ejection[7].

There are many approaches to stabilize AF750 PECs against opsonization. One strategy would be to enshroud the PECs within a protective layer of hydrophilic polymers, such as polyethylene glycol (PEG)[13], in addition to the Pluronic F-68 already present. The surface modifications can be accomplished by activated linkages to sufficiently 'coat' the PECs, avoid phagocyte-mediated clearance, increase the circulatory time, and enhance complex stability.

References

1. Vuu, K.; Xie, J. W.; McDonald, M. A.; Bernardo, M.; Hunter, F.; Zhang, Y. T.; Li, K.; Bednarski, M.; Guccione, S. "Gadolinium-rhodamine nanoparticles for cell labeling and tracking via magnetic resonance and optical imaging" *Bioconjugate Chemistry* **2005,** 16, 995-999.

2. Cheng, Z.; Levi, J.; Xiong, Z. M.; Gheysens, O.; Keren, S.; Chen, X. Y.; Gambhir, S. S. "Near-infrared fluorescent deoxyglucose analogue for tumor optical imaging in cell culture and living mice" *Bioconjugate Chemistry* **2006,** 17, 662-669.

3. Ntziachristos, V.; Bremer, C.; Weissleder, R. "Fluorescence imaging with near-infrared light: new technological advances that enable in vivo molecular imaging" *European Radiology* **2003,** 13, 195-208.

4. Achilefu, S. "Lighting up tumors with receptor-specific optical molecular probes" *Technology In Cancer Research & Treatment* **2004,** 3, 393-409.

5. Mahmood, U.; Weissleder, R. "Near-infrared optical imaging of proteases in cancer" *Molecular Cancer Therapeutics* **2003,** 2, 489-496.

6. Sevick-Muraca, E. M.; Houston, J. P.; Gurfinkel, M. "Fluorescence-enhanced, near infrared diagnostic imaging with contrast agents" *Current Opinion In Chemical Biology* **2002,** 6, 642-650.

7. Owens, D. E.; Peppas, N. A. "Opsonization, biodistribution, and pharmacokinetics of polymeric nanoparticles" *International Journal Of Pharmaceutics* **2006,** 307, 93-102.

8. Dash, P. R.; Read, M. L.; Barrett, L. B.; Wolfert, M.; Seymour, L. W. "Factors affecting blood clearance and in vivo distribution of polyelectrolyte complexes for gene delivery" *Gene Therapy* **1999,** 6, 643-650.

9. Oupicky, D.; Carlisle, R. C.; Seymour, L. W. "Triggered intracellular activation of disulfide crosslinked polyelectrolyte gene delivery complexes with extended systemic circulation in vivo" *Gene Therapy* **2001,** 8, 713-724.

10. Moghimi, S. M. "Mechanisms regulating body distribution of nanospheres conditioned with pluronic and tetronic block copolymers" *Advanced Drug Delivery Reviews* **1995,** 16, 183-193.

11. Oupicky, D.; Ogris, M.; Howard, K. A.; Dash, P. R.; Ulbrich, K.; Seymour, L. W. "Importance of lateral and steric stabilization of polyelectrolyte gene delivery vectors for extended systemic circulation" *Molecular Therapy* **2002,** 5, 463-472.

12. Moghimi, S. M.; Hunter, A. C.; Murray, J. C. "Long-circulating and target-specific nanoparticles: theory to practice" *Pharmacological Reviews* **2001,** 53, 283-318.

13. Wang, J. C.; Goh, B. C.; Lu, W. L.; Zhang, Q.; Chang, A.; Liu, X. Y.; Tan, T. M. C.; Lee, H. S. "In vitro cytotoxicity of Stealth liposomes co-encapsulating doxorubicin and verapamil on doxorubicin-resistant tumor cells" *Biological & Pharmaceutical Bulletin* **2005,** 28, 822-828.

CHAPTER VIII

ASSESSMENT OF NANOPARTICULATE POLYELECTROLYTE COMPLEX PRODUCTION BY KENICS STATIC MIXER

Introduction

The pharmaceuticals and fine chemical industry have shown an increasing interest in alternatives to batch and stirred tank reactor designs and reliable scale-up strategies. Although continuous processing technologies such as static and in-line mixers have been successfully applied in the petroleum industry, literature focusing on their application to the manufacture of excipients, active pharmaceutical ingredients, and nano- and microscale drug delivery systems is limited[1].

Static mixers consist of a series of flow reorientation devices inserted along the axis of a pipe. Pressure, as opposed to mechanical agitation, drives fluids through the device, providing the energy needed to accomplish mixing[2]. They are simply cylindrical pipes with mixing elements fixed inside. The mixing elements are formed by helically twisted rigid plates (usually of the same pitch) each dividing the pipe into two twisted semicircular ducts. The inserts are placed tightly one after another so that the leading edge of the next insert is perpendicular to the trailing edge of the previous one; the length of the elements is one and a half tube diameters[3], as displayed in Figure 8-1. Solutions are radially mixed by rotational circulation around the hydraulic center of each semi-circular channel. Solutions are subsequently forced from the diameter to the outer wall of the element. At the same time, the flow reverses its rotation at each element junction due to the alternate right- and left-hand alignment of the elements. The overall effect is to

cause the stream to be continually inverted radially so that solutions entering at the center of the stream are forced to the outer wall and back again on a continuous basis. Static mixers have achieved throughputs from 10000 m^3/h to approximately 1 m^3/h, offer the potential for achieving liquid-phase plug flow, and pseudo-turbulent conditions at relatively low Reynolds numbers (N Re), laminar flow conditions, and high residence times, without an increase in reactor volume or stream velocity[1,4].

Figure 8-1. Schematic of Kenics mixer geometry.

Here, a new technology is introduced to prepare PECs by means of a Kenics static micromixer. The Kenics static mixer has a bench-top setup, lacks moving parts, can be run continuously for fabrication of large volumes of PECs, and can be sterilized for asceptic processing[5]. LMW and HMW PECs were made at increasing N Re and the physicochemical properties were compared with the goal of a monomodal distribution, decreased sizes, PDIs, and stable ZPs. Furthermore, the mixing efficiency of the device was evaluated by a competitive reaction scheme.

Experimental Procedures

LMW and HMW PECs were fabricated and the mixing properties established, as described in Chapter II, *Process Scale Up with Kenics Static Mixer* and *Qualitative Assessment of Static Mixer Efficiency*, respectively. Figure 8-2 depicts the device, inlets, and outlets. Reynolds numbers were calculated assuming an empty pipe approximation. The Kenics mixer used was 6.35 mm I.D., 21 cm in length, and made of stainless steel.

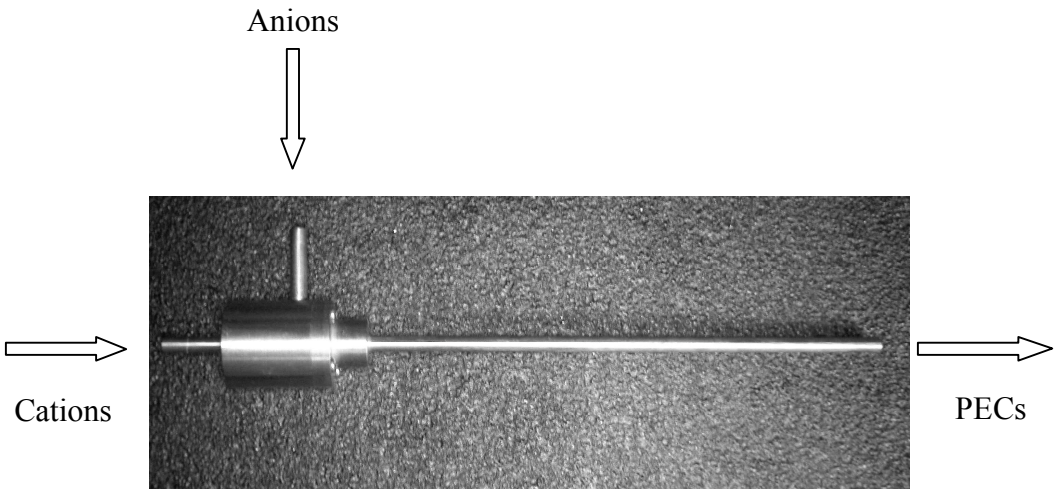

Figure 8-2. Kenics static mixer showing inlets and outlets for PEC production and evaluation of mixing efficiency.

Statistical Analysis

Several statistical methods were applied for evaluation of PEC physicochemistry and the mixing efficiency with JMP-IN 5.1 (SAS, Cary, NC). Subsequent to the fabrication of LMW and HMW PECs, size, polydispersity index (PDI), and zeta potential (ZP) were assessed by ANOVA to statistically determine the heterogeneity of both populations as a function of increasing flow rate. Additionally, the Tukey-Kramer

Honestly Significant Difference (HSD) was used to compare mean properties at each N Re. The same method was performed for tri-iodide production as a function of N Re. LMW and HMW systems were also evaluated by two-sample t-tests for every N Re to compare the polyelectrolyte platforms. Linear regressions were calculated for physicochemical properties and tri-iodide concentrations as a function of N Re. Each slope was statistically tested to see if it differed from zero or whether the data trends. Also, ANOVA was used to understand whether or not the metrics followed an upward or downward trend. All analysis was assessed at the 95% confidence interval ($p<0.05$).

Results and Discussion

Mixer Characterization by Competitive Reactions

The mixing efficiency of the Kenics static mixer used for continuous production of LMW and HMW PECs at stoichiometric ratios of 10:1 was evaluated by an ultrafast competitive acid-base reaction scheme originally designed for batch setups[6] but modified for continuous designs[7,8]. The anionic and cationic streams from the PEC process were mimicked by the sulfuric acid and borate/iodide/iodate solutions, respectively, as described in Chapter II, *Qualitative Assessment of Static Mixer Efficiency*. The two solutions, H_2SO_4 and $H_2BO_3/IO_3^-/I^-$, from the test reaction represented limiting and excess reactants in the same ratios as the PEC reaction. The mixing efficiency was quantified by the equilibrium production of iodine (I_3^-) and measurement via spectrophotometer at 353 nm. The first process, Equation 2-9, is a neutralization that is ultra fast and will always mask the slower second reaction (Equation 2-10), namely the

iodine formation as long as no local excess of the strong acid remained; the higher the absorption due to tri-iodide formation, the poorer the quality of mixing in the unit[9].

A linear profile was observed as a function of Reynolds number in the laminar flow regime (Figure 8-3). The slope of this line is statistically different from zero and the physical system exhibits a negative relationship between iodine concentration and Reynolds number as tested by ANOVA. One-Way ANOVA tests were also used to test the homogeneity of means as N Re increased. The analysis showed a 2% probability that all means are equal, therefore at least one mean is statistically significant. This led to the use of the Tukey-Kramer HSD test to define pairs of means that are statistically different. Table 8-1 displays the results. According to this test, Reynolds number does not induce a statistical effect on mixing until N Re reached 730.25.

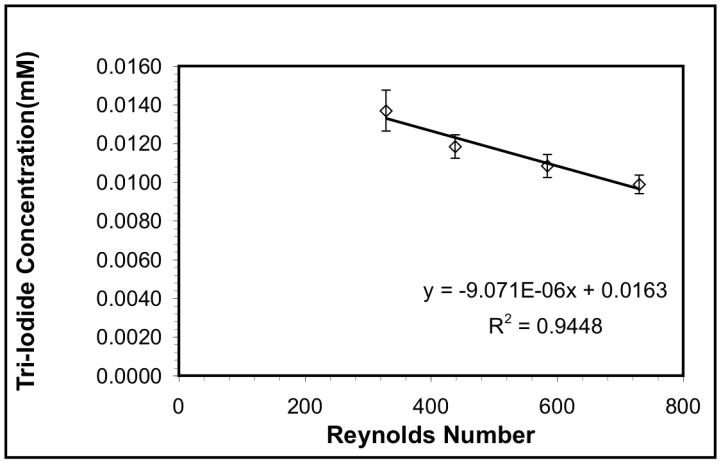

Figure 8-3. Tri-iodide production as a function of Reynolds number for flow rates applied in PEC production. Tri-iodide production with the Kenics static mixer is displayed as the mean±s.e. for 4 independent measurements. Slope and y-intercept are displayed from linear regression analysis.

Table 8-1. Comparison of tri-iodide concentrations using Tukey-Kramer HSD test. Designation of "yes" signifies a concentration in the column heading that is statistically different from the rate for its counterpart in the row heading. "no" means two concentrations are means which are statistically the same.

N Re	328.61	438.15	584.20	730.25
328.61	--	no	no	yes
438.15	no	--	no	no
584.20	no	no	--	no
730.25	yes	no	no	--

Properties of PECs Fabricated by Kenics Static Mixer

PECs were constructed by simple two stream contacting with the Kenics static mixer at laminar flow conditions. The particles exhibited the Tyndall effect, consistent with observations in Chapter III for batchwise preparations. After a 30 s accumulation time, under stirring, the product is sampled for analysis by the Malvern ZetaSizer Nano ZS. Figure 8-4 was separated into two representations. The first (left panels) displays the data as histograms to demonstrate the statistical differences between the LMW and HMW formulations. HMW PEC particle diameter, Figure 8-4A, (250 nm-303 nm) was greater at each N Re in comparison to LMW suspensions (221 nm-250 nm), but none exhibited statistical significance. However, HMW PECs demonstrated greater variability in size as indicated by the standard error. The standard error ranged from 26% (N Re=328.61) to 33% (N Re=584.20) which was indicative of a less reproducible result in comparison to LMW counterparts (standard error 2-4% of average). For zeta potential, only Re=438.15 showed a statistically higher surface charge for HMW (41 mV-42 mV) compared to LMW (32 mV-36 mV), although each HMW ZP was higher as designated in Figure 8-4C. LMW PECs provided statistical decreases for all conditions (Figure 8-4B),

excluding N Re=328.61. The reduction in polydispersity was a sign that the population of LMW PECs became more homogeneous in contrast to the HMW products. Similar results have been seen for other static mixer configurations[10-12].

The second half of Figure 8-4 plots the physicochemical responses as a function of increasing N Re for detection of linearity between size, PDI, ZP, and the flow pattern. A plot of hydrodynamic diameter versus N Re (Figure 8-4D) for HMW PECs showed no statistically unique upward or downward trend while LMW showed a significant decreasing pattern. In fact, this was the case for each characteristic. This would indicate that HMW PECs had a random response to increasing N Re, whereas LMW complexes showed real effects to changes in the flow pattern. Tests on the slopes derived from linear regressions showed that they were statistically different than zero, although ANOVA indicated that only LMW measurements showed a downward trend.

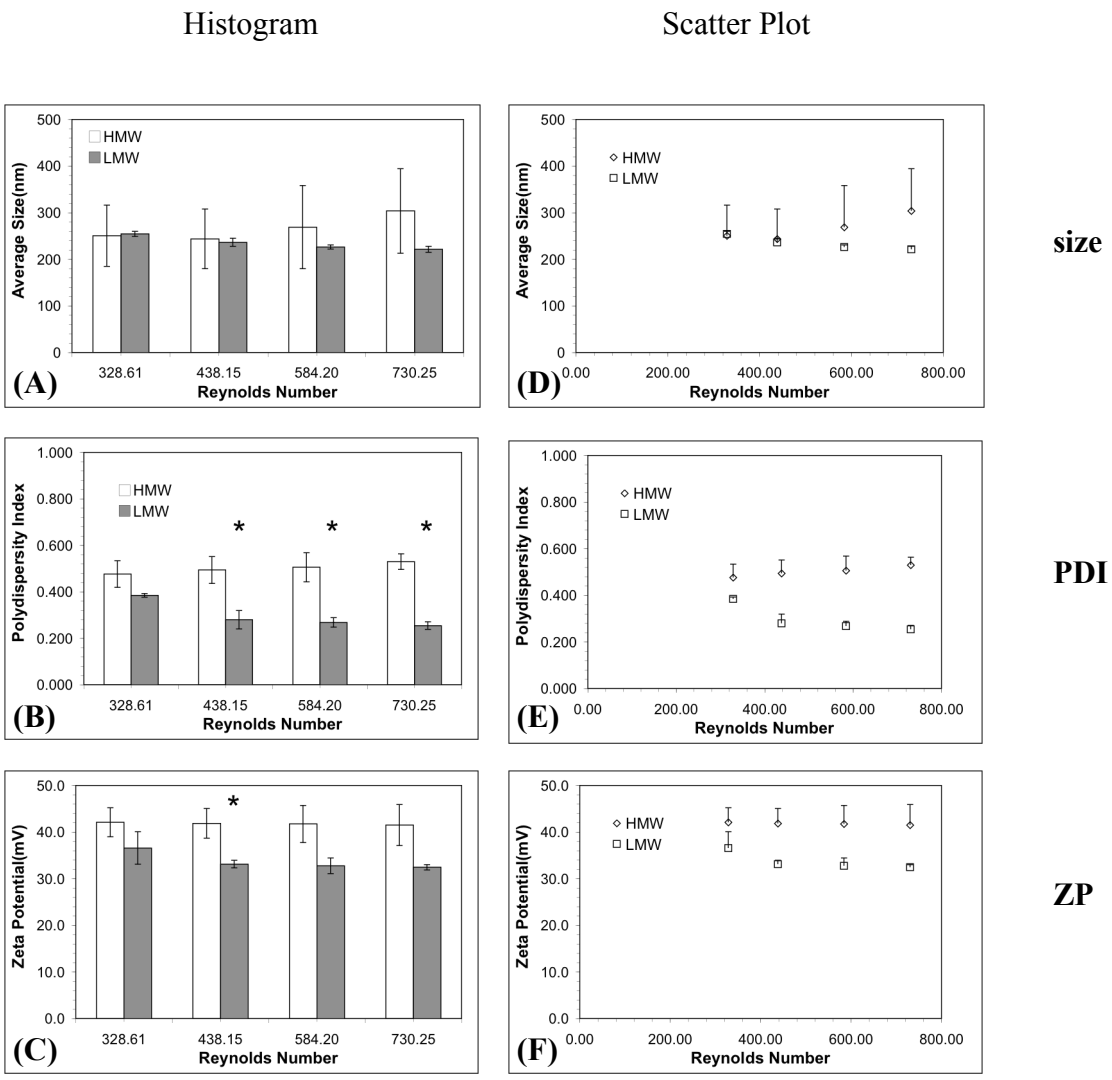

Figure 8-4. Physicochemical properties of LMW and HMW PECs created using the static mixers at increasing Reynolds numbers. Left panels represent histograms while right is the scatter data on a linear scale. Size (A,D), PDI (B,E), and ZP (C,F) are the mean and standard error for at least 3 measurements. Asterisks indicate pairs of means which differ at the 95% confidence level by two-sample t-test.

Conclusions

The results showed that only LMW PECs are affected by preparation by static mixer technology. Also, a parallel competing reaction scheme provided proof that mixing efficiency was enhanced as N Re increased and that further increases in flow rate could result in better mixing. Regardless, the static mixer offered the potential for further improvements. The current configuration of the system does not allow a further buildup of pressure. Better pumps and more robust tubing would have to be used. Additionally, the mixing could be improved by changing inlets to further segregate the streams until they reach the same element.

The more intense the mixing, the better physicochemical results were observed. Large volumes of particles of both systems were produced, ~100-200 ml/min, as opposed to the 22 ml yield for batchwise preparation. This left that the possibility that static mixers could provide a reasonable scale up strategy. Interestingly, only the LMW formulation was sensitive to the rotational mixing inside of the static mixer. This may have implications for the mechanism and ordered assembly of HMW and LMW PECs. A more intense mixing system might be needed to improve the properties of HMW complexes produced by continuous stream contact. Neither static mixer dispersion had more favorable qualities than corresponding complexations by batchwise titration with and without frequency dispergation. Freitas and coworkers[5] argued that re-engineering the outlet section to avoid turbulent flow should reduce the PDI and particle diameter. Other possible improvements might involve reduction of the outlet slit[9] or adding more mixing elements in series. These types of alterations may lead to smaller particle size and reduced polydispersity.

References

1. Brechtelsbauer, C.; Ricard, F. "Reaction engineering evaluation and utilization of static mixer technology for the synthesis of pharmaceuticals" *Organic Process Research & Development* **2001,** 5, 646-651.

2. Szalai, E. S.; Muzzio, F. J. "Fundamental approach to the design and optimization of static mixers" *Aiche Journal* **2003,** 49, 2687-2699.

3. Galaktionov, O. S.; Anderson, R. D.; Peters, G. W. M.; Meijer, H. E. H. "Analysis and optimization of kenics static mixers" *International Polymer Processing* **2003,** 18, 138-150.

4. Werner, B.; Hessel, V.; Lob, P. "Mixers with microstructured foils for chemical production purposes" *Chemical Engineering & Technology* **2005,** 28, 401-407.

5. Freitas, S.; Walz, A.; Merkle, H. P.; Gander, B. "Solvent extraction employing a static micromixer: a simple, robust and versatile technology for the microencapsulation of proteins" *Journal of Microencapsulation* **2003,** 20, 67-85.

6. Fournier, M. C.; Falk, L.; Villermaux, J. "A new parallel competing reaction system for assessing micromixing efficiency - experimental approach" *Chemical Engineering Science* **1996,** 51, 5053-5064.

7. Fang, J. Z.; Lee, D. J. "Micromixing efficiency in static mixer" *Chemical Engineering Science* **2001,** 56, 3797-3802.

8. Guichardon, P.; Falk, L. "Characterisation of micromixing efficiency by the iodide-iodate reaction system. Part I: experimental procedure" *Chemical Engineering Science* **2000,** 55, 4233-4243.

9. Ehrfeld, W.; Golbig, K.; Hessel, V.; Lowe, H.; Richter, T. "Characterization of mixing in micromixers by a test reaction: Single mixing units and mixer arrays" *Industrial & Engineering Chemistry Research* **1999,** 38, 1075-1082.

10. Douroumis, D.; Fahr, A. "Nano- and micro-particulate formulations of poorly water-soluble drugs by using a novel optimized technique" *European Journal Of Pharmaceutics And Biopharmaceutics* **2006,** 63, 173-175.

11. Schwarzer, H. C.; Peukert, W. "Tailoring particle size through nanoparticle precipitation" *Chemical Engineering Communications* **2004,** 191, 580-606.

12. Schwarzer, H. C.; Peukert, W. "Experimental investigation into the influence of mixing on nanoparticle precipitation" *Chemical Engineering & Technology* **2002,** 25, 657-661.

CHAPTER IX

CONCLUSIONS AND FUTURE WORK

Conclusions

The overall work presented herein demonstrates the development and biological properties of a nanoparticulate platform based on the interactions of polyelectrolytes with similar molecular weights that can be prepared through an ultrasonic titration (LMW PECs). The preparation avoids the use of harmful reaction environments, bulk phases such as methylene chloride and chloroform or mineral oils, through the use of water as a solvent, an obvious advantage over many polymeric nanoparticle systems being studied. Common nanotechnological techniques, such as TEM and PCS, can easily provide information on PEC physical properties. PECs have favorable and attractive physicochemical characteristics that are maintained at physiological pH and low concentration, serum-containing media: uniform, attractive size distributions, mean diameters statistically less than or equivalent to 200 nm, and surface charges indicative of stable colloidal suspensions. LMW PECs also assemble into desirable structures without dispergation, a valuable finding for future, viable production and scale-up through simple two-stream, continuous mixing. Such high throughput processing may allow further improvement in downstream manipulation, perhaps through removal of centrifugation as a product isolation method. The system provides an improvement over a system shown to deliver genes to cells of a hematopoietic origin. Additionally, these nanoparticulate architectures can entrap, release, and retain proteins, mimicking therapeutics, over the

course of several days, leading to the possibility of a drug depot for intravenous or systemic administration.

PECs exhibit little or no toxicity in a biological environment. Because of the PEC modular and chemical nature, surface amines and inner core hydroxyl groups permit the efficient incorporation of targeting moieties, chemical linkage of classically insoluble drugs (doxorubicin). The fluorophore incorporation strategy drives both visible and near-infrared fluorescence characterization of PEC fates in cell culture and small animals. Flow cytometry can be utilized to extensively characterize and define the underlying mechanisms of PEC binding and uptake, in common disease state models (endothelial cells), through macropinocytosis. Compartmentalization, uptake and surface binding can be delineated through extracellular FITC quenching; another advantage of flow cytometry. Also, through flow cytometry, cationic PECs bind cells through strictly electrostatic interactions where cells provide an anionic sink to mediate the attachment. Also, a novel, flow cytometric, Scatchard analysis protocol, where the extent of receptor-controlled interactions are dictated by adherence to underlying assumptions of mass action and equilibrium binding. This is the first such flow cytometric Scatchard plot strategy for characterization for nanoparticulate architectures to define true targeting and receptor-ligand interactions; a critical feature due to misleading information from direct kinetic studies. The Scatchard plots can screen targeted delivery systems, in vitro, before expensive animal models are used. This approach is ideal when radioactive nanoparticle components are not currently available or the incorporation of an isotope too cumbersome. LMW PECs hold promise for medical uses and could be utilized as a

targeted drug delivery formulation and also as a non-invasive, real-time imaging construct in humans.

Future Work

It is difficult to produce PECs that possess all ideal in vivo and in vitro performance related properties. The PEC as a whole should exhibit physicochemical properties in biological environments defined pragmatically in the literature: including hydrodynamic diameter less than or equal to 200 nm[1,2], surface charge of greater than $|\pm 30$ mV$|$[3-5], spherical morphology, and a low polydispersity index indicative of a homogeneous size distribution. In this study, LMW PECs were shown to interact in a completely unspecific manner, unless the peptide strategy provided an appropriate geometric and flexible presentation. Another complication was that TSP521 was a weak affinity ligand. An alternative ligand may involve the use of addressins that bind to activated receptors via light, heat, or radiation. Because direct, covalent linkage by EDAC/NHS of TSP521 did not exhibit receptor-mediated behavior, it can be concluded that the peptide was not extended sufficiently from the PEC corona to mitigate charged interactions with the cell surface. This prevented TSP521 from interacting specifically with HSPGs. Additionally, PECs need to be sufficiently modified to avoid uptake by the reticuloendothelial system (RES) to permit accumulation in target tissues.

Proper ligand presentation and a corona adaptation can be improved through the use of polyethylene glycol (PEG). PEG not only provides a coating to prevent opsonization and subsequent recognition by macrophages of the RES, but can link a targeting moiety in a distal conformation to facilitate the appropriate receptor activation.

First introduced by Gref[6], PEG introduction into poly(lactic-co-glycolic acid) nanospheres resulted in dramatic increases in blood circulation times and reduced liver accumulation in mice. Since that discovery in 1994, PEG incorporation into nano- and microparticulate biomaterials has been used extensively in countless studies to improve polymer stability and prevent protein fouling.

Several theories have been proposed to explain the apparent protein resistance and stealth characteristics imparted to materials by grafting of PEG. When opsonins and other plasma proteins are attracted to the surface of the particle, by van der Waals or electrostatic forces, they encounter the PEG chains and begin to compress them. This compression then forces the PEG chains into a more condensed higher energy conformation creating a repulsion and steric hindrance of opsonin or protein adherence[7]. Most research indicates that PEG chains of 2000 molecular weight or greater is required to achieve increased RES avoidance characteristics[6,8,9].

With this in mind, a bifunctional PEG linkage can be used for ligand presentation and introduction of 'stealth' properties. PEG constructs with different activated linkages are available; a chain consisting of an N-hydoxysuccinimide on one end and a maleimide on the other, with at least a 2000 PEG molecular weight polymer in the middle, would be sufficient to link the PEC surface amines to cysteines on a ligand. Previous and similar strategies have been used to link folate, for targeting overexpressed folate receptors on cancer cells, to liposomes[10,11]. Figure 9-1 represents a schematic of this design. The hope is that this PEC chemistry would result in efficient targeting both in vivo and in vitro.

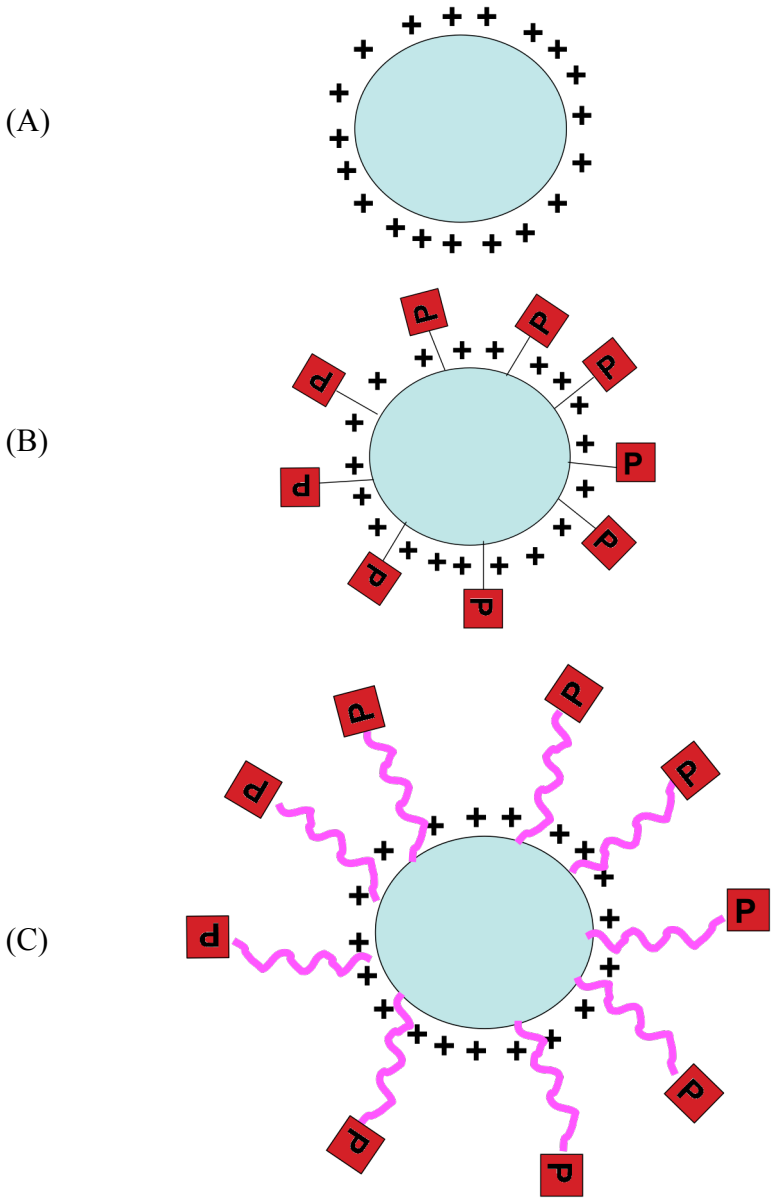

Figure 9-1. Representative peptide modifications of PECs for A) naked, B) direct linkage by EDAC/NHS, and C) extension of peptide away from the surface with PEG. The flexible PEG chains provide a geometric presentation of the ligand and protection from destabilizing opsonins and proteins.

References

1. Carlesso, G.; Kozlov, E.; Prokop, A.; Unutmaz, D.; Davidson, J. M. "Nanoparticulate system for efficient gene transfer into refractory cell targets" *Biomacromolecules* **2005,** 6, 1185-1192.

2. Panyam, P.; Labhasetwar, V. "Biodegradable nanoparticles for drug and gene delivery to cells and tissue" *Advanced Drug Delivery Reviews* **2003,** 55, 329-347.

3. Fatouros, D. G.; Piperoudi, S.; Gortzi, O.; Ioannou, P. V.; Frederik, P.; Antimisiaris, S. G. "Physical stability of sonicated arsonoliposomes: Effect of calcium ions" *Journal of Pharmaceutical Sciences* **2005,** 94, 46-55.

4. Chern, C. S.; Lee, C. K.; Chang, C. J. "Electrostatic interactions between amphoteric latex particles and proteins" *Colloid and Polymer Science* **2004,** 283, 257-264.

5. Sugrue, S. "Predicting and controlling colloid suspension stability using electrophoretic mobility and particle size measurements" *American Laboratory* **1992,** 24, 64-71.

6. Gref, R.; Minamitake, Y.; Peracchia, M. T.; Trubetskoy, V.; Torchilin, V.; Langer, R. "Biodegradable long-circulating polymeric nanospheres" *Science* **1994,** 263, 1600-1603.

7. Owens, D. E.; Peppas, N. A. "Opsonization, biodistribution, and pharmacokinetics of polymeric nanoparticles" *International Journal Of Pharmaceutics* **2006,** 307, 93-102.

8. Leroux, J. C.; Allemann, E.; DeJaeghere, F.; Doelker, E.; Gurny, R. "Biodegradable nanoparticles - from sustained release formulations to improved site specific drug delivery" *Journal of Controlled Release* **1996,** 39, 339-350.

9. Peracchia, M. T.; Harnisch, S.; Pinto-Alphandary, H.; Gulik, A.; Dedieu, J. C.; Desmaele, D.; d'Angelo, J.; Muller, R. H.; Couvreur, P. "Visualization of in vitro protein-rejecting properties of PEGylated stealth (R) polycyanoacrylate nanoparticles" *Biomaterials* **1999,** 20, 1269-1275.

10. Gabizon, A.; Horowitz, A. T.; Goren, D.; Tzemach, D.; Mandelbaum-Shavit, F.; Qazen, M. M.; Zalipsky, S. "Targeting folate receptor with folate linked to extremities of poly(ethylene glycol)-grafted liposomes: In vitro studies" *Bioconjugate Chemistry* **1999,** 10, 289-298.

11. Lee, R. J.; Low, P. S. "Delivery of liposomes into cultured KB cells via folate receptor-mediated endocytosis" *Journal Of Biological Chemistry* **1994,** 269, 3198-3204.

APPENDIX

FITC PMCG Release and Spermine Incorporation

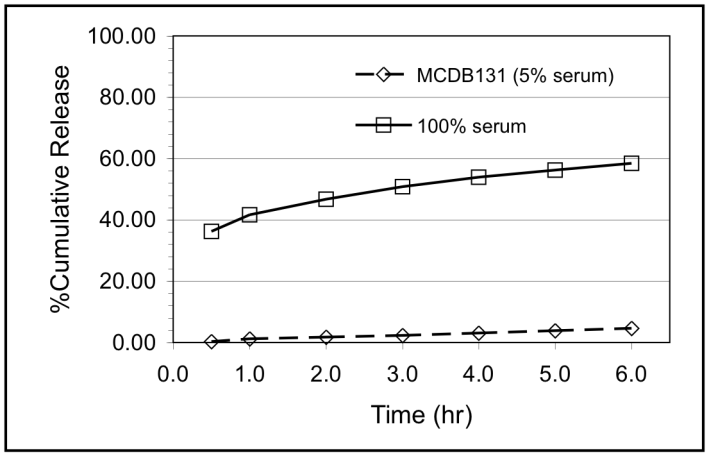

Figure A1. FITC PMCG release depends on serum content. FITC PMCG release was monitored in a similar manner as described in *PEC Protein Release and Monitoring*. For LMW PECs created with dispergation. The release and, therefore, stability of PECs was directly dependent on serum concentration. Cumulative release, after 6 h, in HMVEC media (5% serum) and FCS (100% serum) was 4.62% and 58.42%, respectively (n=1).

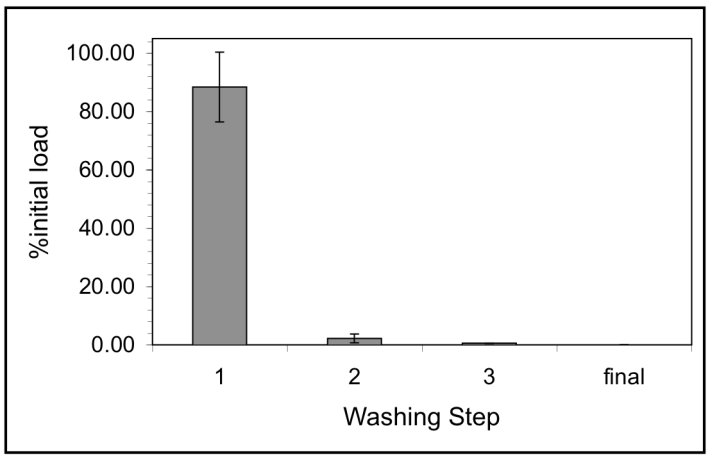

Figure A2. C14 spermine incorporation into LMW PECs with dispergation. C14 spermine (7 μg) was added to the cationic solutions. PECs were fabricated as described in *PEC Fabrication*, centrifuged, and suspended in HMVEC growth media. 0.004% of the labeled material was present in the final suspension.

Early Observations of PEC Association in Mouse Fibroblasts

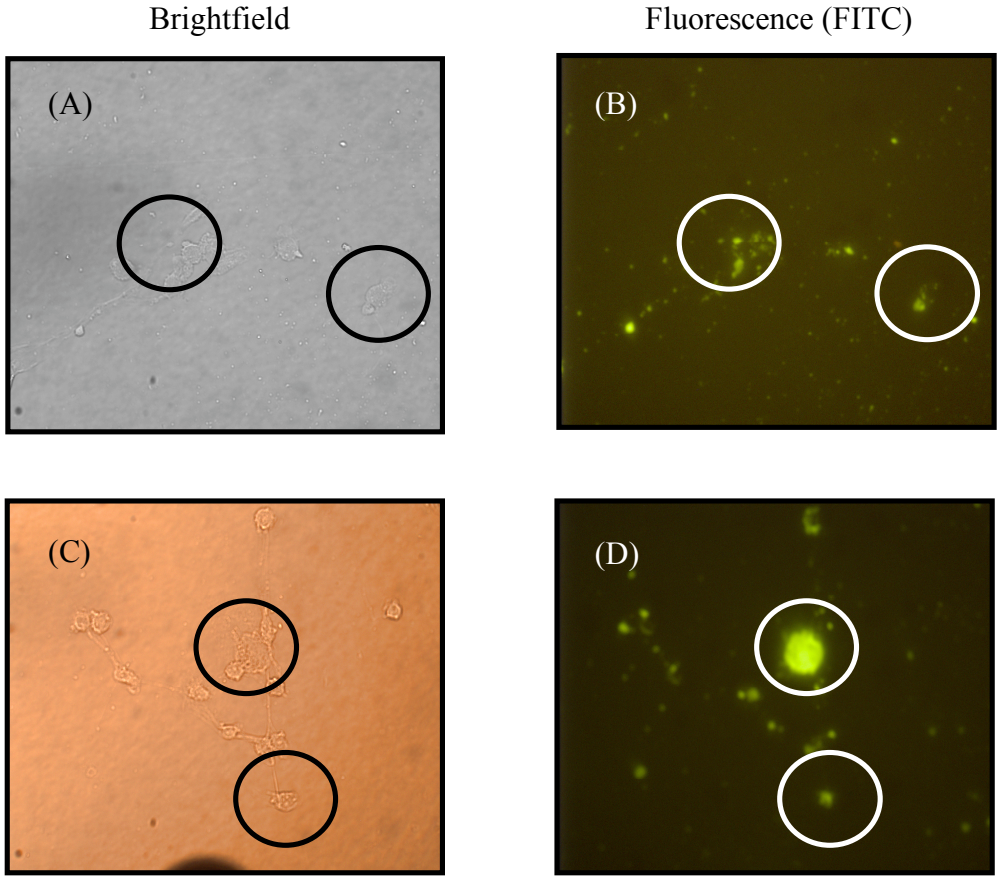

Figure A3. FITC PMCG PECs associate with mouse fibroblasts. FITC PMCG PECs, after suspension in growth media at [PEC]=1.54x10^9 PEC/ml, were incubated with mouse fibroblasts (CRL-10225) for 2 h. Growth media was Dulbecco's Minimum Essential Media (DMEM) supplemented with 10% FCS, 4 mM L-glutamine, 0.05 mg/ml gentamicin, and 1 mM sodium pyruvate. PEC incubations were performed as described in *Confocal Microscopy*. Specimens were viewed with an Olympus BX60 fluorescence microscope. Both brightfield (A,C) and FITC (B,D) filters were applied following a 2 h incubation. Magnification was 400X.

Detection of PEC Association in Mouse Fibroblasts by FACS

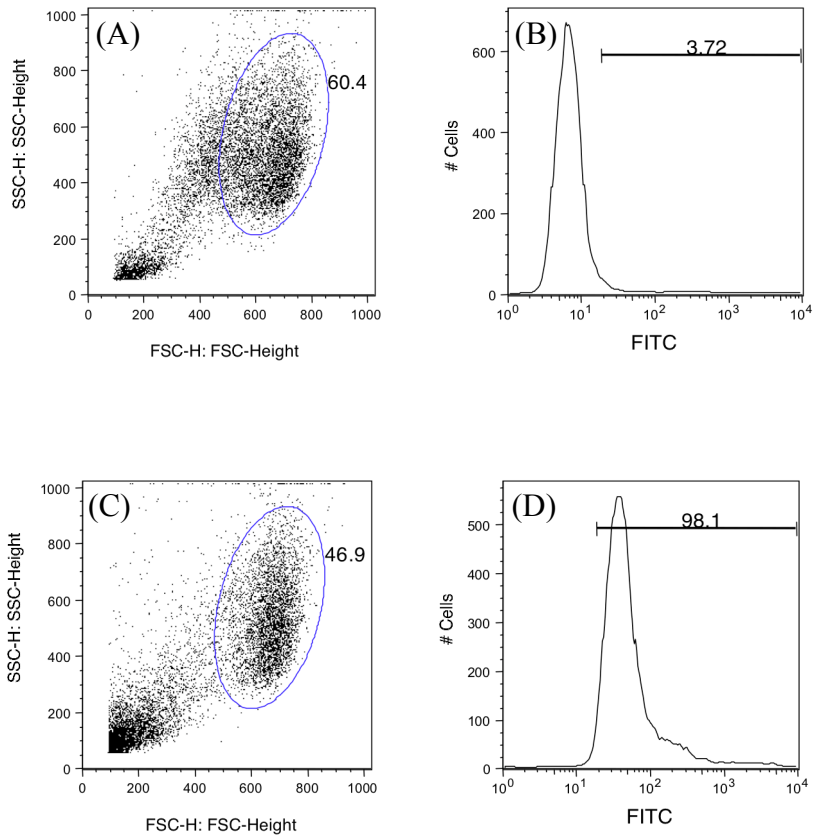

Figure A4. Initial observations of PEC/cell interactions by FACS for mouse fibroblasts (CRL-10225). A 48-well plate containing 50000 cells/well were exposed to 1.54×10^9 PEC/ml for 6 h in standard CHO growth media (C,D). Growth media was Ham's F12 supplemented with 10% FCS, 4 mM L-glutamine, 0.05 mg/ml gentamicin, and 1 mM sodium pyruvate. Subsequent to the exposure period, cells were detached by 0.25% trypsin/0.1% EDTA, and analyzed by FACS. Controls (A,B) were cells in the absence of PECs.

Detection of PEC Association in CHO Cells by FACS

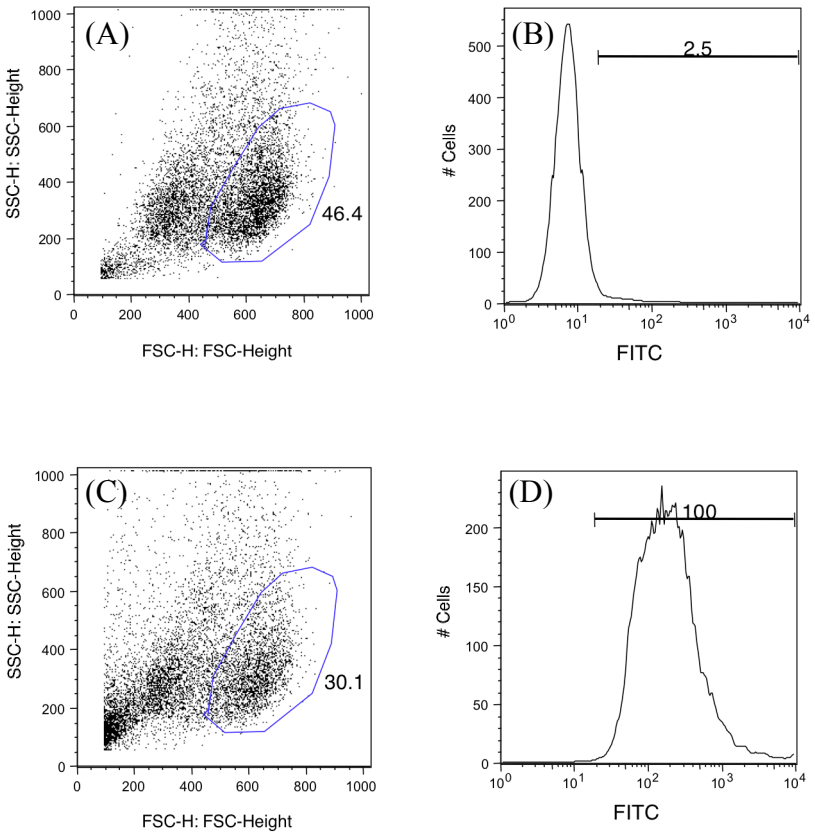

Figure A5. Initial observations of PEC/cell interactions by FACS for Chinese Hamster Ovary cells (CHO). A 48-well plate containing 50000 cells/well were exposed to 1.54×10^9 PEC/ml for 6 h in standard CHO growth media as described in Figure A3 (C,D). Growth media was Ham's F12 supplemented with 10% FCS, 4 mM L-glutamine, and 0.1 mg/ml geneticin. Subsequent to the exposure period, cells were detached by 0.25% trypsin/0.1% EDTA, and analyzed by FACS. Controls (A,B) were cells in the absence of PECs.

Suppression of Surface FITC PMCG with Trypan Blue

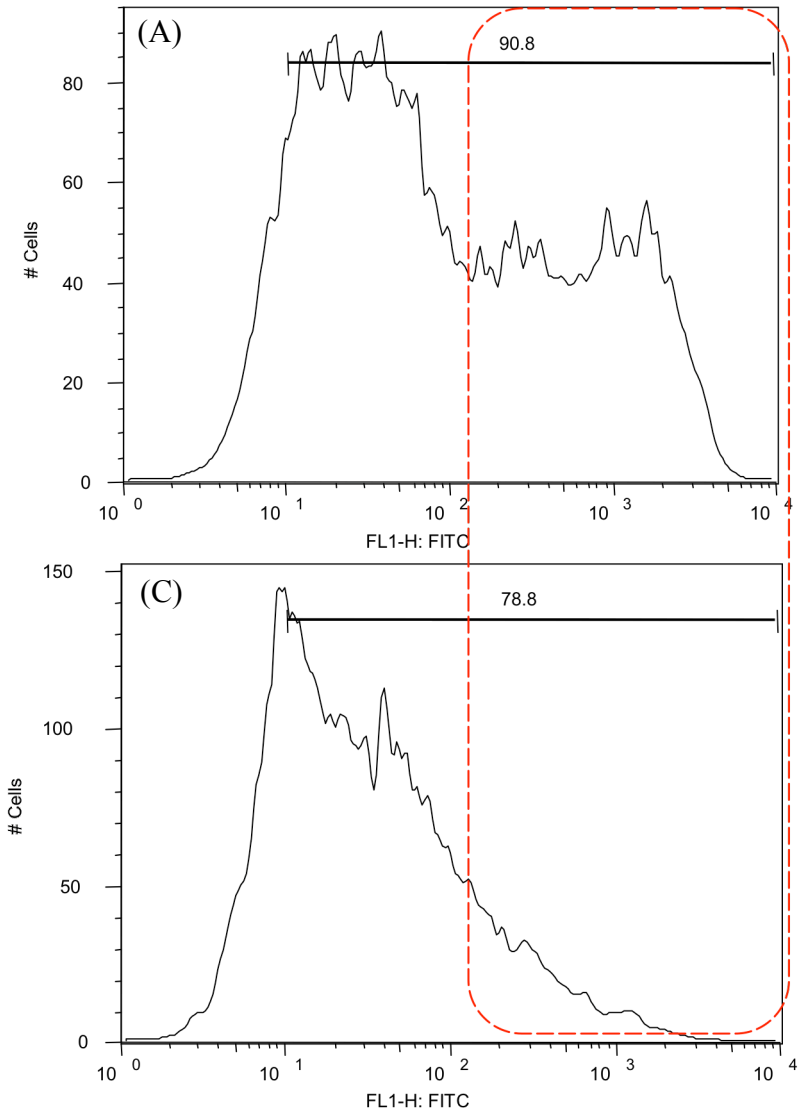

Figure A6. Quenching of a secondary FITC peak with TB. The acquisition of the total MFI (A) was followed by addition of 140 µl of 4 mg/ml TB (B). The result was a disappearance of the peak present in the upper panel.

Two Color FACS Revealed Linkage of TSP521 to PECs

(A)

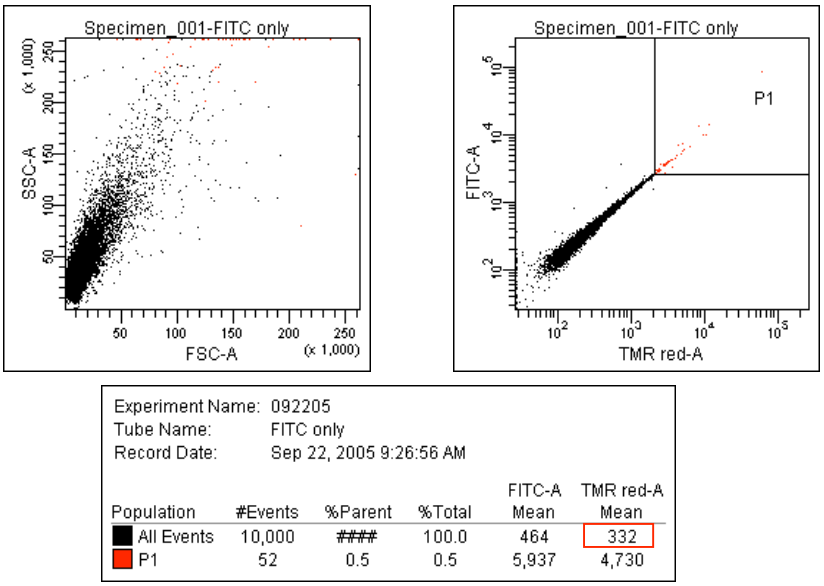

Experiment Name: 092205
Tube Name: FITC only
Record Date: Sep 22, 2005 9:26:56 AM

Population	#Events	%Parent	%Total	FITC-A Mean	TMR red-A Mean
All Events	10,000	####	100.0	464	332
P1	52	0.5	0.5	5,937	4,730

(B)

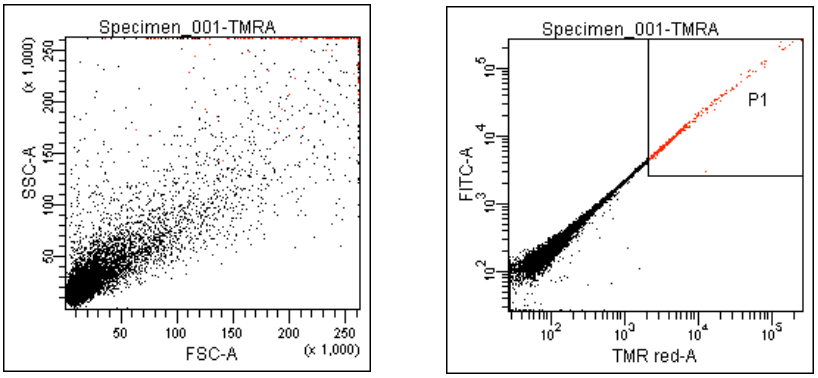

Experiment Name: 092205
Tube Name: TMRA
Record Date: Sep 22, 2005 9:28:41 AM

Population	#Events	%Parent	%Total	FITC-A Mean	TMR red-A Mean
All Events	10,000	####	100.0	1,118	641
P1	276	2.8	2.8	25,154	16,102

Figure A7. Direct linkage of TSP521 by EDAC/NHS verified by two-color FACS. Using the FACSAria system, PECs with (B) and without (A) tetramethylrhodamine (TMRA) TSP521 were analyzed with both TMRA and FITC filters. TSP521 was ligated as elaborated in *Incorporation of TSP521: Direct Surface Coupling and Passive Entrapment*. After preparing dot plots of FITC (vertical) versus TMRA (horizontal), the change in TMRA MFI was calculated with the P1 gate, where P1 described fluorescent indices greater than 10^3 a.u.

Detection of Apoptosis

During the earlier stages of apoptosis, the membrane phospholipid phosphatidylserine (PS) is translocated from the inner to the outer leaflet of the plasma membrane, thereby exposing PS to the external cellular environment. Annexin V is a 36 kDa Ca^{2+} dependent phospholipid-binding protein that has a high affinity for PS, and binds to cells with exposed PS[1]. When conjugated to allophycocyanin (APC), Annexin V binding to PS can be observed by FACS.

The effect of common toxins on HMVEC apoptosis was tested by incubation of epoxomicin (epox), pyrrolidine dithiocarbamate (PDTC), and human tumor necrosis factor alpha (hTNF) for 24 h at varying concentrations (Figure A8). Both PDTC and epox induce apoptosis through inhibition of proteasome activity and NF-κB activation[2, 3]. hTNF turns on apoptotic caspases[4]. This experiment was performed to establish a baseline for the presence or absence of apoptosis through PEC exposure. HMVECs, 5000 cell/well, were seeded to 12-well plates 24 h prior to the addition of Epox, PDTC, and hTNF. After exposure, cells were then detached by 0.25% trypsin/0.1% EDTA and analyzed for Annexin V-APC (BD Pharmingen, San Jose, CA) expression. After monolayer removal, low speed centrifugation, cells were resuspended in 200 μl binding buffer, pH 7.4, consisting of 0.01 M HEPES, 0.14 M NaCl, and 2.5 mM $CaCl_2$. 5 μl of Annexin V-APC was then added and cells stained for 15 min at room temperature in the dark. Cells in the absence of PDTC, epox, and TNF were used as backgrounds and indicated in Figure 8A. Clear shifts were observed as concentrations increased.

PECs, non-targeted (nT PEC) and targeted EDAC/NHS (T PEC) were also tested for their ability to induce apoptosis by incubation at varying, increasing, high concentrations for either 6 h or 24 h (Figure A9). The concentrations evaluated were $1.60x10^9$ PEC/ml, $1.54x10^9$ PEC/ml, $1.01x10^9$, and $6.32x10^8$ PEC/ml. Identical conditions were applied as described for PDTC, epox, and TNF exposures. As shown in Figure 9A, no shift was detected as compared to cells without PECs. The assay does not distinguish between cells that have already undergone an apoptotic cell death and those that have died as a result of necrosis.

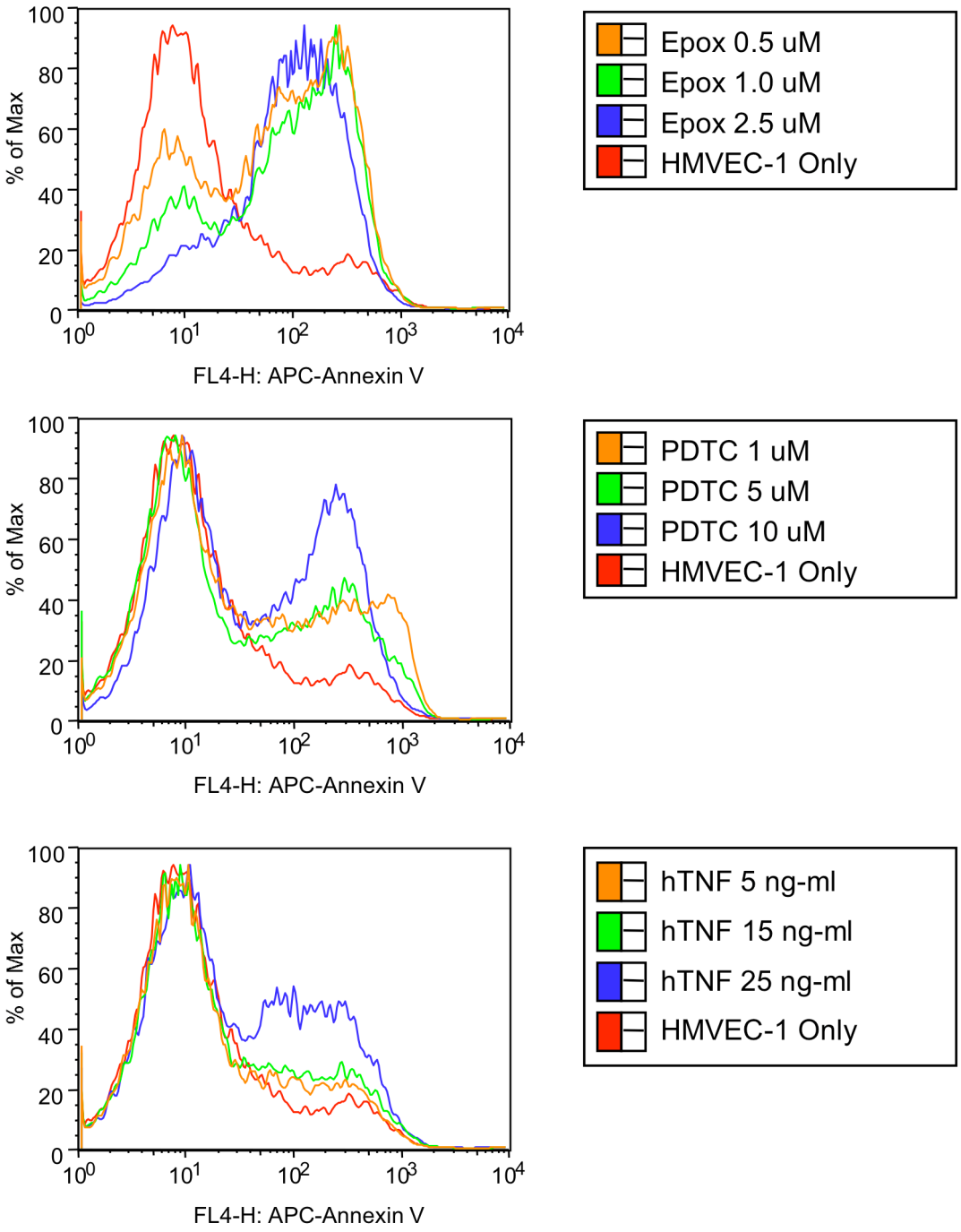

Figure A8. Apoptosis induction by epoxomicin (Epox), pyrrolidine dithiocarbamate (PDTC), and human tumor necrosis factor alpha (hTNF).

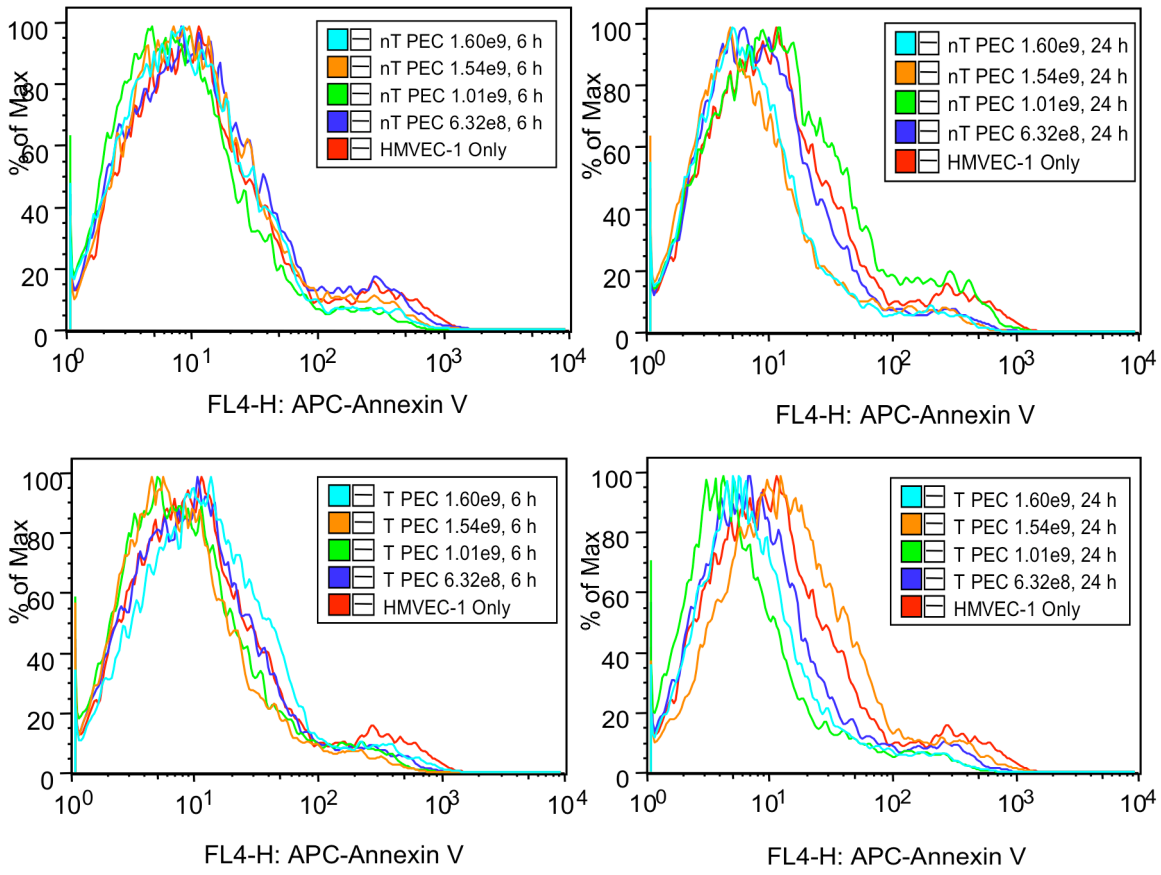

Figure A9. Annexin V-APC expression of HMVECs in the presence or absence of nT or T EDAC/NHS PECs.

Confocal Imaging

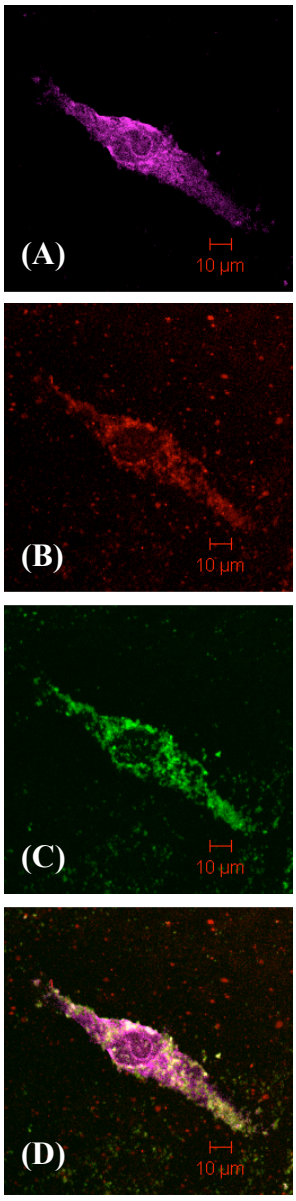

Figure A10. FITC PMCG PECs accumulate inside HMVECs after 24 h. FITC PMCG PECs, after suspension in growth media at [PEC]=1.54x10^9 PEC/ml, were incubated with HMVECs overnight. PEC incubations were performed as described in *Confocal Microscopy*. Filters were (A) concanavalin A-AF647, (B) TMRA, (C) FITC, and (D) merged. Concanavalin A was applied as a lectin stain to visualize the cell membrane Additionally, 100 µg of TMRA TSP521 was coupled to PECs as outlined in *Incorporation of TSP521: Direct Surface Coupling and Passive Entrapment*.

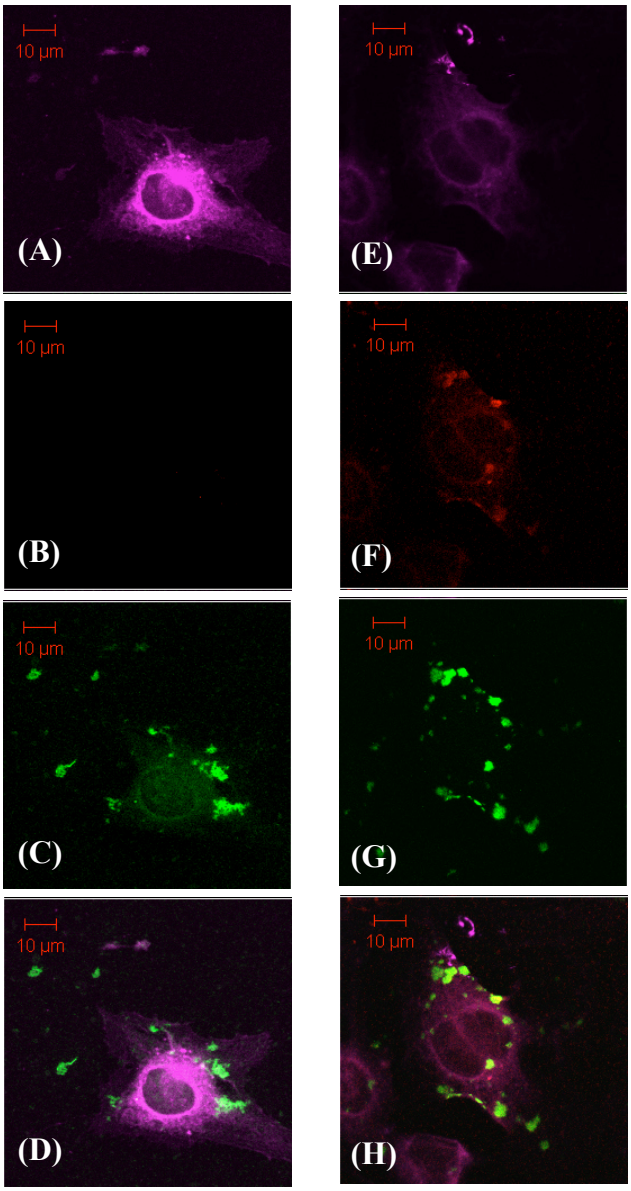

Figure A11. Targeted EDAC/NHS and FITC PMCG PEC confocal imaging. After suspension in growth media at [PEC]=1.54x10^9 PEC/ml, were incubated with HMVECs for 2 h. PEC incubations were performed as described in *Confocal Microscopy*. 100 µg of TMRA TSP521 was coupled to PECs as outlined in *Incorporation of TSP521: Direct Surface Coupling and Passive Entrapment.* Filters were (A) and (E) concanavalin A-AF647, (B) and (F) TMRA, (C) and (G) FITC, and (D) and (H) merged. Concanavalin A was applied as a lectin stain to visualize the cell membrane.

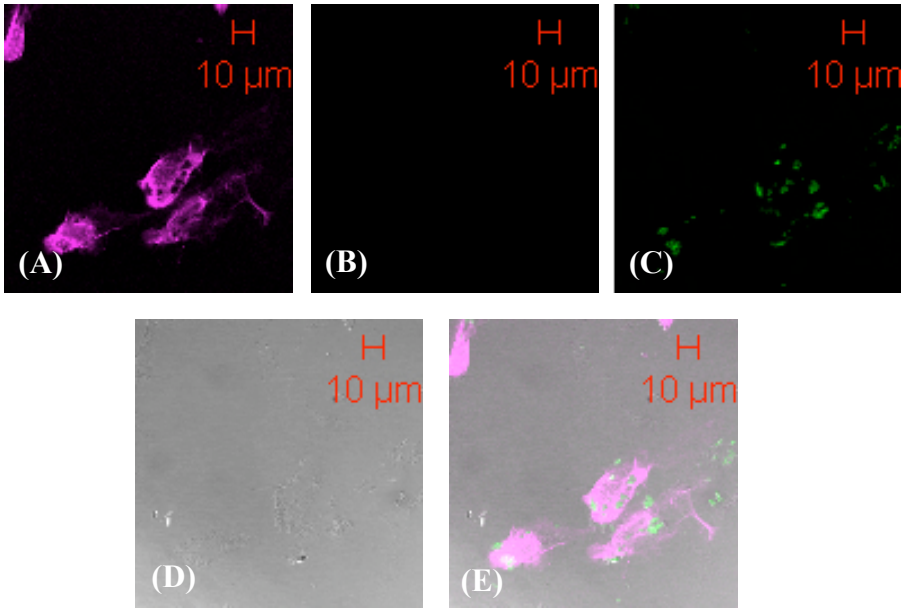

Figure A12. Non-targeted FITC PMCG PEC four-track confocal imaging. After suspension in growth media at [PEC]=1.54x10^9 PEC/ml, were incubated with HMVECs for 2 h. PEC incubations were performed as described in *Confocal Microscopy*. Filters were (A) TOPRO-3, (B) TMRA, (C) FITC, (D) differential interference constrast and (E) merged. TOPRO-3 was applied as a nuclear stain to visualize PEC intracellular localization.

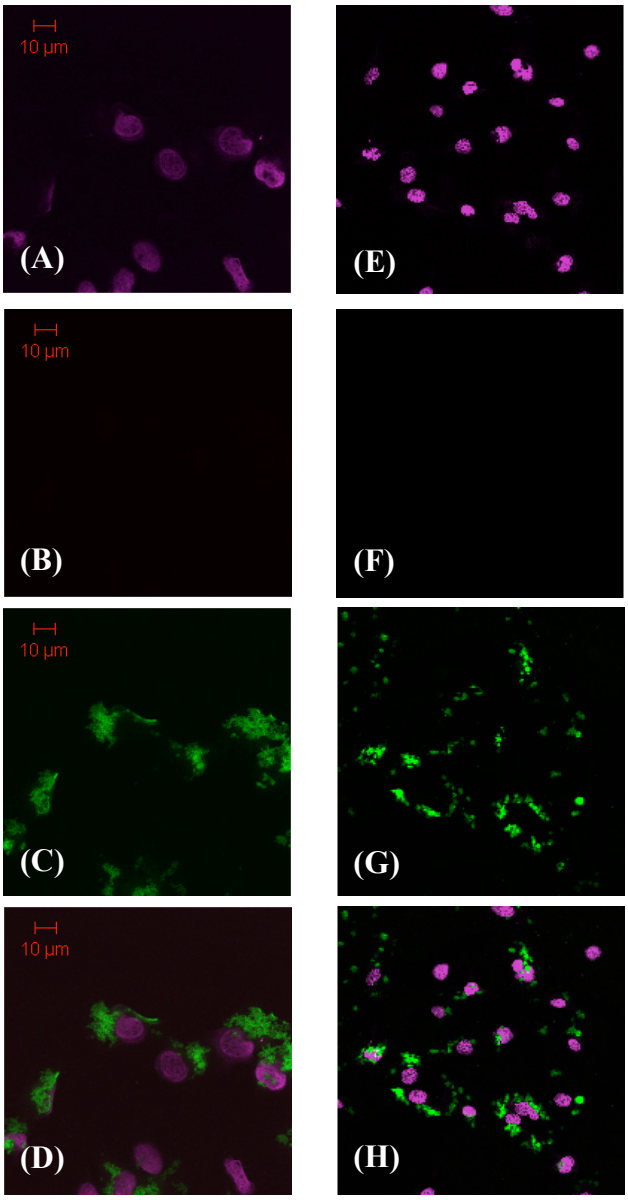

Figure A13. Non-targeted FITC PMCG PEC three-track confocal imaging. After suspension in growth media at [PEC]=1.54x10^9 PEC/ml, were incubated with HMVECs for 2 h. PEC incubations were performed as described in *Confocal Microscopy*. Filters were (A) and (E) TOPRO-3, (B) and (F) TMRA, (C) and (G) FITC, and (D) and (H) merged. TOPRO-3 was applied as a nuclear stain to visualize PEC intracellular localization.

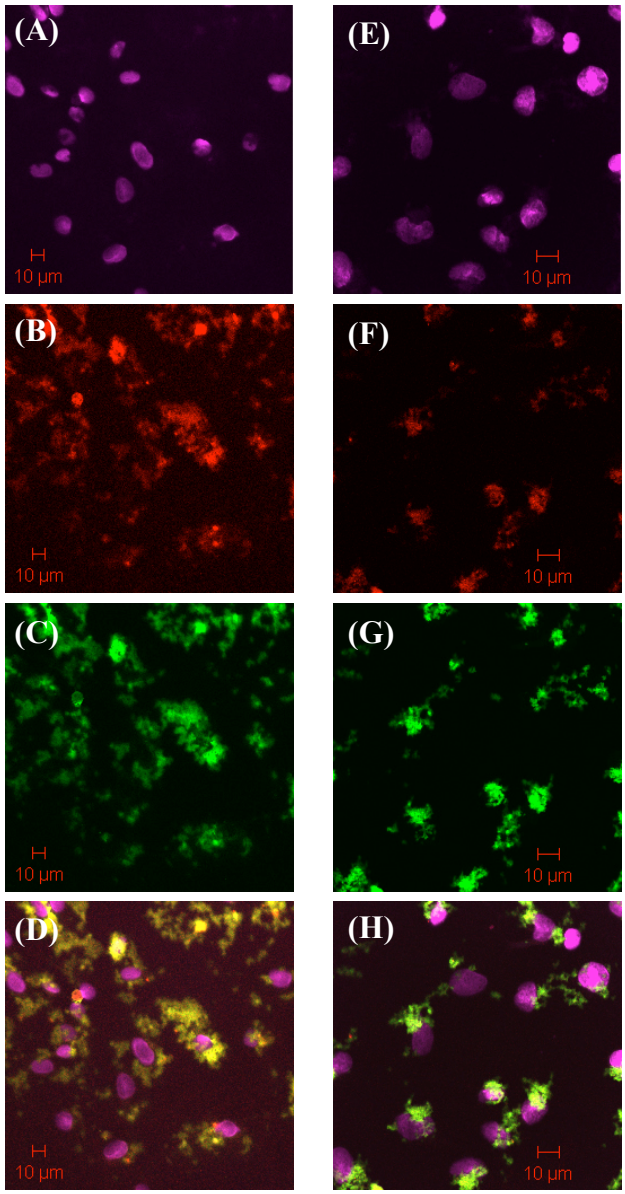

Figure A14. Targeted EDAC/NHS PEC three-track confocal imaging. After suspension in growth media at [PEC]=1.54x10^9 PEC/ml, were incubated with HMVECs for 2 h. PEC incubations were performed as described in *Confocal Microscopy*. 100 µg of TMRA TSP521 was coupled to PECs as outlined in *Incorporation of TSP521: Direct Surface Coupling and Passive Entrapment.* Filters were (A) and (E) TOPRO-3, (B) and (F) TMRA, (C) and (G) FITC, and (D) and (H) merged. TOPRO-3 was applied as a nuclear stain to visualize PEC intracellular localization.

References

1. Vermes, I.; Haanen, C.; Reutelingsperger, C. "Flow cytometry of apoptotic cell death" *Journal Of Immunological Methods* **2000,** 243, 167-190.

2. Erl, W.; Weber, C.; Hansson, G. K. "Pyrrolidine dithiocarbamate-induced apoptosis depends on cell type, density, and the presence of Cu2+ and Zn2+" *American Journal Of Physiology-Cell Physiology* **2000,** 278, C1116-C1125.

3. Meng, L. H.; Mohan, R.; Kwok, B. H. B.; Elofsson, M.; Sin, N.; Crews, C. M. "Epoxomicin, a potent and selective proteasome inhibitor, exhibits in vivo antiinflammatory activity" *Proceedings Of The National Academy Of Sciences Of The United States Of America* **1999,** 96, 10403-10408.

4. Vandenabeele, P.; Declercq, W.; Vanhaesebroeck, B.; Grooten, J.; Fiers, W. "Both TNF Receptors Are Required For Tnf-Mediated Induction Of Apoptosis In PC60 Cells" *Journal Of Immunology* **1995,** 154, 2904-2913.